MALDI MS BASED ASSAYS FOR SCREENING AMINOGLYCOSIDE KINASES

MALDI MASS SPECTROMETRY BASED ASSAYS FOR SCREENING AMINOGLYCOSIDE KINASES

By

ANNE MARIE ELIZABETH SMITH, B.SC.

A Thesis

Submitted to the School of Graduate Studies

In Partial Fulfillment of the Requirements

For the Degree

Doctor of Philosophy

McMaster University

DOCTOR OF PHILOSOPHY (2014) McMaster University

Chemistry and Chemical Biology Hamilton, Ontario

TITLE: MALDI Mass Spectrometry based Assays for Screening Aminoglycoside Kinases

AUTHOR: Anne Marie Elizabeth Smith, B.Sc. Honours (McMaster University)

SUPERVISOR: Dr. John D. Brennan

NUMBER OF PAGES: xv, 164

Abstract

Aminoglycoside antibiotics are commonly used to treat bacterial infections but are highly susceptible to chemical modification, leading to resistance. Chemical modification can be hindered through the use of small molecule inhibitors that target bacterial enzymes involved in resistance, most notably kinases. Current methods for the discovery of small molecule inhibitors of kinases and related "kinase-like" enzymes are limited in throughput and utilize slow, tedious, and expensive assays. This thesis is focused on the development of highly versatile and scaleable kinase and "kinase-like" screening platforms for the discovery of small molecule inhibitors of these drug targets. The work begins with the validation of a matrix-assisted laser desorption/ionization tandem mass spectrometry (MALDI-MS/MS) platform utilizing phosphorylation of kanamycin, an aminoglycoside antibiotic, by aminoglycoside phosphotransferase 3′IIIa (APH 3′IIIa) as a model system. Using a product-to-substrate signal ratio as an internal standard, the assay was used to functionally screen over 200 compounds, combined into mixtures to enhance assay throughput. Moreover, the assay was used to determine inhibitory dissocation constants for newly discovered modulators. Throughput was further increased to a novel dual-kinase assay targeting a bacterial enzyme, APH 3′IIIa and a human kinase, protein kinase A (PKA), which was validated using the previous small molecule library. Alternative assay development platforms were also studied using imaging mass spectrometry of reaction microarrays and the fabrication of sol-gel derived bioaffinity chromatography columns. The MS-based kinase assays developed herein are highly

amenable to high throughput screening, and have the potential to be extended to other important therapeutic targets.

Acknowledgements

I thank my supervisor Dr. John D. Brennan, for direction and support through the duration of this thesis. In addition, I would like to further direct my thanks to my committee members: Dr. B.E. McCarry, Dr. N.A. Magarvey and Dr. A. Capretta for suggestions to advance this project, and my learning. I would also like to thank Dr. P. Lock for advice throughout my thesis.

I would like to thank my fellow lab members, past and present for support and interesting discussions throughout the past 4.5 years, specifically Meghan McFadden, Jessamyn Little, and Christy Hui.

My gratitude to my family and friends for their ongoing support cannot fully be expressed. To my parents, for making it easy for me to get to and from school each and every day either through giving me a ride or maintenance of my car. For making meals and clean laundry easily available, the hours I would have spent doing all those things would surely have made completion of this degree more challenging and lengthy. To my grandmother, for always believing in me and lending an ear. To one of my best friends, Sarah, you have been beyond supportive and encouraging. And lastly, to my boyfriend, your unwavering support and belief in me has made truly stressful times more bearable and brought me so much happiness.

TABLE OF CONTENTS

List of Figures and Tables

Abbreviations

AChE	acetylcholine esterase
ADP	adenosine diphosphate
AP	atmospheric pressure
APH	aminoglycoside phosphotransferase
APTES	aminopropyltriethoxysilane
ALPHA	amplified luminescent proximity homogeneous assay
AMP	adenosine monophosphate
ASMS	affinity selection/mass spectrometry
ATP	adenosine 5'- triphosphate
BIS-TRIS	bis(2-hydroxyethyl)amino-tris(hydroxymethyl)-methane
c-AMP	cyclic adenosine monophosphate
CE	collision energy
CHCA	α-cyano-4-hydroxy-cinnamic acid
DESI	desorption electrospray ionization
DGS	diglycerylsilane
DMSO	dimethyl sulfoxide
DTNB	5,5'-dithiobis(2-nitrobenzoic acid)
EDTA	ethylenediaminetetraacetic acid
ELISA	enzyme-linked immunosorbent assay
ESI	electrospray ionization
EtOH	ethanol
FAC	frontal affinity chromatrography
FLEXIQinase	full-length expressed stable isotope-labeled protein for quantification strategy
FMAT	fluorometric microvolume assay technology
GPCR	G-protein-coupled receptor
HC	high control
HEPES	4-(2-hydroxyethyl)-1-piperazineethanesulfonic acid
HPLC	high performance liquid chromatography
HTRF	homogeneous time resolved fluorescence
HTS	high-throughput screening
IC_{50}	half maximal inhibitory concentration
i.d.	internal diameter
IM	ion mobility
IMAP	immobilized metal ion affinity-based fluorescence polarization
IMER	immobilized enzyme reactor
IMS	imaging mass spectrometry
IQ	iron quenching
IS	internal standard
ITO	indium tin oxide
KAYAK	kinase activity assay for kinome profiling
k_{cat}	catalytic constant (turnover number)

K_I	inhibition constant
K_M	Michaelis-Menten constant
LC-MS	liquid chromatography mass spectrometry
LDI	laser desorption/ionization
LRRASLG	kemptide
MALDI	matrix-assisted laser/desorption ionization
MeOH	methanol
MNP	magnetic nanoparticle
MS	mass spectrometry
MS/MS	tandem mass spectrometry
m/z	mass-to-charge
NADH	nicotinamide adenine dinucleotide
Nd:YAG	neodymium-doped yttrium aluminum garnet
NTB	2-nitro-5-thiobenzoate
PAC	prespotted anchorchip
PEG	poly(ethylene) glycol
PEP	phosphoenolpyruvate
PGS	polyglyceryl silicate
PKA	protein kinase A or cAMP-dependent protein kinase
PK/LDH	pyruvate kinase/lactate dehydrogenase
RF	RapidFire®
SAMDI	self-assembled monolayer desorption/ionization
SDS-PAGE	sodium dodecyl sulfate - polyacrylamide gel electrophoresis
SEM	scanning electron microscopy
S/N	signal-to-noise
SM	small molecule
SPA	scintillation proximity assay
SRM	selected reaction monitoring
SS	sodium silicate
TEOS	tetraethylorthosilicate
TFA	trifluoroacetic acid
TMOS	tetramethylorthosilicate
TOC	total organic content
TOF	time of flight
TOF-SIMS	time-of-flight secondary-ion mass spectrometry
TR-FRET	time-resolved fluorescence resonance energy transfer
TRIS	tris(hydroxymethyl)aminomethane
UV	ultra violet
v/v	volume-volume
w/v	weight per volume

Chapter 1 : Introduction

1.1 Kinases and Antibiotic Resistance

Kinases are enzymes that transfer a phosphate group from molecules such as ATP to various substrates, a process known as phosphorylation, in the presence of cationic co-factors such as Mg^{2+}. [1] Second to G-protein-coupled receptors (GPCRs), protein kinases are the most important drug target due to their critical function in signal transduction pathways and post translational modifications, leading to their involvement in a multitude of diseases and physiological processes ranging from cancer to metabolism.[2-5] Furthermore, kinases are known to be "highly druggable", where a "druggable" target is one that has a well-defined binding pocket that can be probed by small molecules (SMs) that follow Lipinski's rule of five. [6-8]

While proteins are the most common substrates of kinase reactions, phosphotransferases, or kinase-like enzymes, can also use small molecules as substrates, which can include antibiotics. It is now clear that the overuse or misuse of these drugs lessens their efficacy, owing to a group of processes that are generally termed antibiotic resistance, resulting in less efficient treatment of infections. In general, resistance occurs through a variety of mechanisms including modification of drug targets, alteration of cell permeability, active efflux, and antibiotic inactivation, the latter of which being the most predominant. [9-10] Antibiotic inactivation; modification of a drug resulting in one incapable of treating bacterial infections, [11-15] can occur by one of six modifications involving the transfer of acyl, phosphoryl, thiol, nucleotidyl, ADP-ribosyl, or glycosyl

groups to the antibiotic substrate, where the type of modification is dictated by the type of modifying enzyme. [9] Methods to prevent the onset of resistance include modification of currently successful antibiotics, discovery of novel drugs and use of inhibitors of modifying enzymes.[11-13] Modification of current drugs is a relatively simple approach, however given that the modification results in a drug with a high degree of similarity to the original drug, bacteria quickly develop resistance mechanisms. Novel drugs, which are frequently found in nature, are very promising for overcoming resistance. Unfortunately, they require a great deal of time from discovery to clinical use and hence, are not able to quickly address the rising resistance problem. Alternatively, inhibition of modifying enzymes is potentially a quite useful method to delay the onset of resistance.[11-13] An example of this approach is with the selective inhibition of β-lactamases by compounds that are co-administered with lactamase-sensitive antibiotics, which is marketed under tradenames such as Augmentin®,[16] Clavulin®[17] and Zosyn®[18].

Aminoglycoside Phosphotransferase 3′IIIa

A particular group of kinase-like proteins, known as aminoglycoside phosphotransferases (APHs), specifically target aminoglycoside antibiotics and thus play a major role in antibiotic resistance. The APH family of enzymes contains more than 20 members, all sharing 20-40 % of their primary sequence.[19] One such APH is the 264 residue protein APH 3′IIIa; an enzyme present in *Enterococci* and *Staphylococci* bacteria, which is a modifying enzyme responsible for phosphate group transfer from ATP to the 3′ OH group in aminoglycoside antibiotics. [13, 19-21] APH 3′IIIa has additional structural

similarities with eukaryotic protein kinases, such as protein kinase A (PKA), [13, 22] a protein involved in metabolic regulation and cognition, where misregulation (in this case, activation) of this enzyme can result in a decrease in cognitive function, as described later. [23-24] This provides a key challenge; modulating bacterial kinases such as APH3′IIIa without affecting other kinase-dependent signal transduction pathways.

Aminoglycoside antibiotics bind to the 30S subunit of ribosomes causing cell death and are therefore required for treatment of bacterial infections. [19, 25-26] APH 3′IIIa has more than ten antibiotic substrates that it can modify and inactivate[21] resulting in an enormous need for selective inhibition of the substrate binding site. One commonly studied substrate of APH 3′IIIa is the aminoglycoside antibiotic, kanamycin (K_M = 12.6 ± 2.6 μM).[15] The reaction of kanamycin with the co-factor ATP and APH 3′IIIa proceeds by a Theorell-Chance mechanism described in Figure 1.1, where ATP binds first to the enzyme forming an enzyme-ATP complex, followed by binding of the substrate kanamycin, the rapid release of the phosphorylated product and finally the slow release of ADP.[27]

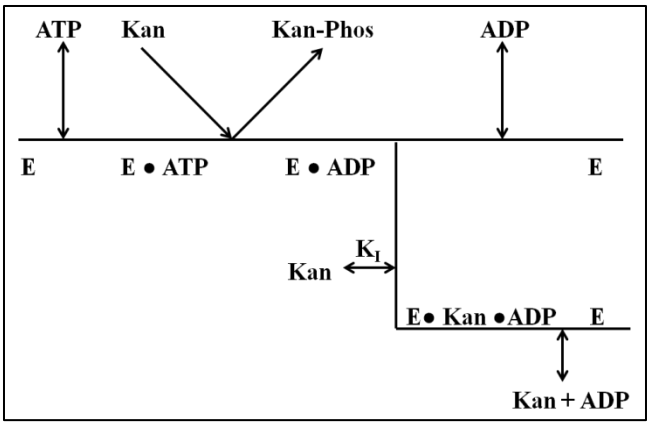

Figure 1.1**:** Theorell Chance Mechanism for kanamycin phosphorylation by APH 3′IIIa. Inhibition of this process is commonly studied with the kanamycin competitive [28] small molecule inhibitor tobramycin (K_I = 2 µM). [15]

Protein Kinase A (PKA)

As noted above, the selective inhibition of the substrate binding site of APH 3′IIIa is of great importance given that this enzyme shares many structural characteristics with eukaryotic protein kinases.[19] Protein kinase A (PKA), or cyclic AMP dependent protein kinase, is a eukaryotic protein kinase involved in neural, cognitive and several other systems throughout the body. [23-24] PKA is a tetramer composed of two regulatory and catalytic subunits, with cAMP activating the complex upon binding the former of the two subunits. [29] Upon activation, catalysis of the transfer of gamma phosphates of ATP to substrates can occur as before. [1] One of the most commonly studied systems involving PKA is the phosphorylation of synthetic peptides such as kemptide (K_M = 16 ± 0.9 µM).[30] The reaction can be inhibited by a variety of small molecules, in particular H-7 (K_I = 3 µM). [31] However, H-7 is an ATP-competitive rather than a substrate-competitive inhibitor and as a result also inhibits the aforementioned “kinase-like” protein, APH 3`IIIa.[28] Consequently, use of PKA and APH3′IIIa provide a useful model system to

develop assays that can identify selective inhibitors of bacterial kinases while leaving the activity of human kinases unaltered.

1.2 Assays for Small Molecule Screening

SMs are compounds less than 500 Da, and are often used for the study of biological processes and have shown great potential for the development of new drugs. [8] With the ever growing number of small molecules synthesized through combinatorial chemistry and the prevalence of bacterial resistance, methods to quickly and reliably evaluate the effects of these molecules on protein systems involved in resistance are needed. The use of high-throughput screening (HTS) methods is thus essential to provide a rapid and inexpensive means to identify modulators of enzyme activity.[32-33]

High Throughput Screening

HTS is a method by which thousands to millions of compounds can be rapidly assayed in an automated fashion, either individually or as mixtures, to determine which ones can modulate enzyme activity or alter biochemical interactions.[32-33] Depending on the assay format, the assay may be used to examine a single target protein, or may be multiplexed so that multiple proteins or cellular pathways are examined at once. A key to development of new HTS methods is the need for a method that is efficient, reliable, inexpensive, robust, and automated. [32] Assay miniaturization is also a key feature of newer HTS methods, as this provides reduced reagent volumes and hence reduced cost, and as noted below can help with multiplexing as in the case of microarrays. [32-33]

Microarrays

Microarray technology is becoming a popular method for screening of compound collections (often small molecules) in a high-throughput, multiplexed manner due to the ability to use nanolitre volumes of reagents and extremely small amounts of proteins, along with the ability to use many different imaging methods to assay microarrays. The technology employs the use of robotic liquid handling instruments, where small spots (ranging from 50-300 μm in diameter) are placed onto glass slides, or an alternative surface in an ordered array using either contact printing or non-contact piezoelectric printing.[34] Each array contains multiple samples along with all required controls, allowing for complete experiments to be carried out on a fraction of a glass slide. This provides a vast amount of data and insight into the biochemical reactions being carried out, with detection typically performed by radiometric, [35] colorimetric, [36-37] fluorimetric [38-39] or luminescence assays, [40] imaging surface plasmon resonance, [41-42] and more recently by mass spectrometric assays. [43-44]

Kinase Screening

As mentioned previously, kinases transfer a gamma phosphate from a co-factor, normally ATP, to a substrate molecule. [1] A variety of methods exist to monitor this reaction, many of which are amenable to HTS assays. The most common methods for performing kinase assays are provided in Table 1.1 below, along with a summary of the key advantages and disadvantages of each method.

Table 1.1: Traditional screening approaches for detection of kinase modulators

Cell Based Assays		
Summary	Advantages (+)/ Disadvantages (-)	Examples
Use of cell lysates in biochemical assays with detection by absorbance, fluorescence or luminescence.	+ Assesses permeability + Occurs within cells – Can involve expensive reagents – Involves handling of cells	• DiscoveRx [45] • AlphaScreen®SureFire® [46] • Homogeneous time resolved fluorescence (HTRF) [47]
ELISA [48-49]		
Summary	Advantages (+)/ Disadvantages (-)	Examples
Antigen binds to an enzyme-linked-antibody. Substrate addition causes a reaction which can be measured with absorbance.	+ Specific – Requires monoclonal antibodies – Expensive – False positives – Laborious – Poor stability – Not always amenable to SM screening	
Fluorescence [47, 50-60]		
Summary	Advantages (+)/ Disadvantages (-)	Examples
Singlet state electron excitation with return to the ground state results in photon emission. Methods vary on proximity of secondary molecules which can result in quenching/excitation, or rotation of molecules in plane polarized light.	+ Inexpensive + Sensitive + High throughput – Poor specificity – Reagent quenching – Requires labels – Compound interferences – Not all amenable to SM screening	• Fluorometric Microvolume Assay Technology (FMAT) [51] • Fluorescence polarization [52-53] • HTRF [47] • TR-FRET Lance assay (time-resolved fluorescence resonance energy transfer) [54] • IMAP (Immobilized metal ion affinity-based fluorescence polarization) [55-56] • Z'lyte [57] • Pro-Q Diamond assay [58] • IQ (Iron Quenching) [59]
Luminescence [50]		
Summary	Advantages (+)/ Disadvantages (-)	Examples
Energy transfer from excited states resulting in light emission caused by reactions such as electrical or chemical reactions. (i.e. ATP consumption in the luciferase-luciferin reaction)	+ Sensitive + Quick – Compound interferences – Can be costly	• PKLight (bioluminescence) [61] • Kinase Glo [62] • Amplified Luminescent Proximity Homogeneous Assay (ALPHA) [63] • Electrochemiluminiscence assays [64]

Absorbance		
Summary	Advantages (+)/ Disadvantages (-)	Examples
Monitors changes in absorbance (i.e. decrease in absorbance at 340 nm; removal of NADH).	+ Simple – Lacks specificity – Secondary screening needed – Inhibition of secondary enzyme – Possible false positives – Limited sensitivity	• NADH coupled reaction [65-66]
Radioactivity[67-71]		
Summary	Advantages (+)/ Disadvantages (-)	Examples
Use radioactivity to monitor phosphorylated reaction products (ie. P^{32})	+ Sensitive – Not very high throughput – Requires labelling – Radioactive	• ^{32}P ATP • Scintillation proximity assay (SPA) [47] • Flash Plate [72]

Among the different kinase screening platforms mentioned above, the most common of these are fluorescence and absorbance based methods due to their simplicity. The expense associated with cell based assays, ELISA, and luminescence, as well as the use of radioactive compounds in radioactivity methods have made these methods less common. Methods which overcome these disadvantages, such as high expense, labelling, false positives, laborious, and specificity, but maintain the advantages are greatly needed. Mass spectrometry is one such method.

1.3 High Throughput Screening using Mass Spectrometry

Although many assays capable of detecting phosphorylation events exist, there are few which allow direct detection without the need for time consuming labelling processes. Mass spectrometry (MS) is a detection method by which substrate molecules (in this case, an antibiotic) and their corresponding phosphorylated products can be directly detected through the use of a mass-to-charge (*m/z*) ratio. Mass spectrometers provide information about molecular formula, structure, and isotopic ratios, and can be

applied to both qualitative and quantitative analyses. [73] MS is also a robust and versatile technique. For instance, depending on analyte, specific ionization methods and mass analyzers can be used to enhance sensitivity and mass accuracy.[73] Some of the key features of mass spectrometers are discussed below as they relate to their use in HTS.

ESI and MALDI

Typical MS methods employ electrospray ionization (ESI); a soft ionization process which creates fewer fragmented ions compared to other ionization sources and hence is ideal for proteomics.[74] The ESI process involves the transfer of analytes from liquid to gas phase through the use of a capillary where ejection of the solution in an electric field results in an aerosol spray, followed by solvent evaporation leading to small charged ions that are pulled by a vacuum into the mass spectrometer for analysis (Figure 1.2). [75] Unfortunately, the presence of non-volatile salts and cofactors such as Mg^{2+} can clog the electrospray capillary used for transfer of analyte solutions to the gas phase for detection, resulting in erratic spraying and significant ion suppression, which affects quantification. This leads to the need for volatile buffers such as ammonium acetate and low ionic strength buffers (20 mM or less), as well as extremely low amounts of co-factor ions (e.g., the upper limit for Mg^{2+} is 0.8 mM while the physiological level is 5 mM). [76-77]

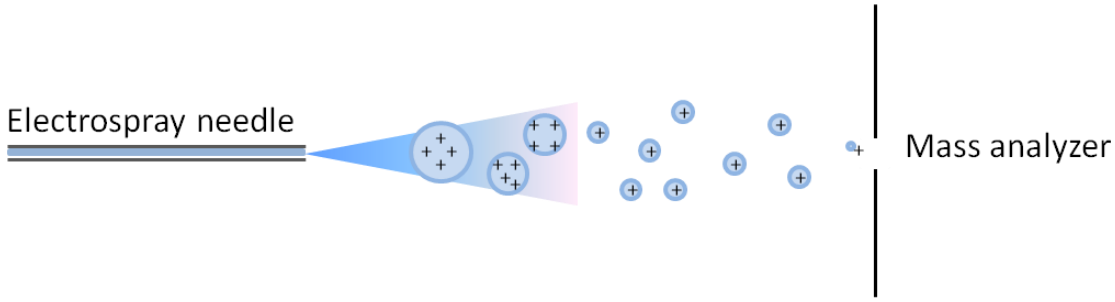

Figure 1.2: Electrospray Ionization process. Analyte molecules are transferred from liquid to gas phase prior to mass analysis. As the solvent droplet evaporates, charged analytes emerge, which are introduced into the mass analyzer. [78]

An alternative soft ionization source that provides the benefit of improved salt tolerance is matrix-assisted laser desorption/ionization (MALDI).[73-74] MALDI ionization uses a pulsed UV laser to irradiate a crystalline material composed of a MALDI matrix (commonly aromatic acids) mixed with the analyte of interest, normally at a 1000:1 molar ratio. The matrix absorbs the UV radiation causing desorption from the surface, followed by analyte ionization and extraction of the ions into the mass analyzer, as illustrated in Figure 1.3. [79-80]

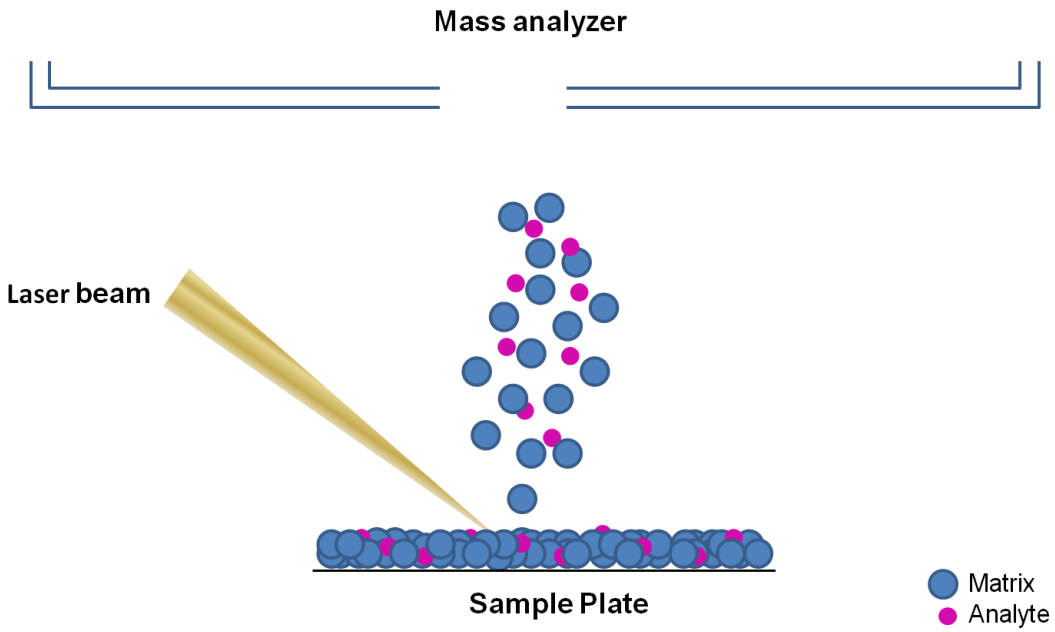

Figure 1.3: MALDI process whereby irradiation of the sample with a laser beam results in desorption and ionization of matrix and analyte molecules that are pulled into the mass spectrometer for analysis. [80]

MALDI-MS has traditionally been used for high molecular weight analytes (MW > 1000) owing to a significant amount of noise in the lower molecular weight region due to matrix ions. However, the method has still found some use in HTS studies, either based on higher molecular weight peptides as analytes to overcome the molecular weight issue, or by employing techniques that allow for detection of small molecules analytes, such as the use of special matrix materials, [81-82] direct laser desorption/ionization (LDI), [83] tandem mass spectrometry, [84] or high resolution mass spectrometry [85] (see below). Such methods could allow for the rapid detection of modulators of the aforementioned aminoglycoside kinase at low cost. Furthermore, direct detection of kinase phosphorylation events by MALDI-MS would allow facile identification of kinase modulators, overcoming a deficiency in current kinase assay platforms.

MALDI and ESI-MS are ideal for proteomics because they create fewer fragmented ions, have low limits of detection and can detect compounds of varying molecular weight.[74] In some applications, MALDI has additional advantages over ESI, where it creates primarily singly charged species, decreases ion suppression and has semi-permanent deposition, allowing reuse of samples, and can be used with samples that contain significantly higher levels of salts and buffers than can be tolerated by ESI.[86] Furthermore, MALDI-MS presents an additional advantage to typical ESI methods, which is increased speed and simplified spectra due to the presence of primarily singly charged species. [87-93]

As noted above, the detection of small molecules with the use of MALDI had not been widely reported due to the high presence of interfering matrix peaks. However, with current advances in MALDI technology, the technique is now being more widely used for small molecule analysis, as opposed to traditional macromolecular studies. [92, 94] Two main disadvantages associated with SM-MALDI are matrix interference and irreproducibility.[95] The emergence of new, high molecular weight (>1000 Da) matrices which result in limited interferences within low molecular mass range [95] have allowed the use of MALDI for SM screening, with specific success detected on a MALDI triple quadrupole instrument[87-93] Furthermore, surfactants can be used to eliminate or substantially suppress matrix interferences by reducing formation of matrix adducts, however, a tradeoff of decreased analyte response by an order of magnitude is observed.[82, 96] Additional sample preparation techniques can also be performed to reduce

matrix interference, for example, washing of matrix crystals with buffers containing ammonium salts. [97]

The use of direct LDI MALDI is another means by which the analysis of SMs can be performed. These techniques typically involve the direct ionization off of porous silicon surfaces where the analyte is trapped within the porous surface and ionized using UV laser irradiation. The ionization is made possible because of the high UV absorbing nature of the silicon surface. The lack of matrix interferences makes this method highly amenable to SM analysis.[83]

Upon use of matrix, the interferences previously discussed only occur when performing full scan MS analysis. Tandem MS (known as MS/MS) is a process by which fragmentation of precursor ions is performed resulting in a spectrum of product ions. MS/MS experiments consist of two mass analyzers surrounding a collision cell, where the first mass analyzer acts as a filter to select precursor ions, the precursor ions are then collided with a neutral gas in the collision cell to create product ions that are separated by the second analyzer and detected (Figure 1.4). [78] Use of this process makes matrix and other background interferences negligible, resulting in enhanced sensitivity and noise reduction.

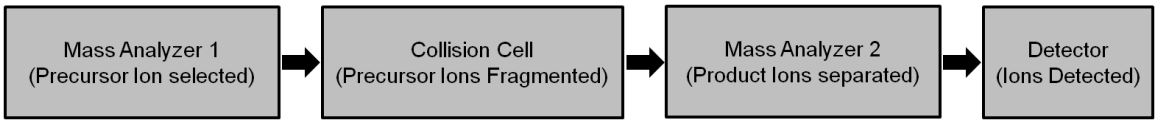

Figure 1.4: Tandem mass spectrometry process.

Further benefits can be seen depending on the type of mass analyzer used. Two types of analyzers of particular interest are the ion trap and time of flight (TOF) analyzers. An ion trap is a three dimensional trap that restricts ions by a combination of three electrodes (Figure 1.5A). A change in voltage to one electrode causes ejection of the ions through small holes in the end-cap electrodes, which are monitored by an electron multiplier detector. Ion traps have the advantage of being sensitive and inexpensive instruments, however they suffer from low reproducibility and resolution compared to other analyzers. [78] TOF analyzers exploit the relationship between mass and velocity at a specific kinetic energy, and measure the time it takes for the ions to travel the distance of the high vacuum instrument tube. These instruments have the advantages of being able to measure high masses and high resolution. Resolution can be further increased through the use of reflectron mode, which corrects for the variation in kinetic energy, by adjusting the velocity of the ions that were initially ionized so that ions of the same mass will reach the detector at the same time (Figure 1.5B). [78]

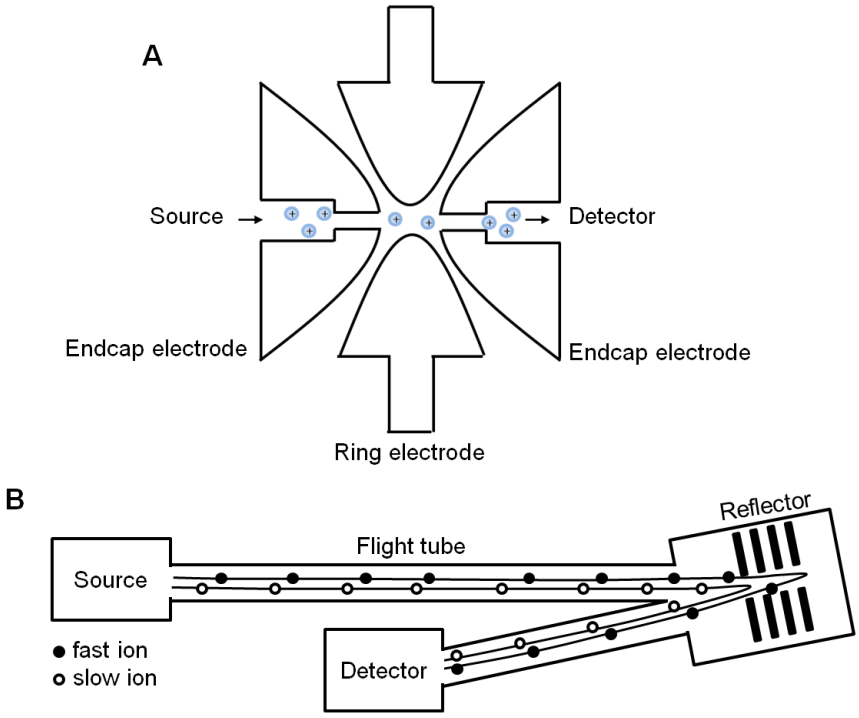

Figure 1.5: A) Ion trap mass analyzer and B) Reflectron time-of-flight mass analyzer. [78]

Recently, TOF analyzers have also been linked to imaging techniques, in particular, MALDI-TOFs (or TOF/TOFs). Imaging technologies provide an automated and high-throughput means of data acquisition for large sample sets. The technology records a mass spectrum for each pixel designated by the user, creating an image. Imaging MALDI has found great use in the analysis of tissue samples by means of protein analysis allowing for determination of molecular features. Use of imaging MALDI in conjunction with microarray technologies is also starting to emerge. [44, 98]

Mass Spectrometry and Kinase Screening

MS is heavily used in drug discovery and with the importance of kinases in signal transduction, it is not surprising that more studies involving MS analyses of kinases are

being reported. [77, 99-100] Quantitative detection of phosphorylated peptides from the enzymatic reaction with PKA has been shown through the use of ESI-MS, however, because of the type of ionization, low salt concentration (Mg^{2+}) was required, which results in reduced product formation.[99] Similarly, Partserniak et al. developed a semi-automated direct detection method for glycogen synthase kinase 3β screening of inhibitors. Again, the authors were required to work at low salt concentrations due to the need for ESI compatible solvents for ionization which can limit the activity of some enzymes. The authors were also required to work at low inhibitor concentrations for screening due to the intolerance of ESI to DMSO; a common solvent in chemical libraries that results in ion suppression. [77] Table 1.2 summarizes a large selection of additional MS methods for kinase screening.

Table 1.2: Mass Spectrometry Techniques for Kinase Screening

Technique	Summary
Affinity Selection/Mass Spectrometry (ASMS) [101]	A screening method of compounds in mixtures where a mixture of ligands are left to react with a target protein, following several ultrafiltration steps to remove unbound ligands samples, the protein is denatured and compounds are identified by the MS.
Time-of-flight secondary-ion mass spectrometry (TOF-SIMS) [102]	Gold Nanoparticles are conjugated to the peptide surface for signal enhancement with a cysteine group attached to maintain protein orientation on the surface. Secondary ion is measured in the MS.
Electrospray ionization MS/MS (ESI-MS/MS) [77, 99]	Substrate and product (+80 Da) signals are monitored through the use of MS/MS.
Frontal affinity chromatography MS (FAC-MS) [103]	Equilibrium established ligand and immobilized kinase. The affinity of the ligand for the target dictates the binding duration. The eluted molecule can be detected by MS analysis which allows for the determination of binding site.
Full-length expressed stable isotope-labeled protein for quantification strategy (FLEXIQinase) [104]	Combines isotope-labelled peptide substrates with typical kinase assays and monitors a shift in signal from substrate to product (+ 80 Da). Provides information about target binding sites.
Immobilized Enzyme Reactor-MS (IMER MS) [105]	Monitors the turnover (phosphorylation or dephosphorylatio) of peptide substrates of an immobilized protein within silica capillary on an ESI-MS instrument.

Ion Mobility MS (IM-MS) [106]	Monitors the protein-ligand complex and the ions produced. Ions are filtered in the first quadrupole by m/z and are separated by the collision cross section with respect to time on a millisecond timescale. Generally used for structure analysis.
Kinase ActivitY Assay for Kinome profiling (KAYAK) [107-108]	Measures the phosphorylation ratio from cell lystates of multiple peptide substrates simultaneously following incubation of SM with cell culture, incubation of the cell lystate with the substrates and desalting.
MALDI- MS [92, 100]	Directly measures substrate and product (+80 Da) signals.
BioTrove RapidFire® Mass Spectrometry (RF-MS) [109]	Couples micro-scale solid-phase extraction with a triple quadrupole mass spectrometer for automated, integrated sample purification and label-free detection.
Structure Assited Matrix Desorption Ionization (SAMDI) [110-111]	Semi-quantitative evaluation of multiple kinase activities from an immobilized peptide substrate on a self-assembled monolayer surface. Monitors substrate and product signals.

Mass spectrometric methods have proven to be invaluable in HTS for kinase drug discovery because of its high selectivity and specificity. However, these approaches typically involve the use of state-of-the art spectrometers. Methods involving inexpensive instrumentation allowing for screening methods to be performed by a larger quantity of people would provide a long-lasting, useful benefit.

Solid Phase Assays utilizing Mass Spectrometry

An alternative method to increasing assay throughput and decreasing assay cost is through the use of bioaffinity chromatography columns. Previously, the use of IMER-MS was found to be a useful method in the screening of small molecules against kinases. [105] However, conventional chromatography columns require linkage of the protein to the inner wall of a fused-silica capillary. Covalent linkage of proteins can result in reduced activity of the target molecule.

The sol-gel process provides another route to protein immobilization without covalent linkage. This is a room-temperature process where a porous matrix is created at a neutral pH, typically through the hydrolysis of a metal alkoxide precursor. The process,

described by Figure 1.6, involves hydrolysis, followed by polycondensation, condensation, and gelation of the desired precursor. [112-119]

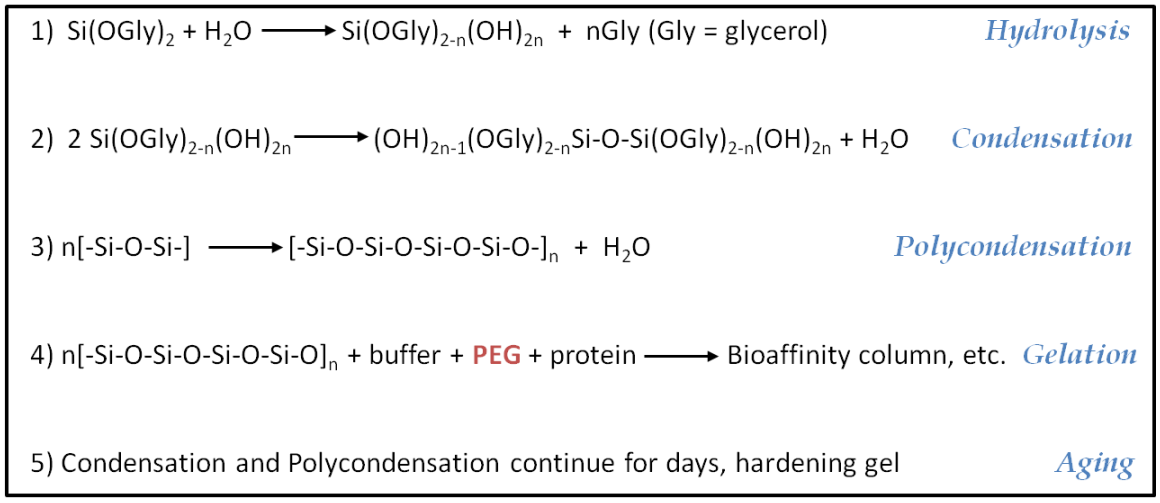

Figure 1.6: Schematic of biofriendly sol-gel processing. [120]

Various metal alkoxides, such as tetramethylorthosilicate (TMOS) and tetraethylorthosilicate (TEOS)[115] have been used as precursors for the sol-gel process. Proteins entrapped within materials derived from the sol-gel process mentioned above, suffer from lack of long-term stability, due to alcohol liberation upon hydrolysis.[113] The development of glycerated silanes, improves the long-term stability in sol-gel derived materials [113, 119, 121-123] through hydrolysis to release glycerol, a protein stabilizer. These glycerated silanes, such as diglycerylsilane (DGS) [119, 123] or poly(glyceryl) silicate (PGS) [124] along with a commercially available precursor, sodium silicate (SS) [112] have shown great utility in facile biofriendly sol-gel processing, enhancing stability for use in bioaffinity and biologically functional based methods. [119] Unfortunately, very little work has been completed involving SS, leading to a need for material development.

Materials can be finely tuned to create a range in porosities from mesopores (2-50 nm) for enhanced surface area and transparency, or macropore formation (>50nm, noted through the presence of phase separation). [125-127] The pore dimensions are easily modified through alteration of buffer pH, type, and concentration, along with inclusion of a variety of additives including polyethylene glycol. For column chromatography, such as IMER, the material porosity is crucial to allow low backpressure while retaining the immobilized protein.[125, 128-129]

Typically column chromatography is coupled to an ESI-MS instrument due to the ease of interfacing this ionization source with liquid chromatography. Since kinases require moderate to high salt concentrations that are incompatible with ESI without the use of sample preparation techniques such as solid-phase extraction, [130] alternative methods are needed. Performing offline reactions with deposition of analytes onto a MALDI sample plate makes this technology a promising approach to MS-based kinase inhibitor screening.

1.4 Thesis Goals and Outline

The current research aims to develop and study kinase screening platforms for the phosphorylation event catalyzed by the bacterial kinase, APH 3′IIIa using MALDI-MS. Chapter 2 discusses the prevalence of antibiotic resistance as it relates to modifying enzymes, specifically APH3'IIIa. The work evaluates the kinetic properties of the enzyme in solution for further use in activity and inhibition studies. The phosphorylation reaction catalyzed by APH3'IIIa requires the use of two co-factors. The presence of

these co-factors in large amounts can hinder the crystallization of the MALDI matrix and as such, the assay requires optimization of such conditions for use with the chosen matrix, CHCA. The first goal of this chapter is to develop a direct screening methodology to examine enzymatic turnover of an antibiotic substrate by APH 3`IIIa, resulting in an inactivated, phosphorylated antibiotic. Furthermore, goals include the validation of the assay and screening of a selection of potential kinase modulators using an atmospheric pressure (AP)- MALDI ion trap MS platform in the presence of difficult reagents such as DMSO. Screening conditions, involving the presence of DMSO, will be assessed to allow mixture screening of a selection of compounds known to interact with the APH3'IIIa in addition to a kinase directed collection.

Chapter 3 expands the work in chapter 2 to multiplexed assays. The second thesis goal is to enhance the previously designed MALDI-MS/MS assay for the presence of two kinase phosphorylation events with simultaneous detection of enzyme activity. The ability to selectively inhibit one kinase while leaving others unaffected is of great importance because a selective inhibitor would reduce cross reactions which lead to unwanted medical side effects. However, kinase substrate promiscuity is a known dilemma due in part to structurally conserved binding pockets and structural similarity, leading to a lack of substrate specificity. The addition of a second kinase will not only allow the study of specificity and selectivity of potential inhibitors, but also provide insight on the potential mechanism of action of these modulators. The goal is to screen two kinases simultaneously against a multitude of potential modulators. Screening of the

same compounds to those in Chapter 2 will allow for further validation of the multiplexed assay.

The discovery of APH modulators can be a long and tedious process. With the increasing emergence of resistant bacteria, rapid methods such as HTS need to be employed. This leads to an additional thesis goal. Chapter 4 will study APH 3`IIIa through the implementation of technological advances including liquid handlers and imaging MALDI-MS (IMS) as a means to increase assay throughput. The use of liquid handlers will increase efficiency and hopefully result in quicker and potentially more accurate dispensing than traditional manual pipetting techniques, allowing a decrease in assay cost and time. By employing the microarray platform, thousands of assays could be performed on a small solid support. The use of microarrays will also create a reduced region for imaging leading to a decrease in time needed for imaging, and reduced laser use, preventing laser burnouts during an experiment. IMS can be used to increase throughput, but also allows for a quick qualitative, detection method through the creation of an image showing increasing colour intensity for a specified ion, simplifying analysis, while also allowing extraction of MS spectra from all imaged regions for quantitative analysis. The main goal of this chapter is to demonstrate a proof of concept model that could be used to screen thousands of potential modulators of APH 3`IIIa and several other kinases for inhibitory effects.

The final goal of this thesis is to study IMER as an alternative screening method, with the hopes of interfacing the technique to a MALDI system. Chapter 6 will identify

an HTS process for the identification of sol-gel derived materials amenable to bioaffinity column chromatography. Through use of a combination of high throughput (opacity), moderate throughput (visual inspection) and low throughput (backpressure, SEM, porosimetry) testing, a process for the identification of optimal materials for HTS will be developed to identify optimal materials. Furthermore, the material can be used in an IMER-MS-based platform.

Lastly, Chapter 6 recapitulates the conclusions of the work discussed and recommends future directions for the extension of this project. Expansion of this work involves the effect of entrapment of APH3'IIIa in the newly synthesized monolithic SS columns with a furtherance to HTS of kinase modulators. Finally, the use of magnetic beads with automation may provide additional benefits in allowing direct identification of kinase modulators directly from the bead surface.

1.5 References

[1] S. A. Johnson, T. Hunter, *Nature Methods* **2005**, *2*, 17-25.

[2] P. Cohen, *Nature Reviews Drug Discovery* **2002**, *1*, 309-315.

[3] P. Hohmann, *International Journal of Cancer* **1989**, *43*, 863-869.

[4] S. S. Taylor, J. A. Buechler, W. Yonemoto, *Annual Review of Biochemistry* **1990**, *59*, 971-1005.

[5] G. Manning, D. B. Whyte, R. Martinez, T. Hunter, S. Sudarsanam, *Science* **2002**, *298*, 1912-1934.

[6] A. L. Hopkins, C. R. Groom, *Nature Reviews Drug Discovery* **2002**, *1*, 727-730.

[7] C. A. Lipinski, F. Lombardo, B. W. Dominy, P. J. Feeney, *Advanced Drug Discovery Reviews* **1997**, *23*, 3-25.

[8] C. M. Dobson, *Nature* **2004**, *432*, 824-828.

[9] G. D. Wright, *Advanced Drug Discovery Reviews* **2005**, *57*, 1451-1470.

[10] G. D. Wright, *Nature Reviews Microbiology* **2007**, *5*, 175-186.

[11] G. D. Wright, *Expert Opinion on Drug Discovery* **2010**, *5*, 779-788.

[12] G. D. Wright, *Chemistry & Biology* **2000**, *7*, R127-R132.

[13] G. D. Wright, *Current Opinion in Microbiology* **1999**, *2*, 499-503.

[14] G. D. Wright, *Current Opinion in Chemical Biology* **2003**, *7*, 563-569.

[15] G. A. McKay, P. R. Thompson, G. D. Wright, *Biochemistry* **1994**, *33*, 6936-6944.

[16] D. A. Leigh, K. Bradnock, J. M. Marriner, *Journal of Antimicrobial Chemotherapy* **1981**, *7*, 229-236.

[17] *Canadian Medical Association Journal* **1985**, *133*, 739.

[18] M. Akova, Y. Yang, D. M. Livermore, *Journal of Antimicrobial Chemotherapy* **1990**, *25*, 199-208.

[19] W.-C. Hon, G. A. McKay, P. R. Thompson, R. M. Sweet, D. S. C. Yang, G. D. Wright, A. M. Berghuis, *Cell* **1997**, *89*, 887-895.

[20] C. Kim, S. Mobashery, *Bioorganic Chemistry* **2005**, *33*, 149-158.

[21] D. H. Fong, A. M. Berghuis, *Embo Journal* **2002**, *21*, 2323-2331.

[22] D. Peisach, P. Gee, C. Kent, Z. Xu, *Structure* **2003**, *11*, 703-713.

[23] A. F. T. Arnsten, B. P. Ramos, S. G. Birnbaum, J. R. Taylor, *TRENDS in Molecular Medicine* **2005**, *11*, 121-127.

[24] B. P. Ramos, S. G. Birnbaum, I. Lindenmayer, S. S. Newton, R. S. Duman, A. F. T. Arnsten, *Neuron* **2003**, *40*, 835-845.

[25] M. A. Owston, E. H. Serpersu, *Biochemistry-Us* **2002**, *41*, 10764-10770.

[26] J. E. Davies, Antibiotics in Laboratory Medicine, 3rd ed. (Ed.: V. Lorian), Williams & Wilkins, Baltimore, **1991**, pp. 691-713.

[27] G. A. McKay, G. D. Wright, *The Journal of Biological Chemistry* **1995**, *270*, 24686-24692.

[28] D. M. Daigle, G. A. McKay, G. D. Wright, *The Journal of Biological Chemistry* **1997**, *272*, 24755-24758.

[29] C. Kim, N.-H. Xuong, S. S. Taylor, *Science* **2005**, *307*, 690-695.

[30] B. E. Kemp, D. J. Graves, E. Benjamini, E. G. Krebs, The *Journal of Biological Chemistry* **1977**, *252*, 4888-4894.

[31] H. Hidaka, M. Inagaki, S. Kawamoto, Y. Sasaki, *Biochemistry* **1984**, *23*, 5036-5041.

[32] J. Major, *Journal of Biomolecular Screening* **1998**, *3*, 13-17.

[33] A. Persidis, *Nat Biotechnology* **1998**, *16*, 488-489.

[34] R. L. Nicholson, M. Welch, M. Ladlow, D. R. Spring, *ACS Chemical Biology* **2007**, *2*, 24-30.

[35] B. Posner, Y. Hong, E. Benvenuti, M. Potchoiba, D. Nettleton, L. Lui, A. Ferrie, F. Lai, Y. Fang, J. Miret, C. Wielis, B. Webb, *Analytical Biochemistry* **2007**, *356*, 266-273.

[36] R.-Q. Liang, C.-Y. Tan, K.-C. Ruan, *Journal of Immunological Methods* **2004**, *285*, 157-163.

[37] B. Quinones, M. S. Swimley, K.-E. Narm, R. N. Patel, M. B. Cooley, R. E. Mandrell, *Frontiers in Cellular and Infection Microbiology* **2012**, *2*, 1-10.

[38] M. R. N. Monton, J. M. Lebert, J. R. L. Little, J. J. Nair, J. McNulty, J. D. Brennan, *Analytical Chemistry* **2010**, *82*, 9365-9373.

[39] A. Asanov, A. Zepeda, L. Vaca, *Sensors* **2012**, *12*, 1800-1815.

[40] L. Yao, K. Y. Yung, R. Khan, V. P. Chodavarapu, F. V. Bright, *IEEE Sensors Journal* **2010**, *10*, 1824-1832.

[41] B. P. Nelson, T. E. Grimsrud, M. R. Liles, R. M. Goodman, R. M. Corn, *Analytical Chemistry* **2001**, *73*, 1-7.

[42] Y. Li, J. Lee, R. M. Corn, *Analytical Chemistry* **2007**, *79*, 1082-1088.

[43] M. Pabst, S. R. Fagerer, R. Kohling, S. K. Kuster, R. Steinhoff, M. Badertscher, F. Wahl, P. S. Dittrich, K. Jefimovs, R. Zenobi, *Analytical Chemistry* **2013**, *85*, 9771-9776.

[44] M. R. Groseclose, P. P. Massion, P. Chaurand, R. M. Caprioli, *Proteomics* **2008**, *8*, 3716-3724.

[45] R. M. Eglen, *ASSAY and Drug Development Technologies* **2002**, *1*, 97-104.

[46] R. I. W. Osmond, S. Das, M. F. Crouch, *Analytical Biochemistry* **2010**, *403*, 94-101.

[47] Y. W. Park, R. T. Cummings, L. Wu, S. Zheng, P. M. Cameron, A. Woods, D. M. Aller, A. I. Marcy, J. D. Hermes, *Analytical Biochemistry* **1999**, *269*, 94-104.

[48] H. Bohm, J. K. H. Petersen-Von Gehr, H. P. Neubauer, F. E. Mehnert, H. P. Jennissen, *Journal of Immunological Methods* **1984**, *70*, 193-209.

[49] E. Engvall, P. Perlmann, *Journal of Immunology* **1972**, *109*, 129-135.

[50] J. R. Lakowicz, Principles of Fluorescence Spectroscopy, 3rd ed., Springer, New York, **2006**.

[51] S. Miraglia, E. E. Swartzman, J. Mellentin-Michelotti, L. Evangelista, C. Smith, I. Gunawan, K. Lohman, E. M. Goldberg, B. Manian, P.-M. Yuan, *Journal of Biomolecular Screening* **1999**, *4*, 193-204.

[52] A. Fowler, D. Swift, E. Longman, A. Acornley, P. Hemsley, D. Murray, J. Unitt, I. Dale, E. Sillivan, M. Coldwell, *Analytical Chemistry* **2002**, *308*, 223-231.

[53] T. C. Turek-Etienne, M. Lei, J. S. Terracciano, E. F. Langsdorf, R. W. Bryant, R. F. Hart, A. C. Horan, *Journal of Biomolecular Screening* **2004**, *9*, 53-61.

[54] W.-G. Zhang, B. Shor, K. Yu, *Protein Expressioin and Purification* **2006**, *46*, 414-420.

[55] J. R. Beasley, D. A. Dunn, T. L. Walker, S. M. Parlato, J. M. Lehrach, D. S. Auld, *Assay and Drug Development Technology* **2003**, *1*, 455-459.

[56] E. M. G. Loomans, A. M. van Doornmalen, J. W. Y. Wat, G. J. R. Zaman, *Assay and Drug Development Technology* **2003**, *1*, 445-453.

[57] *Z'-Lyte™ Kinase Assay Kits. Invitrogen. <<invitrogen.com>>.*

[58] K. Martin, T. H. Steinberg, L. A. Cooley, K. R. Gee, J. M. Beechem, W. F. Patton, *Proteomics* **2003**, *3*, 1244-1255.

[59] T. J. McCauley, M. L. Stanaitis, M. D. Savage, J. Onken, S. Z. Milis, *Journal of the Association for Laboratory Automation* **2003**, *8*, 36-40.

[60] S. Negash, Q. Yao, H. Y. Sun, J. H. Li, D. J. Bigelow, T. C. Squier, *Biochemical Journal* **2000**, *351*, 195-205.

[61] K.-Y. Lin, Y.-H. Uen, *Oncology Letters* **2010**, *1*, 541-547.

[62] K. Kupcho, R. Somberg, B. Bulleit, S. A. Goueli, *Analytical Biochemistry* **2003**, *317*, 210-217.

[63] Y. Li, R. T. Cummings, B. R. Cunningham, Y. Chen, G. Zhou, *Analytical Biochemistry* **2003**, *321*, 151-156.

[64] S.-H. Xiao, E. Farrelly, J. Anzola, D. Crawford, X. Y. Jiao, J. Liu, M. Ayres, S. Li, L. Huang, R. Sharma, F. Kayser, H. Wesche, S. W. Young, *Analytical Biochemistry* **2007**, *367*, 179-189.

[65] N. W. Charter, L. Kauffman, R. Singh, R. M. Eglen, *Journal of Biomolecular Screening* **2006**, *11*, 390-399.

[66] K. Kiianitsa, J. A. Solinger, W.-D. Heyer, *Analytical Biochemistry* **2003**, *321*, 266-271.

[67] A. R. de Boer, T. Letzel, D. A. van Elswijk, H. Lingeman, W. M. A. Niessen, H. Irth, *Analytical Chemistry* **2004**, *76*, 3155-3161.

[68] E. G. Allwood, D. R. Davies, C. Gerrish, B. E. Ellis, G. P. Bolwell, *FEBS Letters* **1999**, *457*, 47-52.

[69] X. Ge, T. L. Sirich, M. K. Beyer, H. Desaire, J. A. Leary, *Analytical Chemistry* **2001**, *73*, 5078-5082.

[70] D. B. Glass, H. C. Cheng, L. Mendemueller, J. Reed, D. A. Walsh, *The Journal of Biological Chemistry* **1989**, *264*, 8802-8810.

[71] J. J. Witt, R. Roskoski, *Analytical Biochemistry* **1975**, *66*, 253-258.

[72] *FlashPlate® Technology. PerkinElmer. <<perkinelmer.ca>>.*

[73] A. El-Aneed, A. Cohen, J. Banoub, *Applied Spectroscopy Reviews* **2009**, *44*, 210-230.

[74] J. B. Fenn, M. Mann, C. K. Meng, S. F. Wong, C. M. Whitehouse, *Mass Spectrometry Reviews* **1990**, *9*, 37-70.

[75] C. G. Enke, *Analytical Chemistry* **1997**, *69*, 4885-4893.

[76] J. R. Yates, *Journal of Mass Spectrometry* **1998**, *33*, 1-19.

[77] I. Partserniak, G. Werstuck, A. Capretta, J. D. Brennan, *Chembiochem* **2008**, *9*, 1065-1073.

[78] F. Rouessac, A. Rouessac, *Chemical Analysis: Modern Instrumentation Methods and Techniques*, 2nd ed., Wiley, Chichester, **2007**.

[79] S. D. Friess, J. M. Daniel, R. Zenobi, *Physical Chemistry Chemical Physics* **2004**, *6*, 2664-2675.

[80] D. A. Skoog, 6 ed., *Principles of Instrumental Analysis*, Thomson Brooks/Cole, Belmont, **2007**.

[81] N. Srinivasan, C. A. Haney, J. S. Lindsey, W. Z. Zhang, B. T. Chait, *Journal of Porphyrins and Phthalocyanines* **1999**, *3*, 283-291.

[82] Z. Guo, Q. C. Zhang, H. F. Zou, B. C. Guo, J. Y. Ni, *Analytical Chemistry* **2002**, *74*, 1637-1641.

[83] J. Wei, J. M. Buriak, G. Siuzdak, *Nature* **1999**, *399*, 243-246.

[84] D. A. Pirman, R. F. Reich, A. Kiss, R. M. A. Heeren, R. A. Yost, *Analytical Chemistry* **2013**, *85*, 1081-1089.

[85] M. Peukert, A. Matros, G. Lattanzio, S. Kaspar, J. Abadia, H.-P. Mock, *New Phytologist* **2012**, *193*, 806-815.

[86] E. J. Zaluzec, D. A. Gage, J. T. Watson, *Protein Expression and Purification* **1995**, *6*, 109-123.

[87] P. Kovarik, R. J. Hodgson, T. Covey, M. A. Brook, J. D. Brennan, *Analytical Chemistry* **2005**, *77*, 3340-3350.

[88] J. J. Corr, P. Kovarik, B. B. Schneider, J. Hendrikse, A. Loboda, T. R. Covey, *Journal of the American Society for Mass Spectrometry* **2006**, *17*, 1129-1141.

[89] J. Gobey, M. Cole, J. Janiszewski, T. Covey, T. Chau, P. Kovarik, J. Corr, *Analytical Chemistry* **2005**, *77*, 5643-5654.

[90] P. Hatsis, S. Brombacher, J. Corr, P. Kovarik, D. A. Volmer, *Rapid Communications in Mass Spectrometry* **2003**, *17*, 2303-2309.

[91] P. Kovarik, C. Grivet, E. Bourgogne, G. Hopfgartner, *Rapid Communications in Mass Spectrometry* **2007**, *21*, 911-919.

[92] R. Rathore, J. Corr, G. Scott, P. Vollmerhaus, K. D. Greis, *Journal of Biomolecular Screening* **2008**, *13*, 1007-1013.

[93] R. Rathore, J. J. Corr, D. T. Lebre, W. L. Seibel, K. D. Greis, *Rapid Communications in Mass Spectrometry* **2009**, *23*, 3293-3300.

[94] L. Sleno, D. A. Volmer, *Rapid Communications in Mass Spectrometry* **2005**, *19*, 1928-1936.

[95] J. J. A. van Kampen, P. C. Burgers, R. de Groot, R. A. Gruters, T. M. Luider, *Mass Spectrometry Reviews* **2011**, *30*, 101-120.

[96] S. Yamaguchi, T. Fujita, T. Fujino, T. Korenaga, *Analytical Sciences* **2008**, *24*, 1497-1500.

[97] I. P. Smirnov, X. Zhu, T. Taylor, Y. Huang, P. Ross, I. A. Papayanopoulos, S. A. Martin, D. J. Pappin, *Analytical Chemistry* **2004**, *76*, 2958-2965.

[98] D. S. Cornett, M. L. Reyzer, P. Chaurand, R. M. Caprioli, *Nature Methods* **2007**, *4*, 828-833.

[99] A. R. de Boer, T. Letzel, H. Lingeman, H. Irth, *Analytical and Bioanalytical Chemistry* **2005**, *381*, 647-655.

[100] H. S. Nam, E. Ban, E. Yoo, Y. S. Yoo, *Journal of Chromatography A* **2002**, *976*, 79-85.

[101] K. M. Comess, J. D. Trumbull, C. Park, Z. H. Chen, R. A. Judge, M. J. Voorbach, M. Coen, L. Gao, H. Tang, P. Kovar, X. H. Cheng, M. E. Schurdak, H. Y. Zhang, T. Sowin, D. J. Burns, *Journal of Biomolecular Screening* **2006**, *11*, 755-764.

[102] Y.-P. Kim, E. Oh, D. W. Moon, T. G. Lee, H.-S. Kim, *Angewandte Chemie* **2007**, *119*, 6940-6943.

[103] J. J. Slon-Usakiewicz, J. R. Dai, W. Ng, J. E. Foster, E. Deretey, L. Toledo-Sherman, P. R. Redden, A. Pasternak, N. Reid, *Analytical Chemistry* **2005**, *77*, 1268-1274.

[104] S. A. Singh, D. Winter, P. M. Bilimoria, A. Bonni, A. Steen, J. A. Steen, *Nature Methods* **2012**, *9*, 504-508.

[105] L. N. Amankwa, K. Harder, F. Jirik, R. Aebersold, *Protein Science* **1995**, *4*, 113-125.

[106] J. N. Rabuck, S.-J. Hyung, K. S. Ko, C. C. Fox, M. B. Soellner, B. T. Ruotolo, *Analytical Chemistry* **2013**, *85*, 6995-7002.

[107] R. C. Kunz, M. F.E., J. Rush, S. P. Gygi, *Analytical Chemistry* **2012**, *84*, 6233-6239.

[108] Y. Yu, R. Anjum, K. Kubota, J. Rush, J. Villen, S. P. Gygi, *Proceedings of the National Academy of Science* **2009**, *106*, 11606-11611.

[109] M. K. Highkin, M. P. Yates, O. V. Nemirovsky, W. A. Lamarr, G. E. Munie, J. W. Rains, J. L. Masferrer, M. M. Nagiec, *Journal of Biomolecular Screening* **2011**, *16*, 272-277.

[110] B. T. Houseman, J. H. Huh, S. J. Kron, M. Mrksich, *Nat Biotechnology* **2002**, *20*, 270-274.

[111] D. H. Min, J. Su, M. Mrksich, *Angewandte Chemie International Edition* **2004**, *43*, 5973-5977.

[112] R. B. Bhatia, C. J. Brinker, A. K. Gupta, A. K. Singh, *Chemistry of Materials* **2000**, *12*, 2434-2441.

[113] J. D. Brennan, *Accounts of Chemical Research* **2007**, *40*, 827-835.

[114] D. Avnir, S. Braun, O. Lev, M. Ottolenghi, *Chemistry of Materials* **1994**, *6*, 1605-1614.

[115] D. Avnir, T. Coradin, O. Lev, J. Livage, *Journal of Materials Chemistry* **2006**, *16*, 1013-1030.

[116] S. Braun, S. Rappoport, R. Zusman, D. Avnir, M. Ottolenghi, *Materials Letters* **1990**, *10*, 1-5.

[117] C. J. Brinker, G. W. Scherer, *Sol-Gel Science: The Physics and Chemistry of Sol-Gel Processing*, Academic Press, New York, **1990**.

[118] M. L. Ferrer, F. del Monte, D. Levy, *Chemistry of Materials* **2002**, *14*, 3619-3621.

[119] M. A. Brook, Y. Chen, K. Guo, Z. Zhang, W. Jin, A. Deisingh, J. Cruz-Aguado, J. D. Brennan, *Journal of Sol-Gel Science and Technology* **2004**, *31*, 343-348.

[120] J. D. Brennan, T. R. Covey, R. J. Hodgson, Y. Chen, Z. Zhang, D. Tleugabulova, X. Zhao, M. Organ, M. A. Brook, P. Kovarik, in *American Society for Mass Spectrometry*, Nashville, Tennessee, **2004**.

[121] J. D. Brennan, *Applied Spectroscopy* **1999**, *53*, 106a-121a.

[122] J. D. Brennan, D. Benjamin, E. DiBattista, M. D. Gulcev, *Chemistry of Materials* **2003**, *15*, 737-745.

[123] M. A. Brook, Y. Chen, K. Guo, Z. Zhang, J. D. Brennan, *Journal of Materials Chemistry* **2004**, *14*, 1469-1479.

[124] I. Gill, A. Ballesteros, *Journal of the American Chemical Society* **1998**, *120*, 8587-8598.

[125] T. R. Besanger, R. J. Hodgson, D. Guillon, J. D. Brennan, *Analytica Chimica Acta* **2006**, *561*, 107-118.

[126] R. J. Hodgson, Y. Chen, Z. Zhang, D. Tleugabulova, H. Long, X. M. Zhao, M. Organ, M. A. Brook, J. D. Brennan, *Analytical Chemistry* **2004**, *76*, 2780-2790.

[127] J. Rouquerol, D. Avnir, C. W. Fairbridge, D. H. Everett, J. H. Haynes, N. Pernicone, J. D. F. Ramsay, K. S. W. Sing, K. K. Unger, *Pure and Applied Chemistry* **1994**, *66*, 1739-1758.

[128] T. R. Besanger, R. J. Hodgson, J. R. A. Green, J. D. Brennan, *Analytica Chimica Acta* **2006**, *564*, 106-115.

[129] R. J. Hodgson, T. R. Besanger, M. A. Brook, J. D. Brennan, *Analytical Chemistry* **2005**, *77*, 7512-7519.

[130] J. M. Moreno, A. Wojnicz, J. L. Steegman, M. F. Cano-Abad, A. Ruiz-Nuno, *Biomedical Chromatography* **2013**, *27*, 502-508.

Chapter 2 : A Matrix-Assisted Laser Desorption/Ionization Tandem Mass Spectrometry Method for Direct Screening of Small Molecule Mixtures Against an Aminoglycoside Kinase

Author's Preface:

The following chapter was published as a full paper in the journal Analytica Chimica Acta under the citation:

Anne Marie E. Smith, Emelia Awuah, Alfredo Capretta, John D. Brennan, **A Matrix-Assisted Laser Desorption/Ionization Tandem Mass Spectrometry Method for Direct Screening of Small Molecule Mixtures Against an Aminoglycoside Kinase,** *Analytica Chimica Acta*. **2013**, 786, 103-110.

I was responsible for the experimental design, and performance of said experiments, data analysis and interpretation. Emelia Awuah synthesized the compounds for screening under the supervision of Dr. Capretta. I wrote the first draft of the manuscript and Dr. Brennan provided editorial input to generate the final draft for submission.

2.1 Abstract

Aminoglycoside phosphotransferase 3′IIIa (APH3′IIIa) is a bacterial enzyme involved in antibiotic resistance through phosphorylation of aminoglycosides, which can potentially be overcome by co-administration of an APH3′IIIa inhibitor with the antibiotic. Current assay methods for discovery of APH3′IIIa inhibitors suffer from low specificity and high false positive/negative hit rates. Here, we describe a method for screening APH3′IIIa inhibitors based on direct detection of kanamycin A phosphorylation using MALDI-MS/MS, which is more rapid than conventional assays and does not require secondary assays or sample cleanup. The MALDI-MS/MS assay operates at an ionic strength of 45 mM and co-factors can be utilized at near-physiological levels for optimal enzyme activity. Detection via MALDI-MS/MS allowed for improved reproducibility when compared to ESI-MS/MS. Furthermore, the use of MS/MS provided better signal-to-noise ratios relative to MS alone on the MALDI instrument. The assay was validated via generation of Z'-factors, with values of 0.78 and 0.56 in the absence and presence of 0.2 % DMSO, respectively. The assay was used to screen a kinase directed library of >200 compounds, assayed as 21 mixtures of 10 compounds each. Five novel synthetic inhibitors were identified following mixture deconvolution. Inhibition constants were obtained for the aforementioned inhibitors using the MALDI-MS/MS assay, revealing several low to mid micromolar "hits", and highlighting the quantitative nature of the assay.

Keywords. aminoglycoside phosphotransferase, antibiotic resistance, inhibition, matrix assisted laser desorption/ionization, small molecule screening.

2.2 Introduction

Aminoglycosides are frequently used in the treatment of bacterial infections [1]. However, the proliferation of these antibiotics in hospitals, and their natural occurrence, has led to a rapid increase in antibiotic resistance in both gram positive and gram negative bacteria [2]. Resistance to aminoglycosides occurs through a variety of mechanisms, one of which is the expression of modifying enzymes, which catalyze reactions that phosphorylate, adenylate or acetylate the antibiotic substrate, rendering it inactive [1-5]. While there is no way to prevent the emergence of antibiotic resistance, there are currently three proposed methods for delaying the onset of bacterial resistance mechanisms. The first is the development of new antibiotics that are not substrates for modifying enzymes. However, due to the slow rate of development of novel antibiotics in the last several decades, this is not a promising method [2,3]. The second is to synthetically modify currently successful antibiotics. However, even when successful, resistance to such modified antibiotics is likely to develop over time [2,3]. Consequently, the most promising method to treat resistance is through the use of small molecules that inhibit the modifying enzymes, which results in the retention of antibiotic activity. Small molecules that inhibit modifying enzymes may be co-administered with the antibiotic to hinder resistance [1,2] and this method has been successfully used in approved pharmaceuticals such as Clavulin (β-lactamase inhibitor and antibiotic) [6].

Aminoglycoside phosphotransferases (APH's) are a family of enzymes that phosphorylate aminoglycoside antibiotics. The modifying enzyme APH3′IIIa, which catalyzes the transfer of a phosphate group from the γ-phosphate of the co-factor adenosine triphosphate (ATP) to the hydroxyl group at position 3 of the 2,4-disubstituted

antibiotic kanamycin A (Figure 2.1A), is an attractive target for development of inhibitory drugs. However, because this reaction product is a small molecule, there are a limited number of assays available for detecting the phosphorylation event. The most typical method involves a coupled reaction using pyruvate kinase/lactate dehydrogenase (PK/LDH), phosphoenolpyruvate (PEP) and nicotinamide adenine dinucleotide (NADH) to produce a colorimetric product from the ADP produced in the APH reaction [7]. Unfortunately, this method suffers from a long analysis time (30 min) [7], high levels of error [8] due to secondary reactions and a need to screen hits against the secondary reaction to confirm activity, which decreases throughput. Other methods to detect phosphorylation reactions (mostly utilizing protein or peptide substrates) include fluorescence [9], radioactivity-based methods [10-13] and mass-spectrometry-based methods [14-16]. Typical fluorescence methods are not commonly used for small molecule products, while radioactivity-based methods suffer from safe disposal issues and an inability to efficiently label all atoms of interest. Most MS methods use electrospray ionization (ESI), and thus are not compatible with high salt and co-factor (Mg^{2+}) concentrations, which are often needed to promote product formation in phosphorylation reactions. Use of low salt concentrations is possible in some cases [14,15], but is not generally applicable to all phosphotransferases. In addition, most ESI methods are not able to tolerate high levels of DMSO [15,17], which is often used to store compounds used in screening [18].

To overcome issues with the need for high ionic strength and DMSO, and to provide faster analysis times, methods such as desorption electrospray ionization (DESI) [19],

ballistic chromatography [20,21] or matrix assisted laser desorption/ionization tandem mass spectrometry (MALDI-MS/MS) can be utilized. Herein, we show the development of an assay based on MALDI-MS/MS. This platform has an advantage that it could eventually be developed into a microarray platform for increased high-throughput [22]. This method is more tolerant to salt and DMSO and presents many advantages relative to typical ESI-MS/MS methods [23-29]. In the last decade several reports of quantitative small molecule MALDI-MS/MS have emerged, typically interfaced to triple quadrupole instruments [23-29], and frequently using a ratio of product-to-substrate [23,28,29] in place of internal standards for quantification, as these can have more similar ionization efficiencies, and tandem MS to reduce background signals caused by the MALDI matrix, which is critical when using MALDI for analysis of small molecules.

Herein, we describe the development and validation of a quantitative assay using MALDI interfaced to an ion trap mass spectrometer that is amenable to screening of small molecules in reactions in which high salt concentrations are required for enzyme activity. In particular, APH3′IIIa is screened in a quantitative manner through the use of atmospheric pressure (AP) MALDI-MS/MS to increase throughput and minimize time-consuming sample preparation procedures. Tandem MS was also used to assess the potency of identified inhibitors through generation of IC_{50} and K_I values.

2.3 Experimental

Materials

APH3′IIIa was expressed in an *E. coli* host and purified as described by McKay *et al.* with minor modifications [5] (see Supporting Information Figure S2.1). Fluorescein, α-cyanohydroxycinnamic acid (CHCA), adenosine 5'-triphosphate (ATP), magnesium acetate (MgOAc), ammonium acetate (NH_4OAc), tobramycin and kanamycin sulfate (major component A, minor components B and C), were purchased from Sigma Aldrich (Oakville, ON). Compounds for screening assays were synthesized by the Capretta Laboratory (McMaster University, Hamilton, ON) [30] while others were commercially available (Sigma Aldrich, Oakville, ON). All water was distilled and deionized (25 °C, 18.2 MΩ·cm, 1-5 ppb total organic content). All other reagents were of analytical grade and were used as received.

Methods

APH3'IIIa Assay Conditions.

All assays were performed by pre-incubation of the enzyme with co-factors for 5 minutes at 37 °C, followed by initiating reactions by addition of kanamycin (prepared in 9.2 mM NH_4OAc, pH 7.5) and incubation for 15 minutes at 37 °C, final assay conditions were: 150 µM ATP (prepared in 9.2 mM NH_4OAc, pH 7.5) , 0.25 mg mL^{-1} APH3′IIIa (stored in 0.85 mM Tris buffer with 17 mM NaCl and 17 µM EDTA), 58 µM kanamycin, 4.6 mM MgOAc and 9.2 mM NH_4OAC pH 7.5. Reactions were quenched by adding an equal volume of matrix solution (6.2 mg mL^{-1} CHCA in methanol containing 1 % acetic acid and 1 µM fluorescein as a secondary internal standard; fluorescein 333 *m/z* signal

compared to 485 *m/z* signal and 565 *m/z* signal on daily basis) to the assay solution. All data was expressed as conversion to product (%P =100 (P/P+S)).

Spotting of Analytes.

The analyte/matrix solution (2 µL) was spotted onto an ABI-100 stainless steel MALDI plate. The plate was placed on top of the incubator (37 °C) used for reactions for approximately 10 minutes or until the spot was visibly dry (Figure S2.2). For samples containing DMSO, a method to increase the matrix tolerance involving matrix seeding was used with modifications [31-34], wherein 2 µL of a 50:50 mixture of matrix:H_2O was spotted onto the ABI-100 stainless steel MALDI plate and allowed to dry prior to overspotting with a 50:50 mixture of matrix:analyte solution. The two-step matrix application method allows for more reproducible crystallization.

Detection of Product and Substrate – Optimization of MALDI Conditions.

A Thermo Finnigan LCQ DECA interfaced with an AP-MALDI source from MassTech (Columbia, MD) was used for MALDI-MS/MS assays. Product and substrate signals were obtained for a sample of kanamycin and a reaction that was left for 15 minutes to allow adequate phosphorylation of the substrate. The ion trap MS was run in selected reaction monitoring (SRM) mode using the following parameters for mass-to-charge ratio (*m/z*) and collision energy (CE): kanamycin (485 *m/z*→324 *m/z*, CE 24 eV, glycosidic oxygen cleavage), phosphorylated kanamycin (565 *m/z*→404 *m/z*, CE 26 eV, glycosidic oxygen cleavage), fluorescein (333 *m/z*→315 *m/z*, CE 56 eV). Ionization was achieved

using a 355 nm Nd:YAG laser with a frequency of 50 Hz and energy of 30 J corresponding to 1200 laser shots per sample upon firing of the laser for 24 seconds. Furthermore, parameters in the instrument software were desorption time = 24 seconds and delay time = 90 seconds (to reduce background by allowing for a reduction of unwanted ions and adsorbed semi-volatiles within the trap), with the system operated in internal timing mode (see spectra in Figures 2.1B-E).

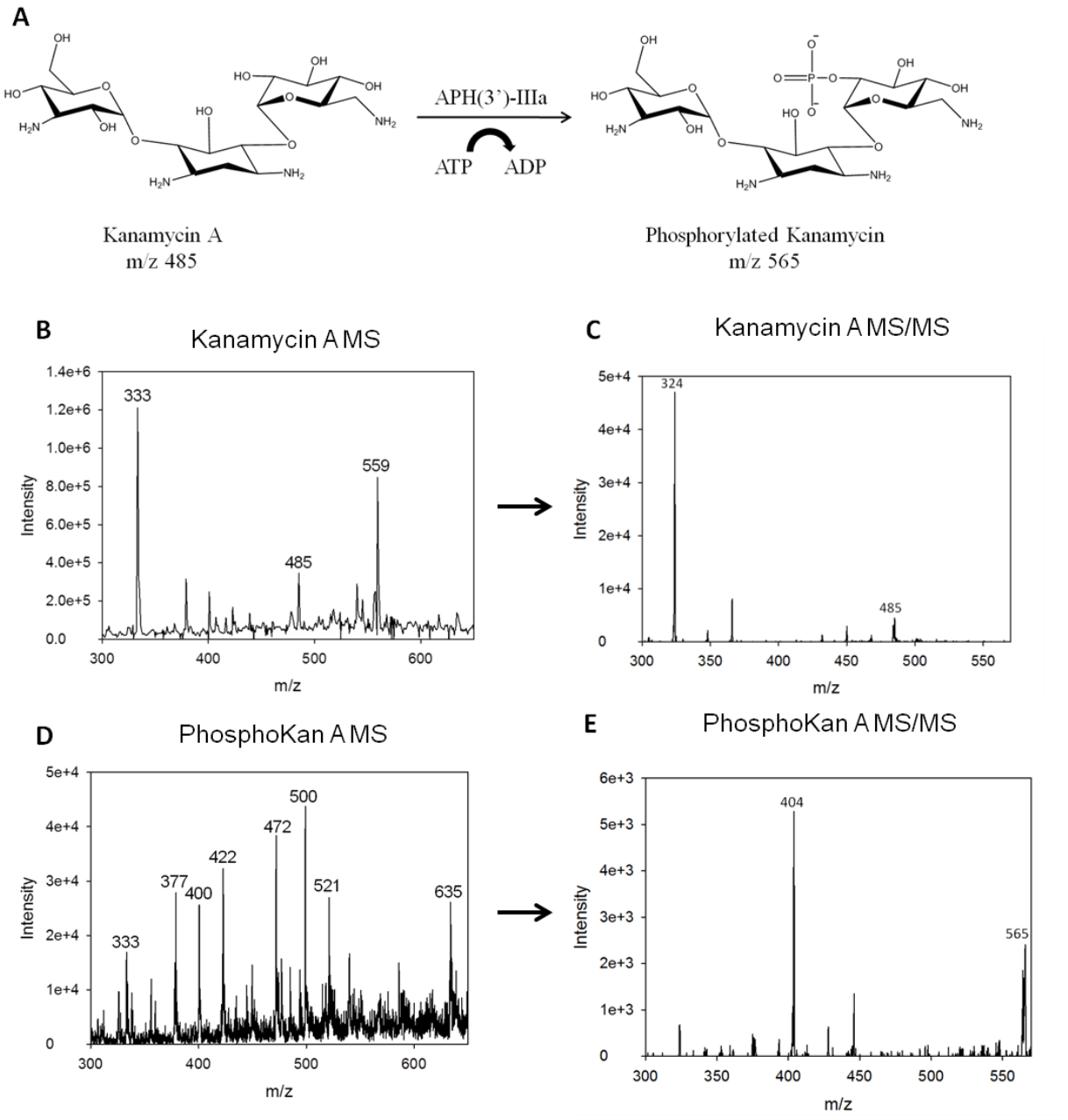

Figure 2.1**:** A) Phosphorylation reaction of Kanamycin A, catalyzed by APH3′IIIa in the presence of co-factors ATP and Mg^{2+}. Detection of MS→MS/MS transitions for B→C) Kanamycin A (500 µM) *m/z* 485→324 and D→E) phosphorylated kanamycin (15 minute reaction at 37ºC, 58 µM Kanamycin, 150 µM ATP, 0.25 mg mL^{-1} APH3′IIIa, 9.2 mM NH_4OAc pH 7.5, 4.6 mM MgOAc pH 7.5) *m/z* 565→404, obtained on an AP-MALDI ion trap MS.

The instrument response of both kanamycin and phosphorylated kanamycin were verified with construction of calibration curves with R^2 values of 0.95 or greater. The kanamycin calibration curve (Figure S2.3A) was obtained by varying concentrations of substrate (0-116 µM) and measuring the response of the instrument (intensity of 485 *m/z*→324 *m/z*). The phosphorylated kanamycin calibration curve (Figure S2.3B) was obtained by varying concentrations of substrate (0-116 µM); and as a result the concentration of phosphorylated kanamycin, performing the reaction under conditions outlined above and measuring the response of the instrument (intensity of 565 *m/z*→404 *m/z*).

ESI-MS/MS.

A Thermo Scientific LCQ FLEET interfaced with an ESI probe in Max-S API source housing and a 10 µL sample loop of 250 μm i.d. (3-aminopropyl)-triethoxysilane (APTES)-coated fused silica capillary was used for sample injections in comparison studies. A flow rate of 15 µL/min was used for all sample injections with a mobile phase of 0.5% acetic acid in 50:50 MeOH:H_2O. Product and substrate signals were tuned on a sample of kanamycin (500 µM) and a reaction left for one hour to allow adequate phosphorylation. SRM transitions were optimized for kanamycin (485 *m/z*→ 324 *m/z*, CE 25 eV) and phosphorylated kanamycin (565 *m/z*→404 *m/z*, CE 28 eV).

APH3'IIIa Assay Validation by MALDI-MS/MS.

Enzyme activity was monitored using the optimized reagent concentrations outlined above (with enzyme stored in 0.85 mM Tris buffer with 17 mM NaCl and 17 μM EDTA) with pre-incubation, incubation and quenching performed as before. Samples (2 μL), consisting of ten high controls (HC, presence of enzyme) and 10 low controls (LC, lack of enzyme) were spotted onto the MALDI plate and analyzed as noted above to obtain %P ratios. Three blank samples were run between high and low samples to ensure sufficient removal of ions from the ion trap and prevent carryover signals. In the presence of 0.2% DMSO (as used in mixture screening), the modified seeding method for matrix crystallization was used to ensure good crystallization of matrix and increase assay reproducibility [33,34].

Ten HC and ten LC samples were included in the Z' assays. The Z' factor was calculated using equation (1) [35]: $Z' = 1-[3(\sigma_{HC}+\sigma_{LC})/(\mu_{HC}-\mu_{LC})]$, where μ_H and μ_L are the average signal of the high and low controls, respectively, and σ_H and σ_L are the standard deviation of the high and low control samples, respectively.

Assay Validation by ESI-MS/MS.

Reactions were performed as before, but were quenched with an equal volume of MeOH. Product and substrate signals were monitored in SRM mode as described above and ten high and low controls were included in the Z' assay.

Mixture Screening.
A total of 207 compounds were obtained as 50 mM stocks in DMSO. Compounds were randomly combined into 21 mixtures of 10 compounds each and diluted in assay buffer to achieve an assay concentration of 10 μM of each compound present in 0.2% (v/v) DMSO. Each mixture was pre-incubated with the enzyme and co-factors for 5 minutes at 37 °C prior to the addition of kanamycin (58 μM) and incubated for 15 minutes before quenching of the reaction. Three controls were included in the mixture screen: two low controls, one containing a known inhibitor, tobramycin (10 μM) within a mixture, and one containing no enzyme, and a high control containing no inhibitory compound. Activity was monitored by MALDI-MS/MS through the conversion to %P.

Mixture Deconvolution.
Identification of active compounds was done for any mixtures that decreased activity by 50% or more in the original duplicate plot. This was done by screening each compound individually at a concentration of 10 μM, using a reduced DMSO concentration of 0.02% (v/v). The compound(s) responsible for inhibition were identified based on their ability to reduce the activity of APH3′IIIa by a minimum of 50%.

IC50 and KI Determination of Potential Inhibitors of APH3'IIIa.
IC_{50} curves were obtained for compounds that were found to reduce the activity of the enzyme by 50% or more when screened at a concentration of 10 μM. Curves were obtained by performing the assay over a concentration range of 0 to 100 μM of the inhibitory compound in 0.2% DMSO. Curves were fit using the four parameter Hill

equation in SigmaPlot 11.0.[36,37] IC_{50} values were obtained from the point where the relative activity was decreased by 50%. The inhibition constant (K_I) was determined from the IC_{50} value using equation (2), as described by Cheng and Prusoff [38]: $K_I = IC_{50}/(1+[S]/K_M)$, where [S] is the concentration of substrate and K_M is the Michaelis constant.

2.4 Results and Discussion

APH3′IIIa Assay for MALDI-MS/MS Analysis.

The activity of APH3′IIIa is highly dependent on the presence of two co-factors, ATP and Mg(II). To maximize signal levels, enzyme activity was measured through the use of an AP-MALDI ion trap system allowing for the presence of an increased ionic strength (45 mM) in comparison to the maximum ionic strength tolerated when using an instrument with an ESI source (~10 mM when using non-volatile salts [15]). Previous studies have shown that the non-volatile component (Mg^{2+}) is particularly detrimental to the signal level obtained on ESI instruments, even at levels as low as 0.8 mM [15].

The use of MALDI-MS/MS was chosen due to an increased signal-to-noise (S/N) relative to typical MALDI-MS systems. Figure 2.1B-E shows the spectra of Kanamycin A and phosphokanamycin when obtained in both MS and MS/MS modes. When observing a range of ± 3 mass units of the ion of interest, the S/N increased more than 10 times upon implementing the MS/MS operation (4→16 for Kanamycin and 1→5 for PhosphoKanamycin). The data suggests that MS could be used in cases where MS/MS

was not available, however it would have poorer reproducibility. As a result, all further assays in this study utilized MS/MS detection.

Validation of assay.

Typically, MALDI-MS is not ideally suited for acquiring quantitative data, although incorporation of suitable internal standards or, as in our case, the use of a ratio of signals, can overcome this issue. To examine the ability to quantitatively determine %P signal ratios in a reproducible manner, the AP-MALDI-MS/MS was operated with a set internal integration time and delay time (to reduce background signals) and %P ratios from ten separate high and low controls were obtained and integrated over 24 s, resulting in signals similar to injection peaks. The use of an enzyme concentration low enough to result in ~10% turnover, as is typically used for determination of k_{cat} and K_M values, did not produce a sufficient difference in MS/MS signals to allow for screening, and indeed produced a Z′-factor of close to 0. Thus, a higher concentration of enzyme (0.25 mg mL^{-1}), resulting in a product signal of ~ 80% was used for all experiments, in accordance with previous MS based asays [39]. Using such conditions, we were able to obtain a Z′-factor of 0.78, corresponding to an "excellent" assay (Figure 2.2A). Excellent assays are characterized by both a large gap between positive and negative samples and a relatively low degree of deviation between replicate samples. Although ten high and low samples is the minimum number for generating a reliable Z′-factor, this has been shown to be successful in other screening assays [15,40].

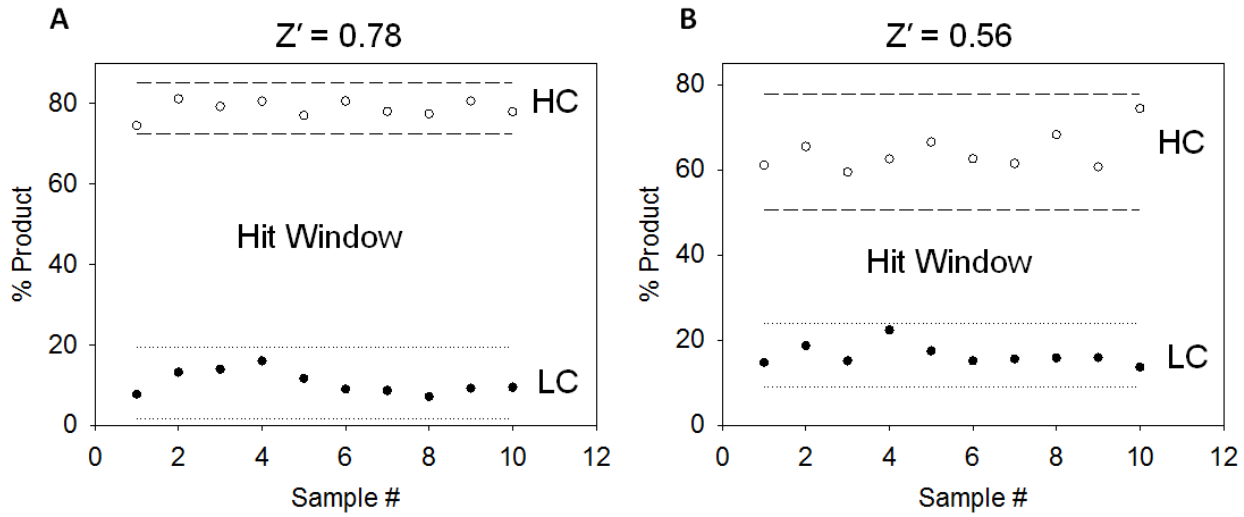

Figure 2.2: Z′-plot for the APH3′IIIa assay (15 minute reaction at 37ºC, 58 µM Kanamycin, 150 µM ATP, 0.25 mg mL^{-1} APH3′IIIa, 9.2 mM NH_4OAc and 4.6 mM MgOAc pH 7.5) using AP-MALDI-MS detection in the presence of (HC ○) and absence of (LC ●) APH 3′IIIa. Dashed lines represent 3 standard deviations of the mean for each control. A) 0 % DMSO, Z'-factor = 0.78 and B) 0.2 % DMSO, Z'- factor = 0.56.

An important aspect of using MALDI for small molecule screening is the ability to tolerate DMSO, which is the standard solvent used for storing compound libraries. For this reason, the assay was also validated in the presence of 0.2% DMSO, which greatly affects the matrix crystallization and thus ionization and assay reproducibility owing to the low volatility and solubilizing nature of the solvent. A somewhat lower Z′-factor of 0.56 was obtained in the presence of DMSO, which still corresponds to an "excellent" assay with a valid "hit window" for screening studies (Figure 2.2B). The primary cause of the reduction in the Z′-factor was a slightly reduced gap between positive and negative controls and somewhat higher noise between replicates, suggesting that DMSO may not affect the enzymatic reaction, but more so the matrix crystallization and ionization process for the APH3'IIIa system, as anticipated.

A particularly strong argument for the use of MALDI in the screening of small molecules was that an acceptable Z′-factor could not be obtained in the presence of 0.2% DMSO with the buffer conditions outlined above (45 mM ionic strength) when using an ESI-MS/MS instrument (Figure S2.4, Z′-factor = 0.25), indicating poor reproducibility. Under such assay conditions, the spray current climbed significantly, making the spray erratic and the signals highly irreproducible, as has been reported previously [41]. In addition, signals could only be acquired for a short time before there was clogging of the ESI needle, as noted by the decrease in convectron gauge pressure (dropping from 1.2 Torr to 0.9 Torr) and a complete lack of ion current at the detector. To overcome these issues additional post-assay sample clean up steps would be required, which would drastically reduce assay throughput.

Mixture Screening.

The AP-MALDI-MS/MS assay was used for the screening of small molecule modulators of the APH3′IIIa catalyzed phosphorylation of kanamycin. We utilized a previously published method that utilized screening of compound mixtures followed by mixture deconvolution as a way of reducing the total number of assays needed to identify hits [17,42]. The data from two independent assays involving a screen of 21 mixtures comprising a total of two hundred and seven synthetic and known kinase inhibitory compounds was expressed as a %P ratio to provide a measure of relative enzyme activity, as shown in the duplicate plot in Figure 2.3A. Compounds were screened at a final concentration of 10 μM to reduce DMSO concentration and still allow for identification

of moderately potent inhibitors. The plot shows relatively good agreement between the two screens as illustrated by the diagonal correlation and an R^2 of 0.74, indicating good reproducibility. While there is a slight offset between the two plots, upon screening as discrete compounds, an excellent agreement is seen, illustrating that valid hits can still be obtained from screening in mixtures, and that the slight offset may be an artifact of screening in mixtures. An additional control was included within one mixture, which contained the known inhibitor, tobramycin (K_I = 2 μM) [5], to ensure that both assays reported significant reductions in enzyme activity when this mixture was assayed. Using 10 compounds per mixture, along with the short analysis time (24 seconds per mixture with a delay of 90 seconds between spots) provided a throughput of one compound every 11.4 seconds (not considering deconvolution or reaction time), almost five times faster than was obtained in similar ESI-MS studies [17]. If screening of all compounds were to be done as discrete molecules, a total of 418 assays (including controls) would have needed to be run compared to 144 assays when using mixtures, including deconvolution, a decrease in analysis time of ~65%. Throughput of the assay could potentially be increased by increasing the mixture complexity to 20 or more compounds, reducing analysis and assay times [17,40], or by replacing DMSO with a solvent that was more suitable for mass spectrometry, to allow far higher numbers of compounds per mixture. Increasing mixture complexity to 20 compounds per mixture would reduce total time (assay, drying and analysis) to ~80 minutes, allowing a throughput of one compound every 26 seconds (not including deconvolution). However, the use of a directed library

results in a high hit rate and, with the goal of minimizing the number of mixtures requiring deconvolution, fewer compounds per mixture is desirable.

As shown in Figure 2.3A, a total of four mixtures were found to produce a reduction in enzyme activity of 50% or greater (in addition to the tobramycin control mixture), which were designated as "hits" in our assay, resulting in a relatively high "hit rate" of 19% for the mixtures (4 of the 21 mixtures, including the control mixture). Such a high hit rate is not common, but in our case is likely due to the use of a kinase directed library rather than a random selection of compounds. Screening of these compounds using discrete compounds would result in a hit rate of ~ 3 % (5 hits in 207 compounds, not including the control compounds).

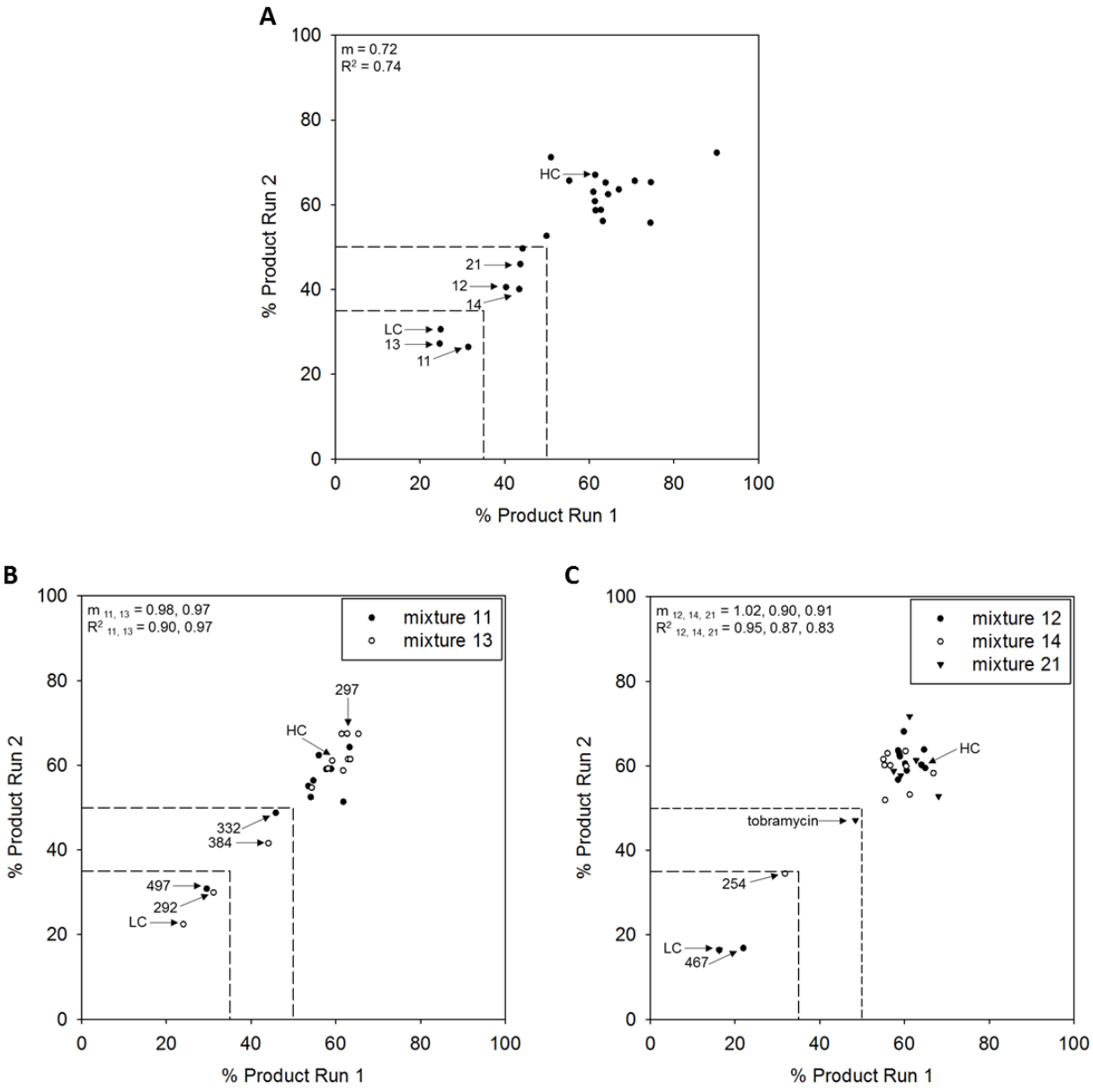

Figure 2.3: (A) Mixture Screen duplicate plot of 207 synthetic compounds (assay concentration of 10 µM each in 0.2 % (v/v) DMSO) from a kinase directed library in addition to few known kinase inhibitors performed on the AP-MALDI ion trap. (B-C) Mixture deconvolution of mixtures 11-14 and 21, those exhibiting a minimum of 50% inhibition. Slope (m) and R^2 values for mixtures illustrate good agreement between plots.

Identification of Inhibitors of APH3′IIIa.

Identification of compounds was done by rescreening each of the 10 compounds present in each of the four "hit" mixtures and the control mixture (47 assays in total, run in duplicate, Figures 2.3B and 2.3C). Through this method of deconvolution, a total of five compounds (in addition to tobramycin, and a previously added blind control) were found to inhibit APH3′IIIa at a concentration of 10 μM, using a value of 50% inhibition (50% residual activity), resulting in a hit rate of nearly 3% for the 207 compounds if screened as discrete compounds. The compounds found to inhibit APH3′IIIa were all synthetic compounds based on an isoquinoline framework, denoted as EME 254 (mixture 14), EME 292 (mixture 13), EME 384 (mixture 13), EME 467 (mixture 12) and EME 497 (mixture 11) (see Figure 2.4 for structures). No other compounds from the 200 remaining members of the kinase directed library were identified as "hits", possibly due to the low concentration used in the assays or the fact that APH3′IIIa is not a protein kinase, but a kinase-like protein and thus may not be strongly inhibited by compounds that typically inhibit protein kinases.

Potency of Inhibitors of APH3′IIIa.

Binding isotherms (Figures 2.4A-E) were generated over a wide range of concentrations for each of the "hits" to further assess the potency of the compounds identified and as a starting point for identifying structural elements that were important for providing inhibition. The curves were analyzed to produce IC_{50} values for each compound, which were then used to determine K_I's using the Cheng-Prusoff equation (2) and a literature K_M value (12.6 μM) [5]. The IC_{50} curves, corresponding K_I values and Hill slopes are

provided in Figure 2.4. All Hill slopes are negative and most are close to -1, indicating a decrease in relative instrument response with increasing concentration of inhibitor and an obtainable inflection point (IC_{50} value). It is expected that all Hill slopes would be -1 due to non co-operative binding. As illustrated in Figure 2.4B, a Hill slope of -0.5 was obtained for EME 292 due to the absence of a plateau at high concentrations of inhibitor, resulting in an inability to obtain an accurate IC_{50} and K_I value. This was also the case for EME 254. Comparing the K_I values and the structures, a qualitative structure-activity relationship can be formulated. The most important structural element within the small series of isoquinolines appears to be the ketone group between ring structures, which is necessary for obtaining single digit micromolar inhibition constants (see Figure 2.4C-E). Compounds lacking the ketone functionality, such as the substituted isoquinoline in Figure 2.4A and the tetrahydroisoquinoline compound shown in Figure 2.4F, exhibit a mid-micromolar inhibition constant and no inhibitory activity, respectively.

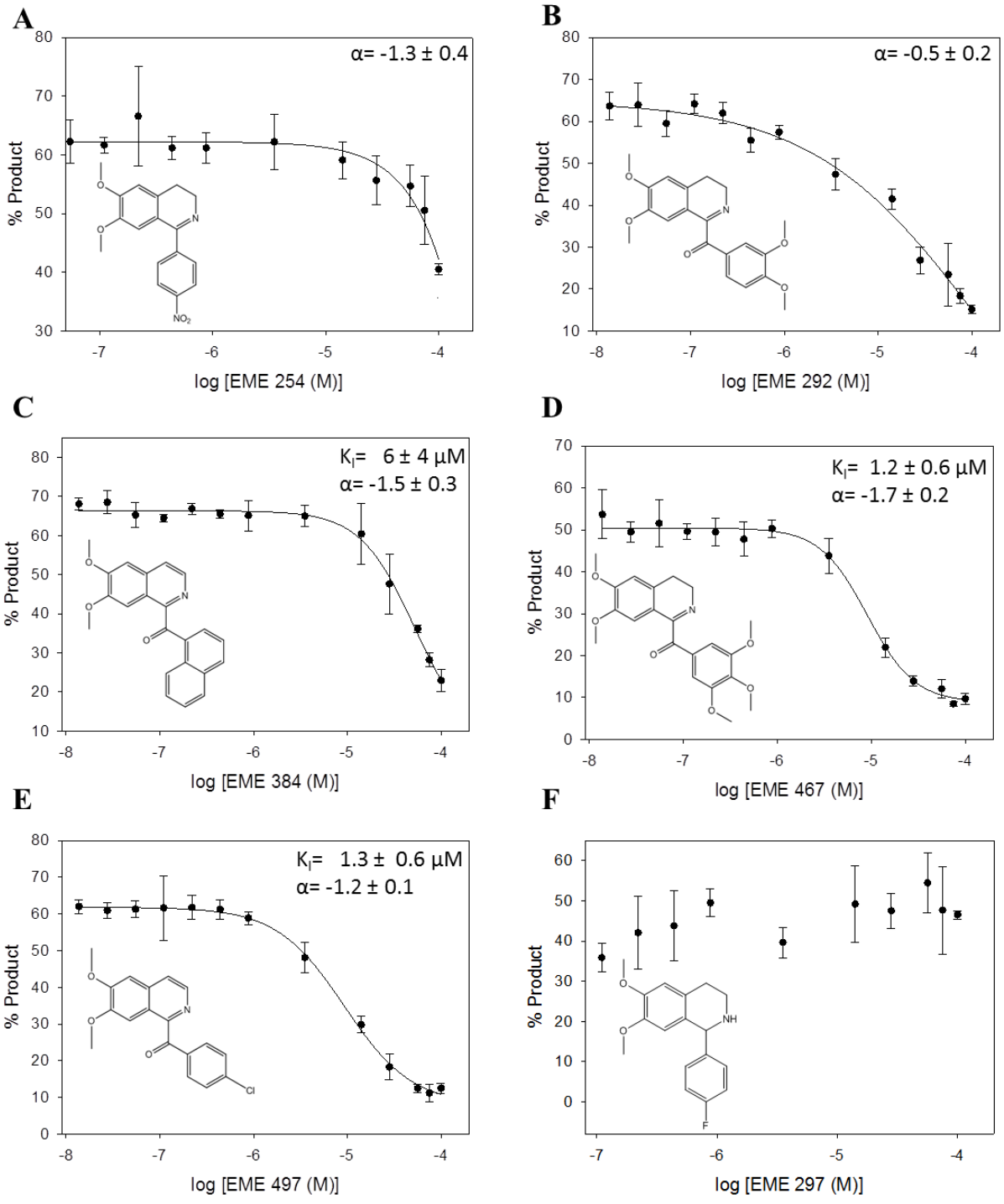

Figure 2.4: (A-E) Dose-dependent response curves, potency and structure of compounds found to inhibit APH3′IIIa at 10 µM. (F) A related compound showing no inhibition towards APH3′IIIa, as determined by no reduction in signal in duplicate plots and in potential dose-response curve.

As a control to ensure the accuracy of our K_I values, we also determined the K_I value for the known inhibitor tobramycin using the AP-MALDI-MS/MS assay, and obtained a value of 0.3 ± 0.1 μM (see Supporting Information Figure S2.5), which was in relatively good agreement with the literature value of 2 μM [5]. It was originally anticipated that the inhibitory compounds identified in our assays would have K_I values less than that of tobramycin, based on the lower %P value obtained in the initial screen (see Figure 2.3A). However, this was not the case, and suggests that synergistic, anti-synergistic or additive effects obtained from screening of mixtures may have lead to variations in %P ratios that altered the relative activity. Owing to targeting of the same active site, it is most likely that additive effects are the source of the difference, This hypothesis is supported by data obtained from a blind study, wherein the supplier of the compounds deliberately labelled one compound with two names (EME 254 or 332). The compound was placed in two different mixtures (EME 254 in mixture 14 and EME 332 in mixture 11) and was found to reduce the activity by different amounts in each of the mixtures (ca. 40% activity for mixture 14 and 35% activity for mixture 11, Figure 2.3A), which while the 5% difference is statistically insignificant, it suggests an effect from surrounding compounds.

2.5 Conclusions

Overall, the data shows that AP-MALDI-MS/MS is useful for direct detection of phosphorylation reactions involving small molecules such as antibiotics. The use of MALDI allows for an increase in salt concentration, including non-volatile components such as co-factors, in reaction samples, which provides a significant enhancement in

enzyme activity relative to low ionic strength assay conditions needed for ESI-MS. The optimization of assay conditions allowed for the validation of the assay (Z'-factor = 0.78 and 0.56 for 0% and 0.2% (v/v) DMSO respectively), making it amenable to screening of standard compound libraries in a high throughput manner. Following the screening of >200 synthetic compounds from a kinase directed library, in addition to known kinase inhibitors, five newly synthesized isoquinoline-based synthetic compounds were identified that inhibited APH3′IIIa. IC_{50} values were quantitatively determined for each compound using the MALDI-MS/MS assay, providing values in the low to mid-micromolar range. Further studies will work towards increasing the throughput of the assay through the use of liquid handlers for solution assays, a MALDI spotter for deposition of analytes onto the MALDI plate and a matrix coater to increase reproducibility and potentially allow higher DMSO levels. The use of automated liquid handling equipment may also increase the reproducibility of the assay and reduce overall assay time, providing a significant increase in throughput. Additionally, throughput could be enhanced through multiplexing the assaying with multiple antibiotic modifying enzymes to rapidly identify lead compounds that can aid in the fight against antibiotic resistance.

2.6 Acknowledgments

The authors thank Dr. G. D. Wright and Tushar Shakya for providing the pPCRG6 plasmid for overexpression of the APH3'IIIa enzyme. The authors thank the Natural Sciences and Engineering Research Council of Canada, the Canada Foundation for Innovation, the Ministry of Research and Innovation, Ontario, and MDS-Sciex for

financial support of this work. JDB holds the Canada Research Chair in Bioanalytical Chemistry and Biointerfaces.

2.7 References

[1] Wright, G. D. Curr. Opin. Microbiol. *2*, (1999) 499-503.

[2] Wright, G. D. Chem. Biol. *7*, (2000) R127-R132.

[3] Wright, G. D. Expert Opin. Drug Discov. *5*, (2010) 779-788.

[4] Wright, G. D. Curr. Opin. Chem. Biol. *7*, (2003) 563-569.

[5] McKay, G. A.; Thompson, P. R.; Wright, G. D. Biochemistry *33*, (1994) 6936-6944.

[6] CMAJ *133*, (1985) 739.

[7] Barker, S. C.; Kassel, D. B.; Weigl, D.; Huang, X. Y.; Luther, M. A.; Knight, W. B. Biochemistry *34*, (1995) 14843-14851.

[8] Morgenstern, S.; Flor, R.; Kessler, G.; Klein, B. Anal. Biochem. *13*, (1965) 149-161.

[9] Negash, S.; Yao, Q.; Sun, H. Y.; Li, J. H.; Bigelow, D. J.; Squier, T. C. Biochem. J. *351*, (2000) 195-205.

[10] de Boer, A. R.; Letzel, T.; van Elswijk, D. A.; Lingeman, H.; Niessen, W. M. A.; Irth, H. Anal. Chem. *76*, (2004) 3155-3161.

[11] Allwood, E. G.; Davies, D. R.; Gerrish, C.; Ellis, B. E.; Bolwell, G. P. FEBS Lett. *457*, (1999) 47-52.

[12] Ge, X.; Sirich, T. L.; Beyer, M. K.; Desaire, H.; Leary, J. A. Anal. Chem. *73*, (2001) 5078-5082.

[13] Glass, D. B.; Cheng, H. C.; Mendemueller, L.; Reed, J.; Walsh, D. A. J. Biol. Chem. *264*, (1989) 8802-8810.

[14] de Boer, A. R.; Letzel, T.; Lingeman, H.; Irth, H. Anal. Bioanal. Chem. *381*, (2005) 647-655.

[15] Partserniak, I.; Werstuck, G.; Capretta, A.; Brennan, J. D. Chembiochem *9*, (2008) 1065-1073.

[16] Nam, H. S.; Ban, E.; Yoo, E.; Yoo, Y. S. J. Chromatogr. A *976*, (2002) 79-85.

[17] Forsberg, E. M.; Green, J. R. A.; Brennan, J. D. Anal. Chem., (2011).

[18] Tjernberg, A.; Markova, N.; Griffiths, W. J.; Hallen, D. J. Biomol. Screening *11*, (2006) 131-137.

[19] Takats, Z.; Wiseman, J. M.; Gologan, B.; Cooks, R. G. Science *306*, (2004) 471-473.

[20] De Nardi, C.; Bonelli, F. Rapid Commun. Mass Spectro. *20*, (2006) 2709-2716.

[21] Romanyshyn, L.; Tiller, P. R.; Hop, C. E. C. A. Rapid Commun. Mass Spectro. *14*, (2000) 1662-1668.

[22] Finnskog, D.; Resssine, A.; Laurell, T.; G., M.-V. J. Proteome Res. *3*, (2004) 988-994.

[23] Kovarik, P.; Hodgson, R. J.; Covey, T.; Brook, M. A.; Brennan, J. D. Anal. Chem. *77*, (2005) 3340-3350.

[24] Corr, J. J.; Kovarik, P.; Schneider, B. B.; Hendrikse, J.; Loboda, A.; Covey, T. R. J. Am. Soc. Mass Spectro. *17*, (2006) 1129-1141.

[25] Gobey, J.; Cole, M.; Janiszewski, J.; Covey, T.; Chau, T.; Kovarik, P.; Corr, J. Anal. Chem. *77*, (2005) 5643-5654.

[26] Hatsis, P.; Brombacher, S.; Corr, J.; Kovarik, P.; Volmer, D. A. Rapid Commun. Mass Spectro. *17*, (2003) 2303-2309.

[27] Kovarik, P.; Grivet, C.; Bourgogne, E.; Hopfgartner, G. Rapid Commun. Mass Spectro. *21*, (2007) 911-919.

[28] Rathore, R.; Corr, J.; Scott, G.; Vollmerhaus, P.; Greis, K. D. J. Biomol. Screen *13*, (2008) 1007-1013.

[29] Rathore, R.; Corr, J. J.; Lebre, D. T.; Seibel, W. L.; Greis, K. D. Rapid Commun. Mass Spectro. *23*, (2009) 3293-3300.

[30] Awuah, E.; Capretta, A. J. Org. Chem. *75*, (2010) 5627-5634.

[31] Dai, Y.; Whittal, R. M.; Li, L. Anal. Chem. *68*, (1996) 2494-2500.

[32] Dai, Y.; Whittal, R. M.; Li, L. Anal.l Chem. *71*, (1999) 1087-1091.

[33] Onnerfjord, P.; Ekstrom, S.; Bergquist, J.; Nilsson, J.; Laurell, T.; Marko-Varga, G. Rapid Commun. Mass Spectro. *13*, (1999) 315-322.

[34] Westman, A.; Nilsson, C. L.; Ekman, R. Rapid Commun. Mass Spectro. *12*, (1998) 1092-1098.

[35] Zhang, J. H.; Chung, T. D. Y.; Oldenburg, K. R. J. Biomol. Screen. *4*, (1999) 67-73.

[36] Healy, M. J. R. Biochem. J. *130*, (1972) 207-210.

[37] Rodbard, D. Clin. Chem. *20*, (1974) 1255-1270.

[38] Cheng, Y.; Prusoff, W. H. Biochem. Pharmacol. *22*, (1973) 3099-3108.

[39] Wu, G.; Yuan, Y.; Hodge, C. N. J. Biomol. Screen. *8*, (2003) 694-700.

[40] McFadden, M. J.; Junop, M. S.; Brennan, J. D. Anal. Chem. *82*, (2010) 9850-9857.

[41] Yates, J. R. J. Mass Spectro. *33*, (1998) 1-19.

[42] Monton, M. R. N.; Lebert, J. M.; Little, J. R. L.; Nair, J. J.; McNulty, J.; Brennan, J. D. Anal. Chem. *82*, (2010) 9365-9373.

2.8 Supporting Information

Expression and Purification of APH3′IIIa**.** APH 3′IIIa was expressed via the pPCRG6 plasmid in an *E.coli* BL21 host as described by McKay *et al*. with minor modification.[1] Briefly, 2x5 cm QSeph columns were used running 0-50% buffer (50 mM Tris, pH 8.0, 1 mM EDTA, 1 M NaCl) at 0.5 mL min^{-1} for 300 min. Fractions were collected and run on a SDS-PAGE gel. Active fractions were pooled and reapplied to the 2x5 cm QSeph columns on a slower gradient (20-50 % at 0.1 mL min^{-1} over 300 min). Fractions were concentrated and run on an SDS-PAGE gel. A sample of the purified enzyme was submitted for accurate mass confirmation on a LC-OrbiTrap-MS and identified using ProMass deconvolution software resulting in a peak at 30841.8 m/z (predicted mass 30978 m/z)[1].

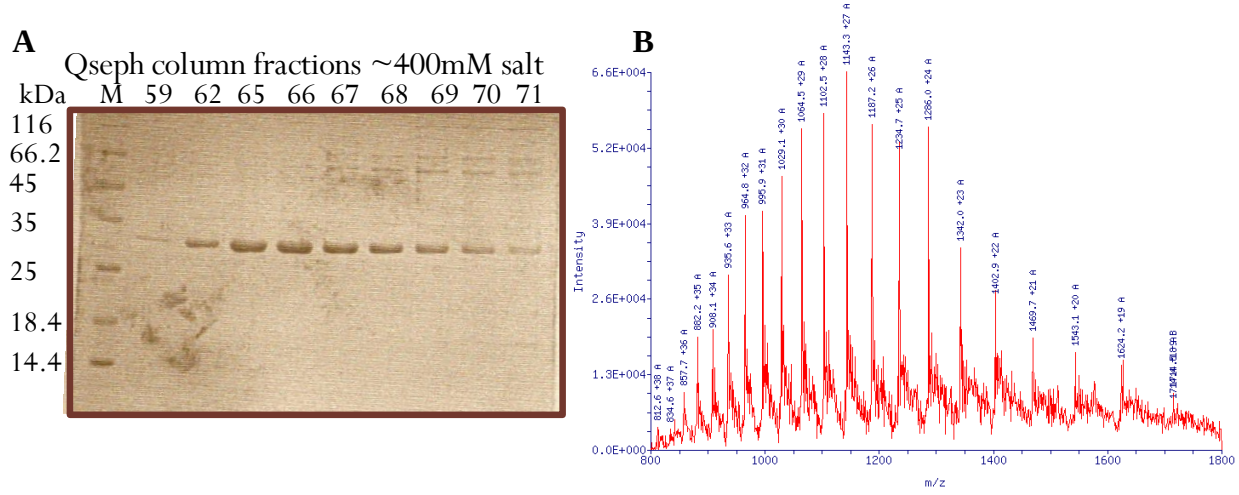

Figure S2.1: A) SDS PAGE Gel showing purity of APH(3')-IIIa and B) confirmation of APH3′IIIa via LC-Orbi-Trap MS.

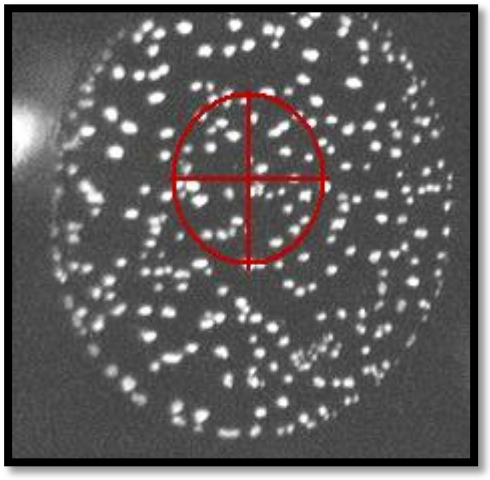

Figure S2.2: Dry spot on MALDI plate, negative control (no enzyme) in the absence of DMSO. A denser matrix composition appears when using seeding.

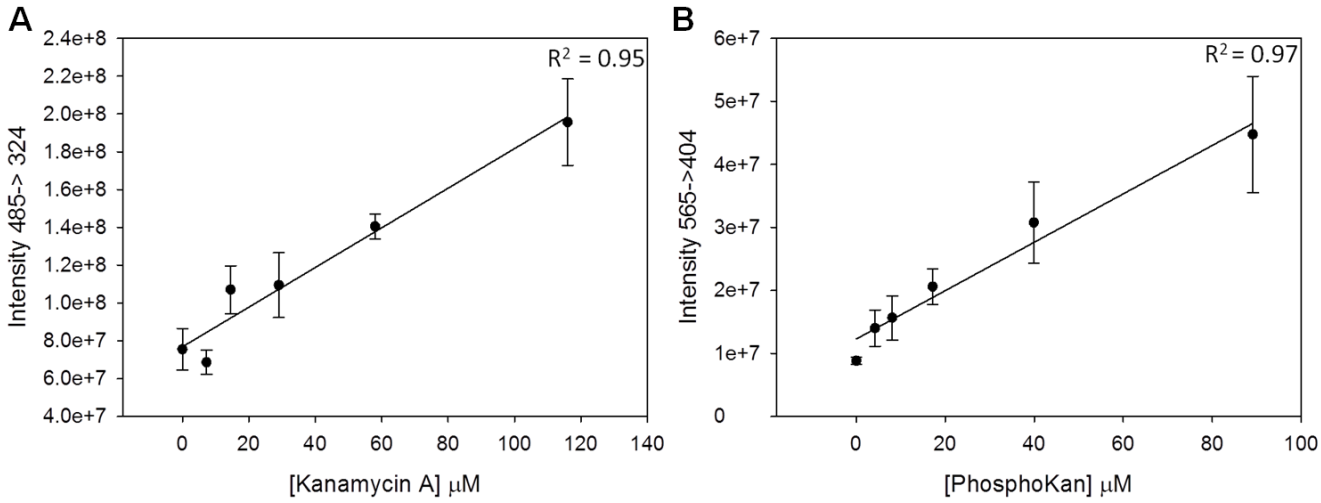

Figure S2.3: Calibration curves for A) Kanamycin and B) Phosphorylated Kanamcyin obtained on an AP-MALDI ion trap.

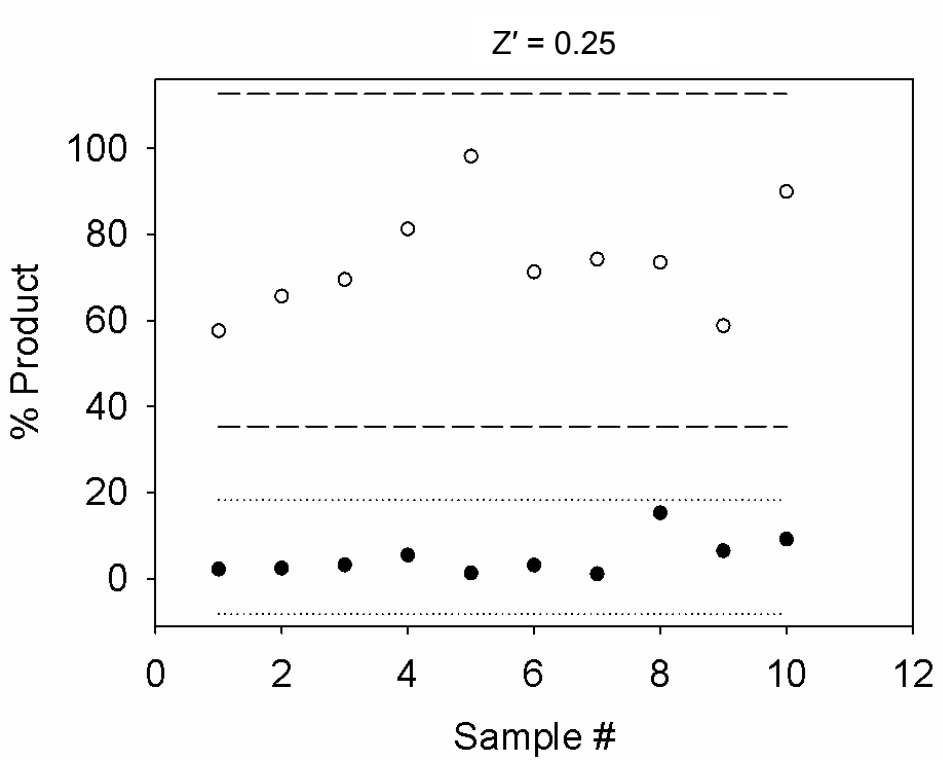

Figure S2.4: Z′ plot using ESI-MS/MS conditions identical to that of Figure 2.2B in the presence of (HC ○) and absence of (LC ●) APH 3′IIIa. Z′-factor = 0.25

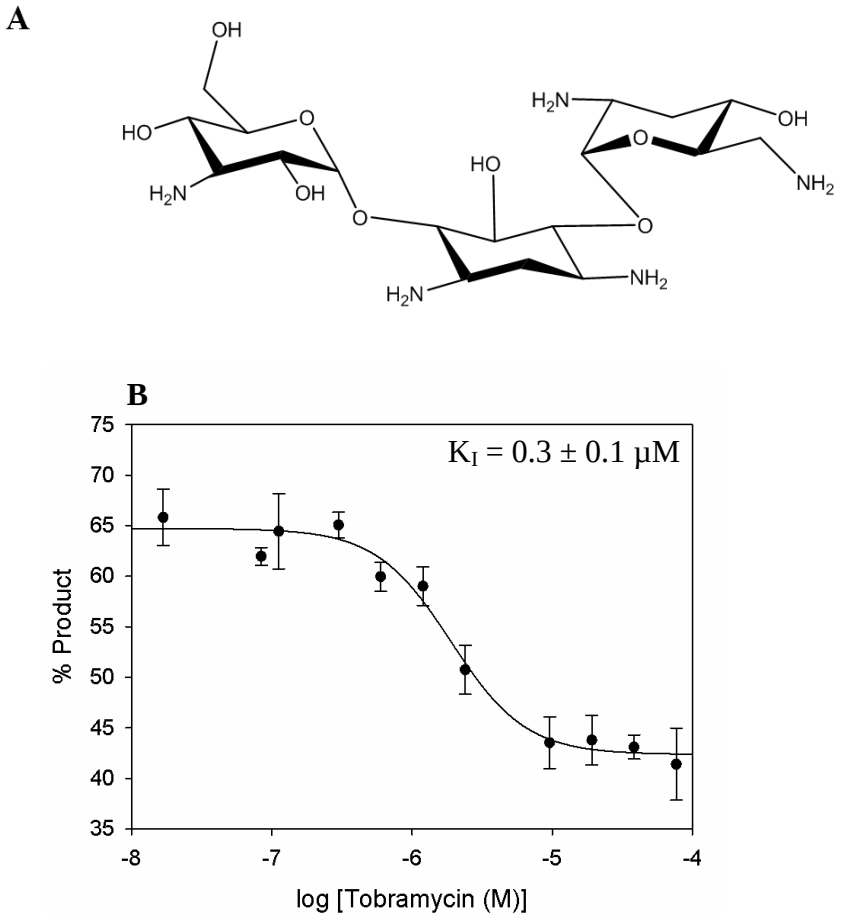

Figure S2.5: A) Structure and B) IC50 curve of a known inhibitor, tobramycin.

2.9 Reference

[1] G. A. McKay; P. R. Thompson; G. D. Wright, Biochemistry. 33 (1994) 6936-6944.

Chapter 3 : Simultaneous Inhibition Assay for Human and Microbial Kinases via MALDI-MS/MS

Author's Preface:

The following chapter is currently in press as a full paper in the journal ChemBioChem under the citation:

Anne Marie E. Smith and John D. Brennan, **Simultaneous Inhibition Assay for Human and Microbial Kinases via MALDI-MS/MS,** *ChemBioChem*. **2014**, 15, 587-594.

I was responsible for the experimental design, and performance of said experiments, data analysis and interpretation. I wrote the first draft of the manuscript and Dr. Brennan provided editorial input to generate the final draft for submission.

3.1 Abstract

Selective inhibition of one kinase over another is a critical issue in drug development. For antimicrobial development, it is particularly important to selectively inhibit bacterial kinases, which can phosphorylate antimicrobial compounds such as aminoglycosides, without affecting human kinases. Previous work from our group showed the development of a MALDI-MS/MS assay for the detection of small molecule modulators of the bacterial aminoglycoside kinase APH3′IIIa. Herein, we demonstrate the development of an enhanced kinase MALDI-MS/MS assay involving simultaneous assaying of two kinase reactions, one for APH 3′IIIa, and the other for the human kinase, protein kinase A (PKA), which leads to an output that provides direct information on selectivity and mechanism of action. Specificity of the respective enzyme substrates were verified and the assay was validated through generation of Z′-factors of 0.55 for APH 3′IIIa with kanamycin, and 0.60 for PKA with kemptide. The assay was used to simultaneously screen a kinase directed library in mixtures of 10 compounds each against both enzymes, leading to the identification of selective inhibitors for each enzyme as well as one non-selective inhibitor following mixture deconvolution.

Keywords. kinase, antibiotic resistance, inhibition, MALDI, high throughput screening.

3.2 Introduction

Kinases are one of the most important drug targets due to their involvement in a myriad of cellular functions related to disease and infection. [1] Kinases play a pivotal role in signal transduction pathways and in post-translational modifications, and hence are responsible for the modulation of most cellular activities. [2-4] Upon mutation or activation of the kinase, diseases such as cancer can occur owing to improper kinase function. [2-4]

Kinases share structural similarities with other proteins known as "kinase-like" proteins. The eukaryotic protein kinase, or c-AMP dependent protein kinase (PKA) is a kinase involved in metabolic regulation in the human body and in the phosphorylation of the peptide substrate, kemptide (LRRASLG). [4-5] PKA shares many similarities with the bacterial enzyme, aminoglycoside phosphotransferase 3`IIIa (APH 3`IIIa); which is involved in the rise of antibiotic resistance through phosphorylation of aminoglycoside antibiotics, resulting in inactive compounds that are unable to treat bacterial infections. [6-10] These similarities include binding domains (two substrate binding sites; ATP and secondary site) as well as additional structural similarities. [11] These similarities can pose significant problems if compounds are introduced that are intended to selectively inhibit only one kinase. In particular, compounds that inhibit bacterial kinase-like proteins (usually denoted as phosphotransferases) as a method to prevent antibiotic resistance can pose a potential problem if the functions of human kinases, such as PKA, are also altered owing to off-target effects. Development of small-molecule screening assays that can simultaneously detect inhibition of multiple kinases and "kinase-like" proteins could

provide a means to rapidly identify selective compounds for target kinases, or quickly reveal off-target effects without the need of additional time consuming reactions. The development and validation of such an assay is a key goal of this study.

A variety of research groups have investigated multiplexed monitoring of enzyme reactions based on three basic approaches: 1) Microarrays; 2) Self-Assembled Monolayer Desorption/Ionization (SAMDI) mass spectrometry; and 3) Electrospray Ionization Mass Spectrometry (ESI-MS). Microarrays have proven themselves to be beneficial for multiplexed assays as they require low volumes and reagent costs, and can be expanded to large numbers of different proteins or several substrates, using peptide substrate arrays. [12] However, they generally require the use of a fluorescent or radioisotope label in order to generate a response. [12-18] Upon combination of multiple kinases, a variety of interferences and cross reactivity can be observed, making multiplexed kinase screening difficult. [12] SAMDI has been widely used for the detection of kinase reactions, however, it relies on immobilization of substrates and as such is only amenable to enzymatic reactions involving peptides. [19] Finally, a variety of research has been reported on the use of ESI-MS for multiplexed assays; however these involve either one enzyme and many substrates, [20] several unrelated proteins [21-22] or pooling of products following an off-line reaction. [23] While, these methods have achieved proof of concept, they have not been applied to simultaneous detection of reactions between enzymes within the same class. Multiplexed assays involving kinase or "kinase-like" systems have not been reported, likely owing to the potential for cross reactivity related to substrate promiscuity.

Previously we reported the development of a MALDI-MS/MS assay that could be used for screening of APH 3'IIIa inhibitors. [24] By monitoring product-to-substrate ratio for an offline reaction, a direct assay for aminoglycoside phosphotransferase activity and inhibition was developed. While the previous work focused heavily on assay development, herein, we show the expansion of the previous assay to a simultaneous, quantitative kinase/"kinase-like" assay through the use of atmospheric pressure (AP) MALDI-MS/MS. Using this assay, we demonstrate for the first time the ability to simultaneously screen two enzymes from the same class to identify compounds that inhibit aminoglycoside phosphotransferase 3`IIIa but do not affect the activity of PKA. A mixture of both proteins and their respective substrates was assayed within a single MALDI spot, rather than performing two separate assays for each enzyme, thus reducing assay time and cost. Furthermore, the ability to screen two kinases simultaneously allows for an internal assessment of likely mode of action, highlighting the ability of the simultaneous assay to identify the biological significance of a given lead compound. We also demonstrate the replacement of DMSO in the assay, which reduced ion suppression effects. The assay has been validated through generation of Z` factors for kemptide and kanamycin phosphorylation by PKA and APH3'IIIa, respectively. A total of 210 kinase directed inhibitors were screened and selective inhibitors for each enzyme were identified and their potency quantified using the MALDI-MS/MS assay.

3.3 Results and Discussion

Substrate Specificity

Kinases are known for substrate promiscuity and hence cross-reactivity is a potential problem when performing two simultaneous reactions. APH 3′IIIa phosphorylates the 3` hydroxyl group of aminoglycoside antibiotics, such as kanamycin, while PKA phosphorylates the hydroxyl group on the serine residue of the synthetic peptide kemptide. Ensuring that one enzyme does not cause phosphorylation of the opposing substrate is important to remove the possibility of false positives or negatives. Supplementary Figure S3.1 shows the MS and MS/MS spectra for kemptide, phosphokemptide, kanamycin A and phosphokanamycin. The spectra indicate that there are unique *m/z* values for each species and unique parent-to-daughter ion transitions, making simultaneous monitoring of the two reactions by selected reaction monitoring possible.

Figure 3.1A shows the intensity ratio of analyte (A)/Internal Standard (IS) from phosphokanamycin/kanamycin obtained by MALDI-MS/MS analysis, and illustrates that only kanamycin is turned over in the presence of APH 3`IIIa, while Figure 3.1B shows the intensity ratio of A/IS from phosphokemptide/kemptide and illustrates that kemptide is also turned over only in the presence of PKA, demonstrating high specificity. Figure 3.1C shows that when kanamycin and APH 3′IIIa are placed together in the presence of either PKA or kemptide, specificity is also obtained, as is confirmed in Figure 3.1D, when kemptide and PKA are together in the presence of APH 3′IIIa or kanamycin. An intensity difference is noted in the ratios for assays utilizing phosphokanamycin (Figure 3.1C) and

phosphokemptide (Figure 3.1D). This difference is attributed partially to differential ionization effects. Indeed, when considering the inherent error in the measurements, as manifested by the error bars, this difference is marginal and is almost within error. This demonstrates that APH 3′IIIa selectively phosphorylates kanamcyin, while PKA selectively phosphorylates kemptide.

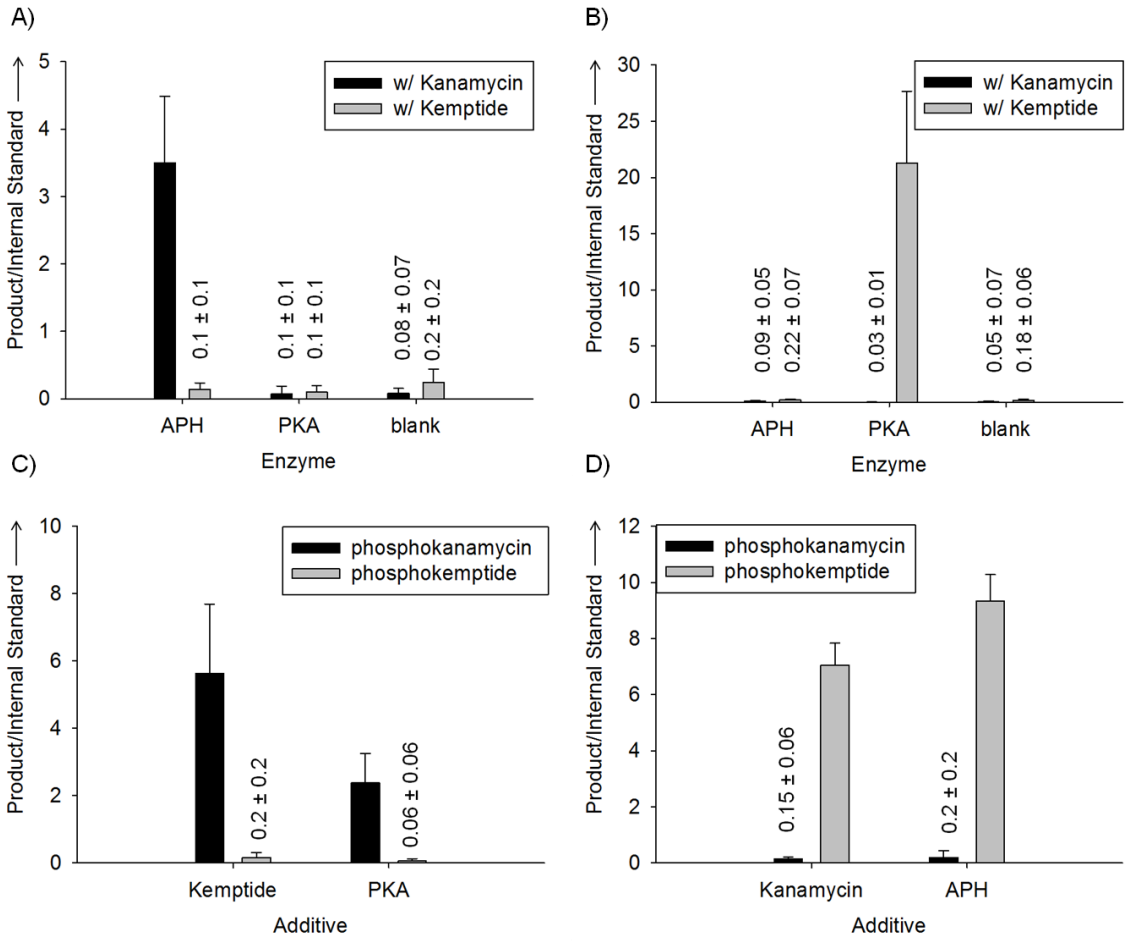

Figure 3.1: Substrate specificity. A) Intensity ratio of A/IS resulting from phosphokanamycin/kanamycin obtained in the presence of kemptide (grey, 0.725 µM) or kanamycin (black, 58 µM) with varying enzymes/blanks, B) Intensity ratio of A/IS resulting from phosphokemptide/kemptide obtained in the presence of kemptide (grey, 0.725 µM) or kanamycin (black, 58 µM) with varying enzymes/blanks, C) Intensity ratio of A/IS resulting from either phosphokanamycin/kanamycin (black) or

phosphokemptide/kemptide (grey) for the phosphorylation of kanamycin by APH 3′IIIa in the presence of either kemptide or PKA, D) Intensity ratio of A/IS resulting from either phosphokanamycin/kanamycin (black) or phosphokemptide/kemptide (grey) for the phosphorylation of kemptide by PKA in the presence of either kanamycin or APH 3`IIIa. In all cases, the concentration of the IS was held constant at 0.5 µM after mixing with analyte.

Instrument Response

The instrument response of phosphorylated kanamycin and phosphorylated kemptide were verified with construction of calibration curves (n = 3), showing a linear response with R^2 values of 0.99, as shown in supplementary Figure S3.2. The absolute signal levels obtained from kemptide and its phosphorylated product are much higher than those of kanamycin and phosphokanamycin, which is likely due to a higher ionization efficiency for the peptide relative to the small molecule. Even so, all species provided sufficient signal-to-noise levels to allow screening at relevant concentrations that were close to the K_M of the respective enzyme.

Validation of assay

While MALDI-MS/MS is not widely used for obtaining quantitative data, several studies, including our previous assay of APH3'IIIa, demonstrate that quantification is possible, particularly when utilizing an ion trap mass analyzer to perform tandem mass spectrometry. [24] Operation of the AP-MALDI ion trap system in internal timing mode with the use of a set internal integration time (24 s) and delay time (90 s) reduced background interferences from matrix ions and allowed for the production of peaks that could be integrated in a manner similar to that of HPLC injection peaks. This approach significantly reduced variability in the signal and also improved overall signal levels.

A Z`-factor was calculated for both enzyme systems in the presence and absence of DMSO to quantitatively assess the reproducibility of the assays using ten positive (+ve) and negative (-ve) controls. The presence of DMSO can greatly affect enzymatic activity, and can have a dramatic effect on ionization efficiency in mass spectrometric assays. In the presence of 0.2% v/v DMSO, a high Z' value of 0.64 was obtained for phosphorylation of kanamycin, indicative of a highly reproducible assay. However, similar levels of DMSO resulted in significant irreproducibility for assays involving phosphorylation of kemptide by PKA (Z' = -0.35; Figure S3.3). Hence, DMSO appears to greatly alter the ionization of the peptide substrate kemptide, likely due to ion suppression. [25] In order to resolve this problem, Z`-factors were obtained in the presence of a more compatible solvent (0.2% v/v MeOH) to allow more efficient ionization for mass spectrometry based assays. 0.2% MeOH was the minimum concentration needed to dissolve compounds in the kinase directed library. A Z`-factor corresponding to an excellent assay was achieved for both enzymes; 0.55 for the kanamycin reaction in the presence of both PKA and kemptide (Figure 3.2A) and 0.60 for the kemptide reaction in the presence of both APH 3′IIIa and kanamycin (Figure 3.2B). Based on these results all further studies were done using compounds dissolved in the MeOH:water solvent system.

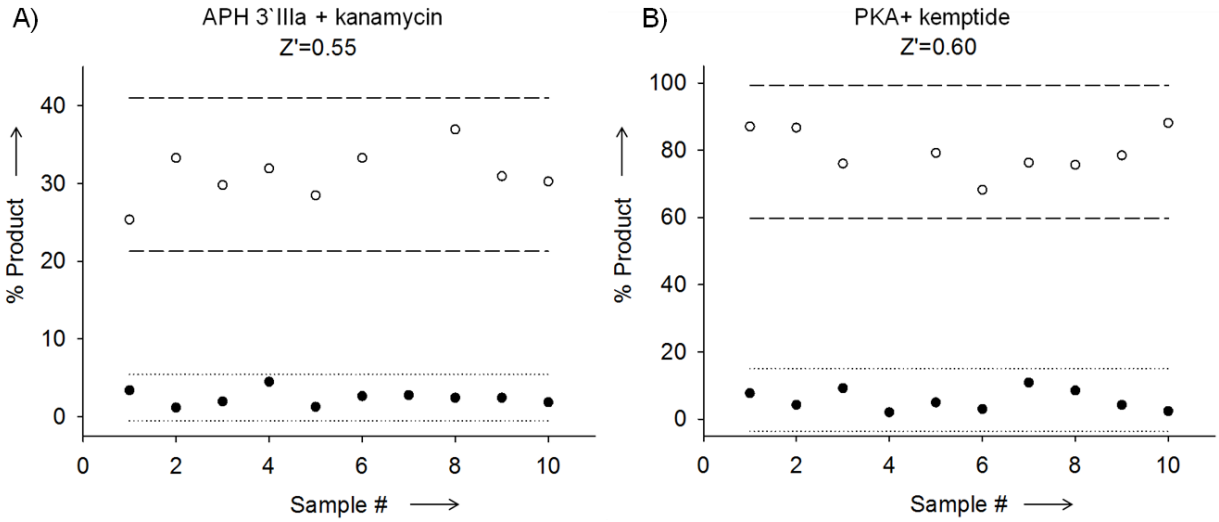

Figure 3.2: Z'-plot of A) APH 3′IIIa with kanamycin, Z` = 0.55 and B) PKA with kemptide, Z` = 0.60 in the presence of 0.2% v/v MeOH in water. Dashed lines signify 3 standard deviations of the average of high and low controls.

Simultaneous Screening of Mixtures

Modulators of the phosphorylation of kanamycin by APH 3′IIIa that do not alter the enzymatic activity of PKA were monitored simultaneously using the optimized AP-MALDI-MS/MS assay. Assay throughput was increased by screening both enzyme reactions simultaneously against mixtures of potential inhibitors rather than discrete compounds. [24, 26-27] A total of 21 mixtures were screened in duplicate with 10 compounds per mixture, including known inhibitors of both enzyme systems as well as +ve (enzyme + substrate) and –ve (no enzyme) controls. While mixture complexity could have been increased to contain 20 or more compounds instead of 10 compounds, however due to the use of a kinase directed library, and a potentially high hit rate, a mixture complexity of 10 compounds per mixture was chosen to avoid having a hit in each mixture. All compounds were initially present in DMSO stock solutions. Evaporation

under vacuum was required to fully remove DMSO and leave compound samples dry, allowing reconstitution in 0.8% v/v MeOH for screening.

Compounds were originally screened at a concentration of 10 μM, a suitable concentration to find inhibitors and a value that was identical to that used in our previous study. [24] Both reactions were run in duplicate for each mixture with the % product monitored simultaneously for both kanamycin (percent product shown in Figure 3.3A) and kemptide (percent product shown in Figure 3.3B). While a few outliers do occur, which is a common occurrence in mixture screening, [24, 26, 28] an important feature of these plots is that the duplicate data lies primarily on the diagonal, showing good reproducibility between assays. The presence of signals at levels greater than 100% are commonly observed in screening assays regardless of the format used (i.e. MS, absorbance, fluorescence, etc.) [21, 23-25] possibly due to compounds increasing enzyme activity or enhancing signals as a result of interference (e.g. enhanced ionization). It should also be noted that the 100% value is the baseline activity for the assay under the conditions use, and does not represent 100% substrate turnover, but rather a defined turnover that is subsequently set at 100%. 100% product formation would in fact be undesirable for any screening assay as it is not within the range where activity changes linearly with substrate concentration. In addition, the mixtures span a broad range of activity, with at least one mixture and the appropriate positive control compounds showing at least 50% inhibition for each reaction, a value selected based on data from the Z' assay which showed no non-inhibitors demonstrating activity below this value .

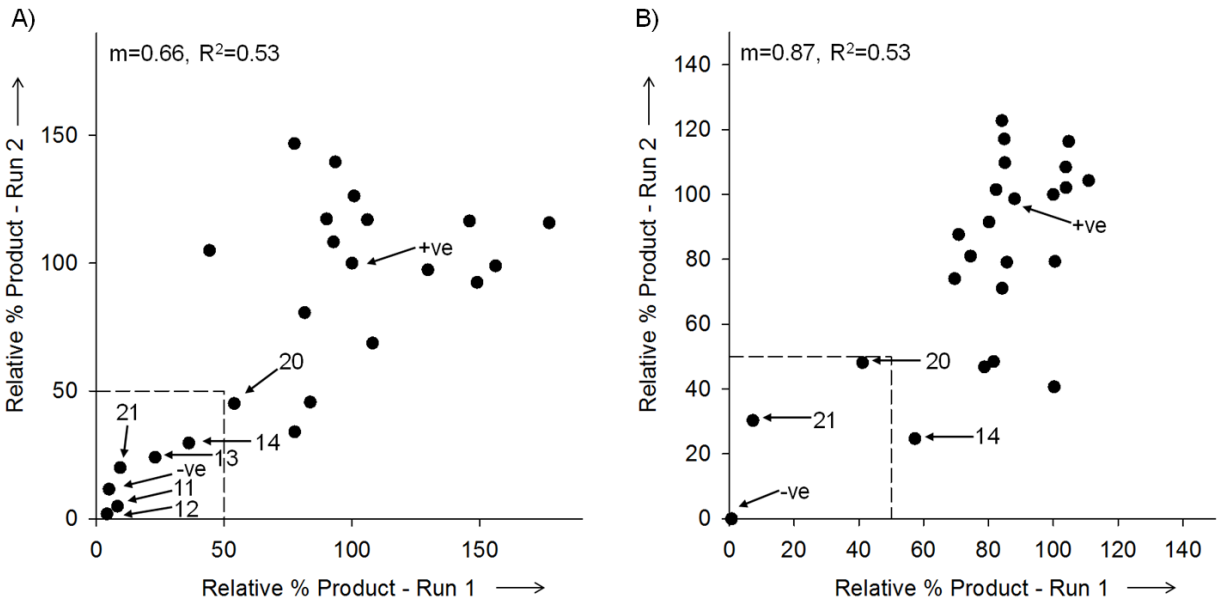

Figure 3.3: Duplicate plot for the simultaneous screen of 210 compounds as 21 mixtures of 10 compounds each against APH 3′IIIa and PKA. % product formed is shown for each assay for A) APH3'IIIa - kanamycin reaction and B) PKA – kemptide reaction as monitored by tandem mass spectrometry. Labels were not included for mixtures showing little to no inhibitory action. Positive (+ve) signifies a sample containing both enzyme and substrate (no inhibitor), while negative (–ve) signifies a samples containing only substrate in the absence of enzyme (and inhibitor).

An important point was that the screening of mixtures against two enzymes simultaneously significantly reduced assay time and cost. To screen all compounds against each enzyme individually, in duplicate, would require 848 individual reactions (210 compounds in duplicate for each enzyme = 840 + 4 controls in duplicate). However, screening as mixtures first, and in the presence of both enzymes, reduces this number to 148; a reduction of over 80%.

Mixture Deconvolution.

Mixtures shown to reduce substrate turnover in either reaction by a minimum of 50%; a value commonly chosen in screening assays [26-28] and that is within the hit

window of the Z' assay, were further examined to determine which compounds were responsible for inhibition and to obtain quantitative data on inhibition constants. Compound identification was obtained by rescreening each compound in a bioactive mixture to identify the specific inhibitor(s). Given our interest in identifying selective inhibitors of APH3'IIIa, we deconvoluted those mixtures showing inhibition towards APH3`IIIa and no inhibition towards PKA (mixtures 11, 12 and 13), and also two mixtures that showed non-selective inhibition of both enzymes (mixtures 14 and 20).

Figure 3.4 shows the deconvolution of mixtures 11, 12 and 13 based on running the assays simultaneously with APH3'IIIa (data shown in Panel A) and PKA (data shown in Panel C). Two identical compounds (denoted as either EME 254 or EME 332, depending on the mixture) were included in two separate mixtures (14 and 11, respectively) as a blind control and further identified as inhibitors upon discrete screening. This further validated the dual-kinase assay and showed that the assay was able to identify selective inhibitors of APH3'IIIa, even in the presence of PKA. Importantly, compounds included in the screen that were expected to be selective inhibitors of APH3'IIIa (tobramycin) were only found to inhibit APH 3`IIIa, ATP competitive inhibitors such as H-7 were found to inhibit kinases, while staurosporine and RO-31-8220, which are kinase inhibitors that are known not to inhibit APH3'IIIa were found to only inhibit PKA, illustrating that selectivity is obtained using the simultaneous dual-kinase assay.

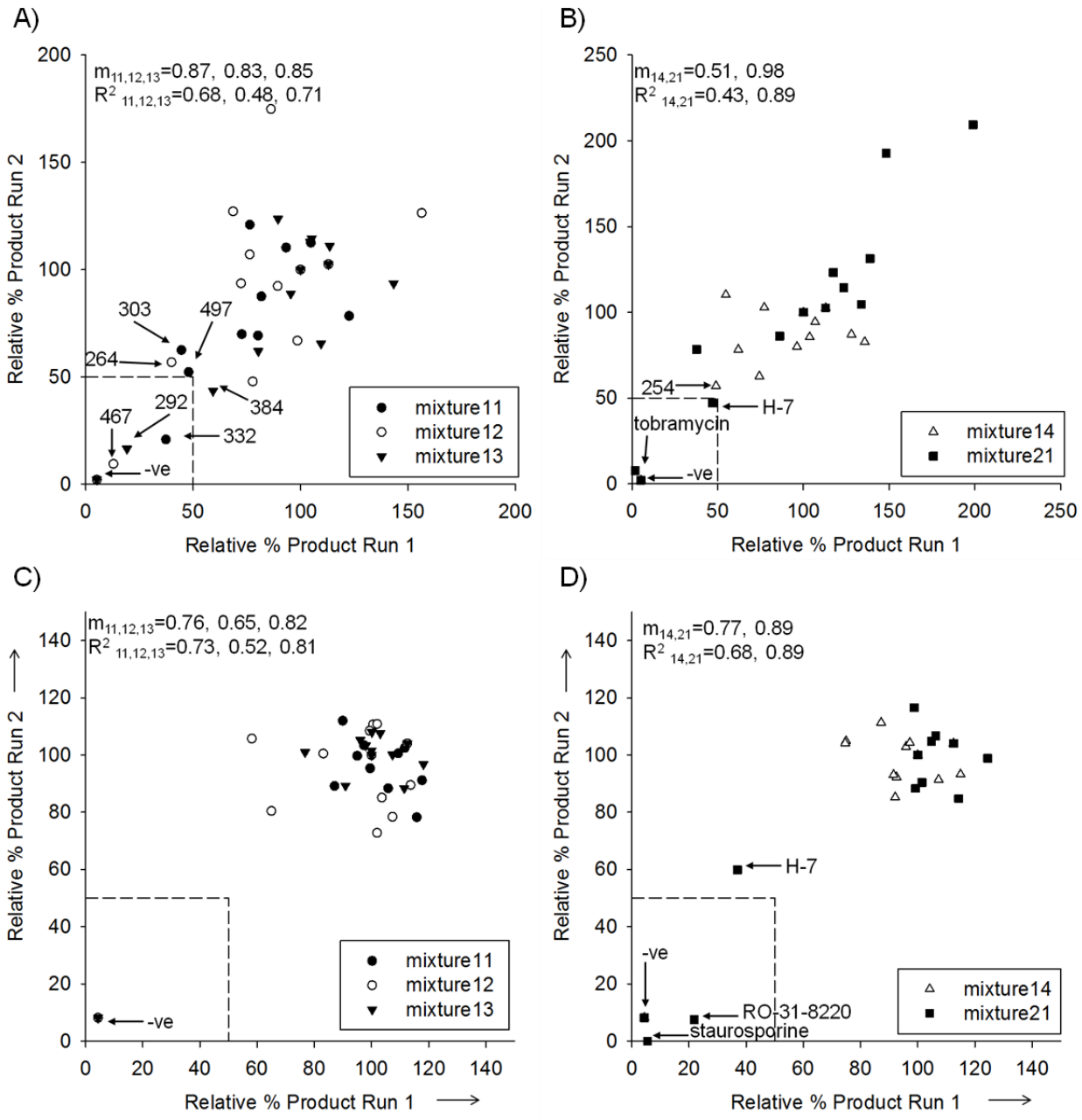

Figure 3.4: Deconvolution of "hit" mixtures from the initial mixture screen. % product formation is shown for A) kanamycin with mixtures 11-13, B) kanamycin with mixtures 14 and 21, C) kemptide with mixtures 11-13 and D) kemptide with mixtures 14 and 21. Compounds identified by deconvolution are shown in the respective plots. Negative samples (-ve) were those containing no enzyme for the given reaction, while positive (+ve) samples were those containing both enzyme and substrate. Labels were not included for compounds showing little to no inhibitory action.

This data also provides some preliminary insight into the mode of action of inhibitors. As previously discussed, both kinases share an ATP binding site. Theoretically, if a compound is ATP competitive, then it should bind to both kinases;, as was found for H7, which is a known ATP competitive inhibitor. [29] If the compound binds to only one of the kinases, then the compound should either be substrate competitive, or bind through an allosteric mechanism. Tobramycin is known to be substrate competitive in its binding with kanamycin to APH 3′IIIa, [6] and as expected was found to inhibit only this enzyme. Finally, compounds staurosporine and RO-31-8220 are analogs of one another and are expected to affect the ATP binding site of PKA allosterically; [11], [30] and thus should inhibit PKA but not APH3'IIIa, since allosteric binding is specific to the enzyme, as observed here. Based on these inhibition patterns, it appears that the synthetic EME compounds that were observed to selectively inhibit APH 3′IIIa are either allosteric or substrate competitive inhibitors of APH 3`IIIa, which may make them useful starting points for designing highly selective and potent compounds that can be used in conjunction with aminoglycoside antibiotics to overcome resistance by altering the ability of APH3′IIIa to modify aminoglycoside antibiotics.

Quantitative Dose-Dependent Response Curves.

Quantitative dose-dependent response curves were collected for a known inhibitor of each of APH 3′IIIa and PKA (tobramycin and H-7 respectively) in the absence of the second enzyme. Through the use of the Cheng-Prusoff equation (2) and using literature K_M values of 12.6 ± 2.6 μM [6] and 16 ± 0.9 μM [31] for APH 3`IIIa/kanamycin and

PKA/kemptide respectively, inhibition constants (K_I) were calculated. In order to improve reproducibility, assay time was increased from 5 min to 15 min for dose-dependent response curves. Literature K_I values for aforementioned inhibitors tobramycin and H-7 are 2 μM [6] and 3 μM, [29] respectively. The values found through the use of the AP-MALDI-MS/MS assay were 0.7 ± 0.2 μM for tobramycin with APH 3′IIIa (Figure 3.5A) and 5 ± 2 μM for H-7 with PKA (Figure 3.5B), showing good agreement with literature values. However the error bars on the IC_{50} plots (n = 3), tend to show a large error for some points; possibly owing to variations in matrix crystallization, which is a common issue for MALDI-MS. The novel inhibitor, EME 467, found in previous work by our group to have a K_I value of 1.2 ± 0.6 μM [24] was found in the current assay to have a K_I value of 1.1 ± 0.2 μM (Figure 3.5C) for APH3'IIIa when run in the presence of PKA and kemptide, showing excellent agreement with the previous published value.

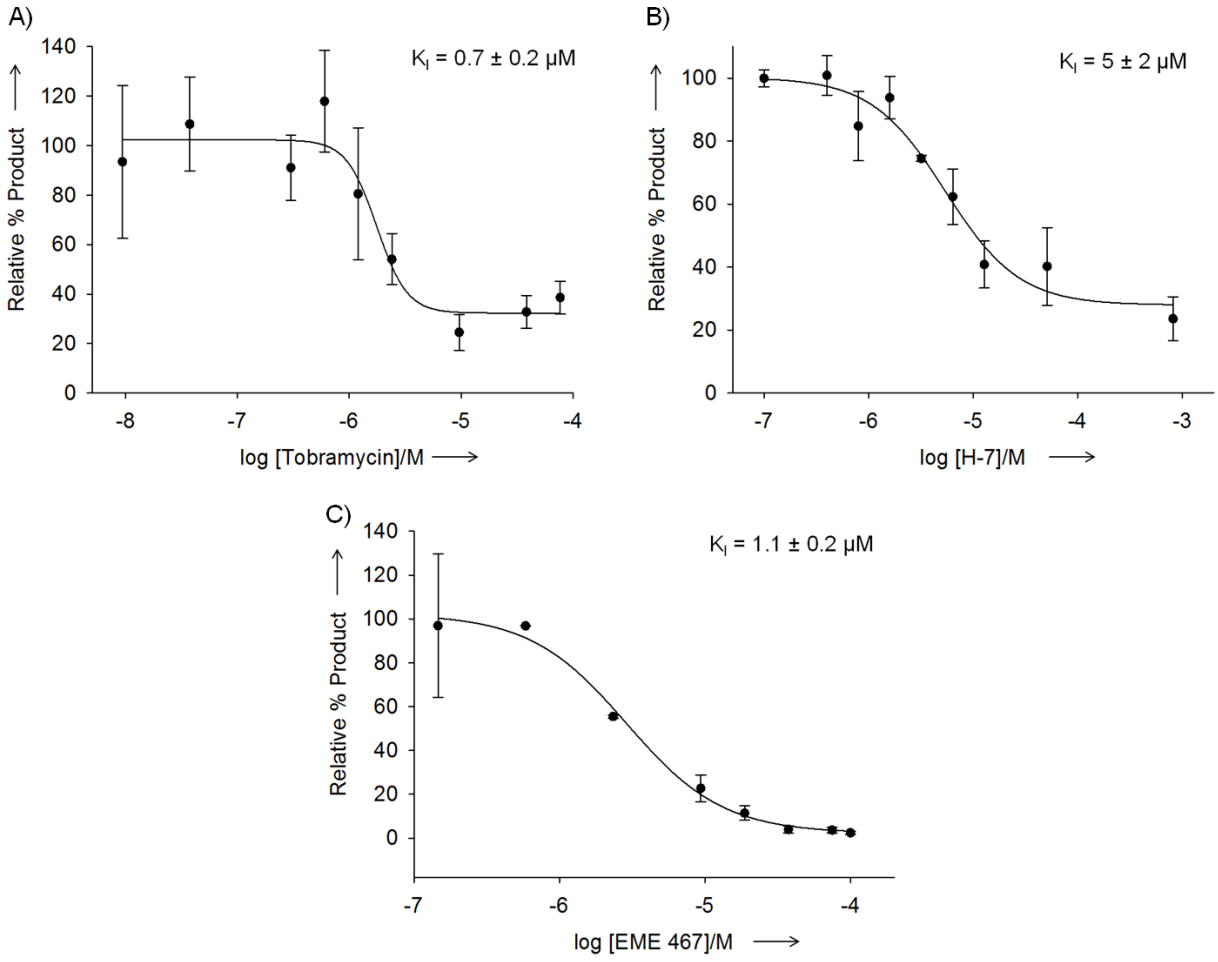

Figure 3.5: Dose-dependent response curves: A) APH 3′IIIa with kanamycin inhibited by tobramycin; B) PKA with kemptide inhibited by H-7 and; C) APH 3′IIIa with kanamycin inhibited by EME 467.

3.4 Conclusions

MALDI-MS/MS has shown the potential to be a promising technique for detection of two simultaneous phosphorylation events within the same MALDI spot. Substrate specificity of APH 3′IIIa and PKA for their respective substrates (kanamycin and kemptide) was verified. Difficulties were encountered in the validation of the assay

in the presence of DMSO, however, upon substitution of DMSO with 0.2% v/v MeOH, Z`-factors of 0.60 and 0.55 were achieved for PKA with kemptide and APH 3′IIIa with kanamycin, respectively. Upon screening and deconvolution of a library of 210 kinase directed compounds, only known inhibitors of either system were found, in addition to those synthetic compounds identified in our previous study involving one kinase and a DMSO solvent system, further illustrating the reliability of this assay. Dose-dependent response curves were also obtained for an inhibitor of each PKA and APH 3′IIIa and one synthetic inhibitor to illustrate the quantitative nature of the assay. The results show that it is possible to simultaneously screen for inhibition of both a bacterial and human kinase, making it possible to identify selective inhibitors of bacterial (or human) kinases more simply rapidly.

3.5 Experimental Section

Materials

APH3′IIIa was expressed in an *E. coli* host and purified as described by McKay *et al.* with minor modifications. [6] The cAMP-dependent protein kinase, catalytic subunit (PKA) was purchased from Promega (Madison, WI). Fluorescein, α-cyanohydroxycinnamic acid (CHCA), adenosine 5'-triphosphate (ATP), magnesium acetate ($Mg(OAc)_2$), ammonium acetate (NH_4OAc), tobramycin, kemptide (LRRASLG) and kanamycin sulfate (major component A, minor components B and C), were purchased from Sigma Aldrich (Oakville, ON). Staurosporine, RO-31-8220 and H-7 dihydrochloride were purchased from Millipore (Billerica, MA). Compounds for

screening assays were synthesized by the Capretta Laboratory (McMaster University, Hamilton, ON) [32] or were commercially available (Sigma Aldrich, Oakville, ON). All water was distilled and deionized (25 °C, 18.2 MΩ·cm, 1-5 ppb TOC). All other reagents were of analytical grade and were used as received.

Methods

Dual-kinase Assay Conditions.

Reaction conditions were similar to our previous report, [24] with minor changes. Briefly: all assays were performed by pre-incubation of the enzymes (APH3`IIIa and/or PKA) with co-factors ($Mg(OAc)_2$ and ATP) for 5 min at 37 °C. Reactions were initiated with addition of kanamycin and/or kemptide (prepared in 9.2 mM NH_4OAc, pH 7.5) followed by incubation for 5 min at 37 °C. Final assay conditions were: 100 µM ATP (prepared in 9.2 mM NH_4OAc, pH 7.5), 0.0125 mg/mL APH3′IIIa (in 2 mM HEPES pH 7.5, 0.5 % v/v glycerol), 0.0625 U/µL PKA (in 1.4 mM potassium phosphate buffer, pH 6.8) 22 µM kanamycin, 0.27 µM kemptide and 0.58 mM $Mg(OAc)_2$. Reactions were quenched by adding an equal volume of matrix solution (6.2 mg/mL CHCA in methanol containing acetic acid (1 % v/v) and fluorescein (1 µM) as a secondary internal standard because it does not react with either enzyme, ionized well at low concentrations, and has been used previously without complications) [24] to the assay solution resulting in a matrix:analyte ratio of ~1500:1 for kanamycin and ~12000:1 for kemptide. All data was smoothed using a 7-point boxcar algorithm available in the Xcalibur software provided by Thermo Finnigan and expressed as conversion to product ($\%P = 100\ (P/P+S)$), where P is

the signal from the product ion and *S* is the signal from the substrate ion. Values for product concentration are based on the 1:1 stoichiometry for substrate-to-product conversion, hence a 20% drop in substrate signal corresponds to a 20% increase in product signal for a given sample.

Spotting of Analytes

The analyte/matrix solution (2 µL) was spotted onto an ABI-100 stainless steel MALDI plate and set to dry on top of an incubator (37 °C) for approximately 10 min or until the spot was visibly dry. Initial assays included DMSO and as such, methods were implemented to improve reproducibility of matrix crystallization. The crushed crystallization method with a cold water wash (2-5 °C) was used, [33-36] wherein 2 µL of a 66:33 mixture of matrix:H_2O was spotted onto the ABI-100 stainless steel MALDI plate and allowed to dry at room temperature prior to crushing of the formed crystals with a glass microscope slide. Debris was removed and samples were overspotted with a 50:50 mixture of matrix:analyte solution and allowed to dry at room temperature. Following drying of the DMSO containing samples, the slide was dipped in a cold water bath (2-5 °C) for 15 s. The plate was removed and allowed to dry at room temperature. The crushed crystallization matrix application method allows for more reproducible crystallization, while the cold water wash allows for the ion suppressing effects of DMSO to be minimized when used at low levels. [25]

Detection of Product and Substrate – Optimization of MALDI Conditions.

MALDI-MS/MS assays were carried out on a Thermo Finnigan LCQ DECA 3D ion trap mass spectrometer interfaced with an AP-MALDI source from MassTech (Columbia, MD) operated in positive ion mode as described previously. [24] Spectra were obtained for a sample of kanamycin (58 µM) or kemptide (1 µM) prepared by mixing the solution 1:1 by volume with CHCA to obtain substrate spectra, while a reaction of each substrate for 15 min was done to allow adequate phosphorylation to obtain product spectra (see Figure S3.1). The ion trap MS was run in selected reaction monitoring (SRM) mode, while the AP MALDI source utilized a 355 nm Nd:YAG laser with an energy and frequency of 30 J and 50 Hz, respectively. In all experiments involving the AP-MALDI-MS/MS instrument, each sample spot was subjected to laser pulses for 24 s at 50 Hz. Additional parameters are listed in Table 3.1 for mass-to-charge ratio (*m/z*) of parent and daughter ions and the collision energy (CE) to induce fragmentation.

Molecule	Parent (*m/z*)	Daughter(s) (*m/z*)	CE (eV)	Cleavage Location
Kanamycin	485	324	24	Glycoside oxygen
Phosphorylated Kanamycin	565	404	26	Glycoside oxygen
Kemptide	773	730, 503	60	Between R/R
Phosphorylated Kemptide	853	737	56	Between L/R
Fluorescein	333	315	56	N/A

Table 3.1: Mass-to-charge ratio, collision energy and fragmentation information for substrate and parent molecules.

Substrate specificity of kanamycin and kemptide

Kanamycin and kemptide were tested for cross-reactivity, as kinases are known to suffer from substrate promiscuity. [37] Samples of Kanamycin (58 µM) and kemptide (0.725 µM) were individually tested in the presence of co-factors (4.6 mM $Mg(OAc)_2$ and

200 µM ATP) with APH 3′IIIa (0.0125 mg/mL), PKA (0.5 U/µL) or no enzyme (corresponding buffer solution). The very low concentration of kemptide was chosen to bias the assay toward identification of selective APH3'IIIa inhibitors, as any off-target effects involving binding to the kemptide site of PKA should be identified when using a kemptide concentration of ~10% of K_M. Furthermore, increased concentrations of kemptide resulted in significant ion suppression of kanamycin. Further studies involved mixtures of a) kanamycin, kemptide and APH 3`IIIa, b) kanamycin, kemptide and PKA, c) kanamycin, APH 3′IIIa and PKA, d) kemptide, PKA and APH 3′IIIa and finally e) the full reaction of kanamycin, kemptide, APH 3′IIIa and PKA at the concentrations listed above. Samples turnover was monitored for conversion of substrate to product and expressed as a ratio to the internal standard, fluorescein (present at 1 µM) for comparison due to the absence of one substrate.

Instrument Response

Following optimization of reagent concentrations, the instrument response of phosphorylated kanamycin and phosphorylated kemptide was verified through construction of calibration curves. The calibration curves were constructed using ATP (100 µM, prepared in 9.2 mM NH_4OAc, pH 7.5), APH3′IIIa (0.0125 mg/mL, in 2 mM HEPES pH 7.5, 0.5 % v/v glycerol), PKA (0.0625 U/µL, in 1.4 mM potassium phosphate buffer, pH 6.8), $Mg(OAc)_2$ (0.58 mM) and NH_4OAC (9.2 mM pH 7.5) with varying substrate concentrations. The phosphorylated kemptide calibration curve was obtained by varying concentrations of kemptide (0.18-0.54 µM), while holding the concentration of kanamycin constant (58 µM) and measuring the response of the instrument (intensity of

853 *m/z*→737 *m/z*). The phosphorylated kanamycin calibration curve was obtained by varying concentrations of kanamycin (11-29 µM), while holding the concentration of kemptide constant (0.27 µM) and measuring the response of the instrument (intensity of 565 *m/z*→404 *m/z*). Final optimized conditions, taking into account both assays, required further reduction of substrate concentrations. Final conditions were 100 µM ATP (prepared in 9.2 mM NH_4OAc, pH 7.5), 0.0125 mg/mL APH3′IIIa (in 2 mM HEPES pH 7.5, 0.5 % v/v glycerol), 0.0625 U/µL PKA (in 1.4 mM potassium phosphate buffer, pH 6.8), 0.58 mM $Mg(OAc)_2$ and 9.2 mM NH_4OAC pH 7.5, 0.27 µM kemptide and 22 µM kanamycin.

Assay Validation by MALDI-MS/MS.

Using the aforementioned assay conditions, 2 µL of each of ten high controls (HC, presence of APH 3′IIIa and PKA) and ten low controls for each of the two individual reactions (LC, lack of APH 3′IIIa or PKA) were spotted onto the MALDI plate and allowed to completely dry as described above. The samples were analyzed using the AP-MALDI-MS/MS method with 1200 laser shots per sample to monitor percent turnover. Three blank samples were run between each of the set of controls (HC, LC-no APH 3′IIIa or LC-no PKA) to prevent carryover signals. Samples were tested in the presence of MeOH (0.2 % v/v), as compounds for screening will contain MeOH following reconstitution of dried library samples.

Ten high control (HC) (○) and ten low control (LC) (●) samples were included in each (PKA/kemptide and APH 3`IIIa/kanamycin) of the Z' assays. The Z' factor was

calculated using equation (1): [38] $Z' = 1-[3(\sigma_{HC}+\sigma_{LC})/(\mu_{HC}-\mu_{LC})]$, where, and σ_H and σ_L are the standard deviation of the high and low control samples, respectively and μ_H and μ_L are the average turnover of the high and low controls, respectively.

Mixture Screening.

A total of 210 compounds were obtained as 50 mM stocks in DMSO. Compounds were randomly combined into 21 mixtures of 10 compounds each and diluted in assay buffer to achieve an assay concentration of 10 μM of each compound present in 0.2% (v/v) DMSO. However, due to problems with reproducibility and ionization in the presence of DMSO, the solvent was removed from samples using a Genevac Evaporator until compound dryness was achieved. Samples were reconstituted in MeOH (0.8% v/v) for assay screening studies. Each mixture was pre-incubated with the enzyme and co-factors for 5 min at 37 °C prior to the addition of substrates (kanamycin 22 μM and kemptide 0.27 μM) and incubated for 5 min before quenching of the reaction. A selection of controls were included in the mixture screen: two low controls, one containing no PKA and one containing no APH 3`IIIa, and a high control containing no inhibitory compound. In addition, a selection of known inhibitors of one or both enzymes was included in the screen: APH 3′IIIa inhibitors tobramycin and H-7 and PKA inhibitors staurosporine, RO-31-8220 and H-7. Activity was monitored by MALDI-MS/MS through the conversion to %P.

Mixture Deconvolution.

Mixtures that caused a decrease in substrate turnover to product (%P) by a minimum of 50% were re-screened as discrete compounds against both enzymes. Each compound was screened in duplicate at a concentration of 10 μM as in the original screen. Those reducing activity of APH3′IIIa by a minimum of 50% were then examined for potency and compared to the literature.

Quantitative Assay: IC50 and KI Determination of Known Inhibitiors

IC_{50} curves were obtained for a set of control compounds; those known to inhibit either PKA or APH 3′IIIa and which were found to reduce the activity of one or both enzymes by 50% or more in the dual kinase screen. Curves were obtained by performing the assay over a concentration range of 9.4 nM to 77 μM and 100 nM to 820 μM of the inhibitory compounds, tobramycin or H-7, respectively in 0.8% v/v MeOH with 15 min reaction time following addition of substrate. Note the increase in assay time from 5 to 15 min was necessary in order to achieve more reproducible data. To confirm assay reproducibility, a curve was also obtained for a hit found in both the dual-assay described as well as the previously published assay. [24] Dose-dependent response curves were fit using the four parameter Hill equation in SigmaPlot 11.0. [39-40] The point where the relative activity was decreased by 50% was taken as the IC_{50} value and used to calculate the inhibition constant (K_I). The equation described by Cheng and Prusoff: [41] $K_I = IC_{50}/(1+[S]/K_M)$, equation (2), was used for conversion of IC_{50} values to K_I's using the concentration of substrate, [S] and Michaelis-Menten constant, K_M.

3.6 Acknowledgments

The authors thank Dr. G. D. Wright and Tushar Shakya for providing the pPCRG6 plasmid for overexpression of the APH3'IIIa enzyme. The authors thank Dr. A. Capretta for providing the EME library of compounds for screening. The authors thank the Natural Sciences and Engineering Research Council of Canada, the Canada Foundation for Innovation, the Ministry of Research and Innovation, Ontario, and MDS-Sciex for financial support of this work. JDB holds the Canada Research Chair in Bioanalytical Chemistry and Biointerfaces.

3.7 References

[1] P. Cohen, *Nat Rev Drug Discovery* **2002**, *1*, 309-315.

[2] P. Hohmann, *Int. J. Cancer* **1989**, *43*, 863-869.

[3] S. S. Taylor, J. A. Buechler, W. Yonemoto, *Annu. Rev. Biochem.* **1990**, *59*, 971-1005.

[4] G. Manning, D. B. Whyte, R. Martinez, T. Hunter, S. Sudarsanam, *Science* **2002**, *298*, 1912-1934.

[5] B. E. Kemp, R. B. Pearson, *Trends Biochem. Sci.* **1990**, *15*, 342-346.

[6] G. A. McKay, P. R. Thompson, G. D. Wright, *Biochemistry* **1994**, *33*, 6936-6944.

[7] G. D. Wright, *Expert Opin. Drug Discovery* **2010**, *5*, 779-788.

[8] G. D. Wright, *Curr. Opin. Chem. Biol.* **2003**, *7*, 563-569.

[9] G. D. Wright, *Chem. Biol.* **2000**, *7*, R127-R132.

[10] G. D. Wright, *Curr. Opin. Microbiol.* **1999**, *2*, 499-503.

[11] D. M. Daigle, G. A. McKay, G. D. Wright, *J. Biol. Chem.* **1997**, *272*, 24755-24758.

[12] M. D. Shults, I. A. Kozlov, N. Nelson, B. G. Kermani, P. C. Melnyk, V. Shevchenko, A. Srinivasan, J. Musmacker, J. P. Hachmann, D. L. Barker, M. Lebl, C. Zhao, *Chembiochem* **2007**, *8*, 933-942.

[13] M.-L. Lesaicherre, M. Uttamchandani, G. Y. J. Chen, S. Q. Yao, *Bioorg. Med. Chem. Lett.* **2002**, *12*, 2085-2088.

[14] K.-C. Ko, M. H. Choi, J. K. Rho, S. H. Park, *Sens. Actuators B* **2013**, *178*, 434-442.

[15] S. H. Park, K.-C. Ko, H. J. Gwon, *J. Labelled Compd Radiopharm.* **2007**, *50*, 724-728.

[16] M. Schutkowski, U. Reimer, S. Panse, L. Y. Dong, J. M. Lizcano, D. R. Alessi, J. Schneider-Mergener, *Angew. Chem. Int. Ed.* **2004**, *43*, 2671-2674.

[17] B. T. Houseman, J. H. Huh, S. J. Kron, M. Mrksich, *Nat. Biotechnol.* **2002**, *20*, 270-274.

[18] U. Reimer, U. Reineke, J. Schneider-Mergener, *Curr. Opin. Biotechnol.* **2002**, *13*, 315-320.

[19] D. H. Min, J. Su, M. Mrksich, *Angew. Chem. Int. Ed.* **2004**, *43*, 5973-5977.

[20] A. Liesener, A. M. Perchuc, R. Schoni, M. Wilmer, U. Karst, *Rapid Commun. Mass Spectrom.* **2005**, *19*, 2923-2928.

[21] F. Hsieh, H. Keshishian, C. Muir, *J. Biomol. Screening* **1998**, *3*, 189-198.

[22] R. Rathore, P. Pribil, J. J. Corr, W. L. Seibel, A. Evdokimov, K. D. Greis, *J. Biomol. Screening* **2010**, *15*, 1001-1007.

[23] D. H. Ko, S. H. Jun, H. D. Park, S. H. Song, K. U. Park, J. Q. Kim, Y. H. Song, J. Song, *Clin. Chem.* **2010**, *56*, 764-771.

[24] A. M. Smith, E. Awuah, A. Capretta, J. D. Brennan, *Anal. Chim. Acta* **2013**, *786*, 103-110.

[25] E. T. Gangl, M. Annan, N. Spooner, P. Vouros, *Anal. Chem.* **2001**, *73*, 5635-5644.

[26] E. M. Forsberg, J. R. A. Green, J. D. Brennan, *Anal. Chem.* **2011**, *83*, 5230-5236.

[27] M. R. N. Monton, J. M. Lebert, J. R. L. Little, J. J. Nair, J. McNulty, J. D. Brennan, *Anal. Chem.* **2010**, *82*, 9365-9373.

[28] M. J. McFadden, M. S. Junop, J. D. Brennan, *Anal. Chem.* **2010**, *82*, 9850-9857.

[29] H. Hidaka, M. Inagaki, S. Kawamoto, Y. Sasaki, *Biochemistry* **1984**, *23*, 5036-5041.

[30] L. H. Elliott, S. E. Wilkinson, A. D. Sedgwick, C. H. Hill, G. Lawton, P. D. Davis, J. S. Nixon, *Biochem.Biophys. Res. Commun.* **1990**, *171*, 148-154.

[31] B. E. Kemp, D. J. Graves, E. Benjamini, E. G. Krebs, *J. Biol. Chem.* **1977**, *252*, 4888-4894.

[32] E. Awuah, A. Capretta, *J. Org. Chem.* **2010**, *75*, 5627-5634.

[33] P. Onnerfjord, S. Ekstrom, J. Bergquist, J. Nilsson, T. Laurell, G. Marko-Varga, *Rapid Commun. Mass Spectrom.* **1999**, *13*, 315-322.

[34] F. Xiang, R. C. Beavis, *Rapid Commun. Mass Spectrom.* **1994**, *8*, 199-204.

[35] F. M. L. Amado, P. Domingues, M. G. SantanaMarques, A. J. FerrerCorreia, K. B. Tomer, *Rapid Commun. Mass Spectrom.* **1997**, *11*, 1347-1352.

[36] S. A. Trauger, W. Webb, G. Siuzdak, *Spectrosc. Int. J.* **2002**, *16*, 15-28.

[37] D. H. Fong, A. M. Berghuis, *EMBO J.* **2002**, *21*, 2323-2331.

[38] J. H. Zhang, T. D. Y. Chung, K. R. Oldenburg, *J. Biomol. Screening* **1999**, *4*, 67-73.

[39] M. J. R. Healy, *Biochem. J.* **1972**, *130*, 207-210.

[40] D. Rodbard, *Clin. Chem.* **1974**, *20*, 1255-1270.

[41] Y. Cheng, W. H. Prusoff, *Biochem. Pharmacol.* **1973**, *22*, 3099-3108.

3.8 Supporting Information

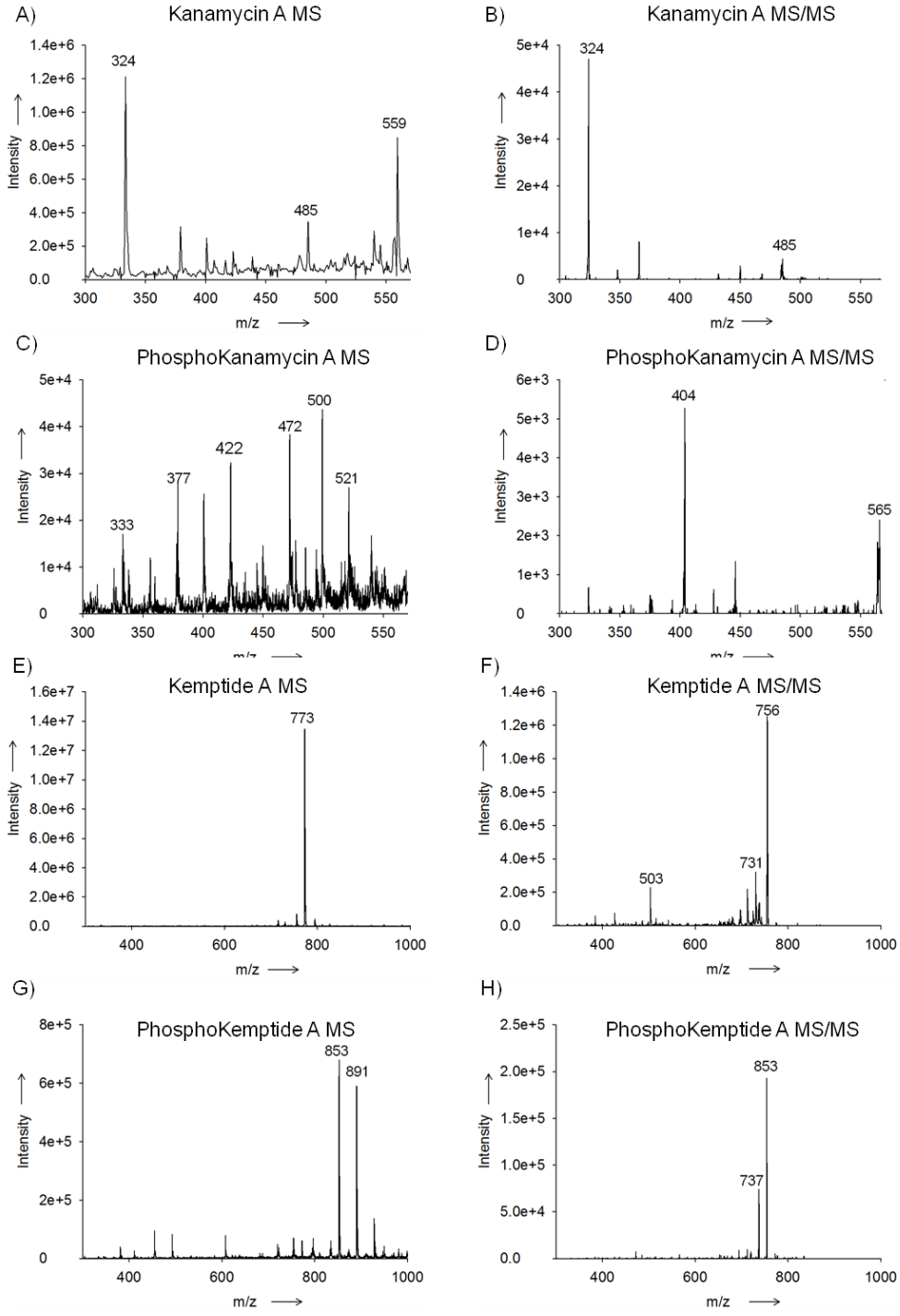

Figure S3.1: Detection of MS→ MS/MS transitions on an AP-MALDI-MS/MS for A→B) kanamycin A, *m/z* 485→ 324, C→D) phosphorylated kanamycin, *m/z* 565→404, E→F) kemptide, *m/z* 773→ 730 & 503, G→H) phosphorylated kemptide, *m/z* 853→ 737

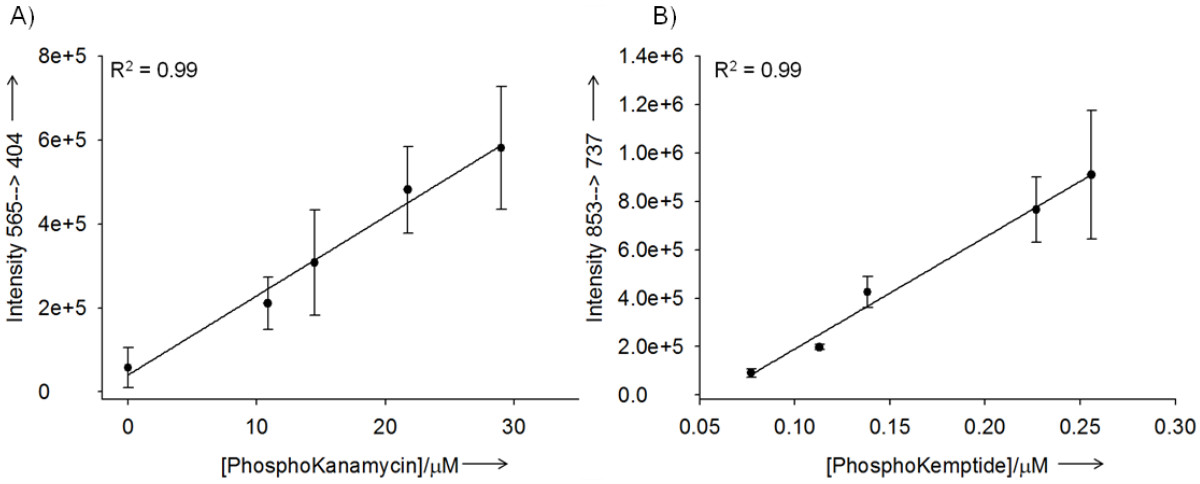

Figure S3.2: Calibration curves for A) phosphorylated kanamycin, and B) phosphorylated kemptide.

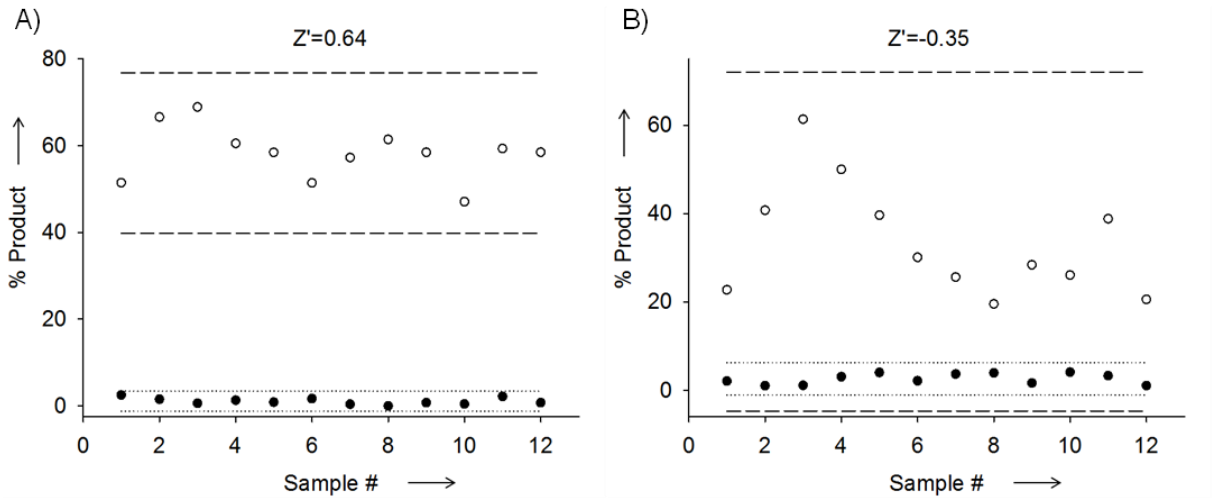

Figure S3.3: Assay Validation Plots in the presence of 0.2 % v/v DMSO A) APH 3′IIIa with kanamycin, B) PKA with kemptide.

Chapter 4 : Imaging MALDI-MS: A High Throughput Detection Method for Analysis of Kinase Inhibition on Microarrays

Author's Preface:

The following chapter provides preliminary data for the production of a high throughput kinase screening method. Elna Luckham and Mehdi Keramane provided training and instrument support on the array printer, matrix deposition system and MALDI IMS system. Brandon Aubie wrote new software to help automate data analysis and reduce processing time. I designed and performed all experiments, data collection, analysis and interpretation. I wrote the first draft of the chapter and Dr. Brennan provided editorial input to generate the final draft of the chapter.

4.1 Abstract

The rising number of new diseases and infections, and in particular the rise of resistance to existing anti-infective agents, has brought a corresponding need to increase the rate of discovery of new agents to fight infection. In turn, this has led to a need for methods to increase assay throughput so that new anti-infective agents can be discovered more rapidly. In this study we focus on modulating aminoglycoside kinases, which have the capability of phosphorylating current aminoglycoside antibiotics to render them ineffective. The key issue is that there are hundreds of protein kinases that are also essential for a variety of processes throughout the human body, and thus selective modulation of aminoglycoside kinases is critical. Unfortunately, kinases tend to suffer from poor substrate specificity, and thus methods to simultaneously screen for compounds that selectively inhibit aminoglycoside kinases and do not affect human kinases are needed. Here we describe a proof-of-principle platform for multiplexed kinase screening, whereby multiple kinases can potentially be screened simultaneously against large libraries of potential modulators using a low volume, high density imaging mass spectrometry (IMS) platform, which could reduce assay cost and time compared to typical kinase assays. Herein we report on the key steps needed to produce the multiplexed assay using a microarray platform, assess methods to optimize reproducibility and quantification of assays using IMS, and demonstrate the ability to identify inhibitors using this method.

Keywords. Imaging MALDI, high throughput screening, kinase, microarray, inhibition.

4.2 Introduction

Next to GPCR's, human kinases are the most important drug target today due their ability to control signalling pathways, the deregulation of which leads to numerous diseases including many cancers, several neurological disorders and Type II Diabetes.[1] In addition, kinase-like proteins, usually termed phosphotransferases, are found in bacteria, and have a role in phosphorylating antibiotic drugs, leading to antimicrobial resistance. Thus it is important to be able to develop new methods that can rapidly detect identify selective inhibitors of key kinases without modulating the multitude of other kinases that are required for normal physiological function. Unfortunately, this task has proven to be difficult owing to the promiscuity of kinase substrates. [2-3] The bacterial kinase aminoglycoside phosphotransferase 3`IIIa (APH 3`IIIa) is an example of a kinase that has been difficult to selectively inhibit. This enzyme, which phosphorylates aminoglycoside antibiotics, has at least 10 known aminoglycoside substrates.[4] On the other hand, it also binds adenosine triphosphate (ATP) as a co-substrate, which is a common substrate amongst human and bacterial kinases. The lack of aminoglycoside specificity coupled with the use of a common co-substrate poses serious difficulties in the identification of selective APH 3'IIIa inhibitors.

Previously we demonstrated that it was possible to simultaneously screen both APH 3'IIIa and a human kinase (protein kinase A) against mixtures of potential inhibitors to identify compounds that selectively inhibited one or the other kinase, or showed non-selective inhibition of both enzymes.[5] However, the method was relatively slow and labor intensive, required manual sample preparation, collection and data analysis, and

used relatively large volumes of reagents. As such, this assay was not ideal for scaling to simultaneous screening of tens or hundreds of kinases to more comprehensively assess the selectivity of potential inhibitors.

One method that has been demonstrated for multiplexed kinase screening is the use of microarrays. As one example, our group has demonstrated that nanovolume screening can be performed using microarrays kinases, and that inhibition assays can be performed against multiple kinases at once, increasing assay throughput and reducing assay cost.[6-8] However, this work required protein kinases and used a fluorescence readout that was not amenable to small-molecule phosphotransferases such as APH 3′IIIa. Other groups have prepared microarrays of multiple peptide substrates and have been able to assess multiple phosphorylation events related to exposure of the array to different kinases, with detection based on mass spectrometry (MS). [3] While this method did show great promise in the detection of multiple kinases within one reaction mixture, it was not amenable to small molecules (which are harder to immobilize on arrays with retention of function) and it could not be used with kinase that were very similar in function, as these would phosphorylate multiple peptide substrates, making it impossible to determine substrate specificity or selectivity of inhibition.

As shown previously, mass spectrometry is an efficient tool for detection of phosphorylation reactions and does not require radioactive or fluorescenct labels to generate a signal, instead operates in a label-free manner. [9-10] The interfacing of MS with microarrays requires the use of matrix-assisted laser desorption/ionization (MALDI) to produce ions from the microarray surface. Incorporation of imaging MALDI MS

(IMS) is a further step that has the potential to display selectivity of inhibition as a spatial image of intensity for specific mass-to-charge (m/z) ratios related to kinase substrates and products, and has been previously used for characterization of tissue microarrays. [11-12] When applied to kinase screening, the implementation of MALDI IMS could provide an enormous benefit for high throughput and low volume assays for discovery of small molecules that selectively inhibit one kinase over several others.

Herein, we show the development of an automated platform for rapid multiplexed kinase screening utilizing reaction microarrays interfaced to MALDI-IMS, which is not limited to peptide substrates. Solution-phase assays were first run manually followed by non-contact printing of assay components as a microarray onto pre-coated MALDI plates. Using high resolution imaging MALDI MS/MS, it was possible to obtain array images that could be used to quantitatively assess substrate and product concentrations for bacterial kinases and thereby assess the effect of an inhibitor of this kinase in an automated manner.

4.3 Experimental

Materials:

APH3′IIIa was expressed in an *E. coli* host and purified as described by McKay *et al.* with minor modifications.[13] Fluorescein, acetic acid, trifluoroacetic acid (TFA), α-cyanohydroxycinnamic acid (CHCA), adenosine 5'-triphosphate (ATP), magnesium acetate ($Mg(OAc)_2$), ammonium acetate (NH_4OAc), tobramycin, glycerol and kanamycin sulfate (major component A, minor components B and C), were purchased from Sigma Aldrich (Oakville, ON). All water was distilled and deionized (25 °C, 18.2 MΩ·cm, 1-5

ppb TOC). Pre-spotted anchor chips (PAC-96 well format) were purchased from Bruker Daltonics. All other reagents were of analytical grade and were used as received.

Methods:

APH3'IIIa Assay Conditions.

Kinase assays were performed in the solution phase and then transferred to a MALDI plate for analysis. Assay conditions were similar to those reported previously[5, 14] with minor alterations. All assays were performed by pre-incubation of the enzyme with co-factors for 5 minutes at 37 °C. Reactions were commenced with the addition of substrate, kanamycin (prepared in 9.2 mM NH_4OAc, pH 7.5) followed by incubation for 15 minutes at 37 °C. Final assay conditions utilized 100 µM ATP (prepared in 9.2 mM NH_4OAc, pH 7.5), 0.0125 mg/mL APH3′IIIa (stored in 2 mM HEPES pH 7.5, 0.5 % v/v glycerol), 22 µM kanamycin, 0.58 mM $Mg(OAc)_2$ and 9.2 mM NH_4OAC, pH 7.5. Reactions were quenched by adding an equal volume of MeOH (containing 0.1 % trifluoroacetic acid and 2% glycerol) when using PAC plates or with matrix solution (6.2 mg/mL CHCA in methanol containing 1 % acetic acid and 1 µM fluorescein) in all other cases.

Microarray Deposition of Matrix and Analytes.

Analyte samples were deposited onto the desired surface using a Scienion SciFlexArrayer S5 Non-Contact Microarray Printer. Three methods were utilized to form microarrays of reaction mixtures that were co-crystallized with MALDI matrix. These were: 1) printing of premixed matrix:analyte solutions onto glass, Indium Tin Oxide (ITO) coated or metal slides; 2) aerosol deposition of matrix using an ImagePrep MALDI matrix sprayer

(Bruker Inc) with overprinting of arrays; and, 3) directly printing the reaction components onto PAC plates that were precoated with a MALDI matrix.

Microarray printing of the solutions was performed using a PDC60 nozzle (resulting in ~260 pL/drop) and a dot pitch of 275 µm. Crucial steps of the deposition method included aspiration of a low volume of analyte (3 µL) from the reaction plate and formulation of the printed solution to allow formation of spherical drops that could be reproducibly dispensed as judged by video imaging of the droplet produced at the tip of the nozzle. In general, this required addition of small amounts of glycerol to adjust viscosity into the optimal range for printing.

Imaging MALDI-TOF Detection of Product and Substrate Ions.

MALDI-IMS analysis was performed using an Ultraflexextreme MALDI-TOF/TOF mass spectrometer (Bruker Inc.) using a Smartbeam^{TM} –II 355 nm laser with a repetition rate of 1 kHz, a pulse width of 100 ns, and a focal diameter of 50 µm to provide sufficient spatial resolution to collect multiple spectra across each array element. Mass analysis was done with a TOF operated in reflectron mode, and data were acquired in imaging mode using a 4 GHz digitizer. Spectra were acquired from the sum of 500 laser shots per spot. The ion source used voltages of 25.00 kV and 22.30 kV for ion sources 1 and 2 respectively, a lens voltage of 7.70 kV and reflectors 1 and 2 set at 26.43 and 13.38 kV respectively. Spectra were obtained for samples of both kanamycin and phosphorylated kanamycin following the APH3'IIIa reaction, as described previously.

Data Analysis.

While the use of IMS with a TOF mass analyzer provides rapid qualitative analysis, quantitative analysis requires both significant care in sample preparation as well as several steps to normalize, manipulate and integrate data peaks. To address the latter issue, a program was produced to automate data analysis. After manually selecting a region of interest within each microarray spot using the FlexImaging software provided by Bruker, the averaged spectrum was exported as a CSV file and imported into mMass (available at mmass.org) to convert to an ASCII/txt file. This file was imported into custom Spectrometer Analysis software (available at birg.mcmaster.ca), which defines a floor cutoff, peak threshold, and area height (value used to calculate peak area) for user specified peaks. In this case, the values were 0.1, 0.2 and 0.05 for peaks related to substrate (m/z = 507.227) and product (m/z = 587.194) respectively, to integrate the designated peaks and ratio the areas, which were expressed as percent conversion to product (%P =100*P/(P+S); where the user must manually multiply by 100).

Instrument Response.

The instrument response to kanamycin and phosphorylated kanamycin was verified through construction of two calibration curves obtained using IMS of reaction microarrays printed onto the PAC-96 well plates. Calibration curves were constructed in the absence of presence of APH 3′IIIa with all other co-factors present. Curves were obtained for a range of concentrations (13 - 101 µM for substrate calibration curve, 13 - 61 µM for product calibration curve) with monitoring of either substrate (507.227 m/z) or product (587.194 m/z) signals. Note that it was not necessary to use MS/MS analysis as

these two peaks were sufficiently removed from any matrix noise peaks to allow for quanification. Quantitative data was extracted from the imaged surface using the peak area as calculated from the Spectrometer Analysis software. The optimal concentration of kanamycin was selected as 22 μM to obtain adequate product turnover.

APH3´ IIIa Assay Validation by MALDI-IMS.

Assay validation was done in two steps, involving the initial determination of a Z' factor followed by construction of an IC_{50} curve for a known inhibitor, tobramycin. The Z' validation was performed by printing three drops of each analyte solution containing, unreacted kanamycin at a concentration of 22 μM in the presence of co-factors and absence of APH3'IIIa (low control, LC) or 22 μM of kanamycin in the presence of co-factors and APH3'IIIa (high control, HC) to produce phosphokanamycin following a 15 minutes reaction. Each LC and HC sample was deposited onto the PAC spot in a 2x2 array, with formation of 10 arrays for each type of sample. Analyte samples contained 0.2 % (v/v) MeOH prior to quenching to account for the solvent that would be present when screening compounds. [5] Following analyte deposition the samples were analyzed using the MALDI-TOF imaging spectrometer and the Z′ factor was calculated using equation (1): [15] $Z' = 1-[3(\sigma_{HC}+\sigma_{LC})/(\mu_{HC}-\mu_{LC})]$ (1) where σ_H and σ_L are the standard deviation of the high and low control samples, respectively and μ_H and μ_L are the average turnover of the high and low controls, respectively. Dose-response curves were constructed using a range of concentrations of tobramycin (19 nM – 80 μM) in 0.2 % (v/v) MeOH with the reaction conditions outlined above.

4.4 Results and Discussion

Printing of Reaction Microarrays.

Reaction microarrays were optimized on a variety of surfaces including glass, ITO coated glass, metal slides and PAC plates. The main parameters for ideal spotting included no bleeding from one spot into the next (i.e. spots too close together), uniform spot sizes (accurate dispensing), and perhaps the most important factor for MALDI imaging, uniform matrix crystallization. Uncoated glass surfaces, which would require the application of a conductive coating, resulted in uncontrollable bleeding of spots into one another, irreproducible printing and irregular spot sizes. ITO coated slides, while commonly used in MALDI tissue imaging, did not work well for microarray imaging owing to uneven matrix crystallization, regardless of whether a mixture of matrix and analyte was printed or matrix was overprinted onto analyte spots, as shown in Figure 4.1A. The uneven crystallization lead to poor resolution and limited ionization in imaging experiments. Furthermore, because of the uneven crystallization, spot sizes were found to be highly variable. The Bruker ImagePrep system was also examined as a means to obtain uniform matrix deposition onto the aforementioned ITO coated slides. However, this system also produced uneven crystallization from one region of the slide to the next and the formation of large crystals (Figure 4.1 B), both of which resulted in a poor resolution in imaging MS.

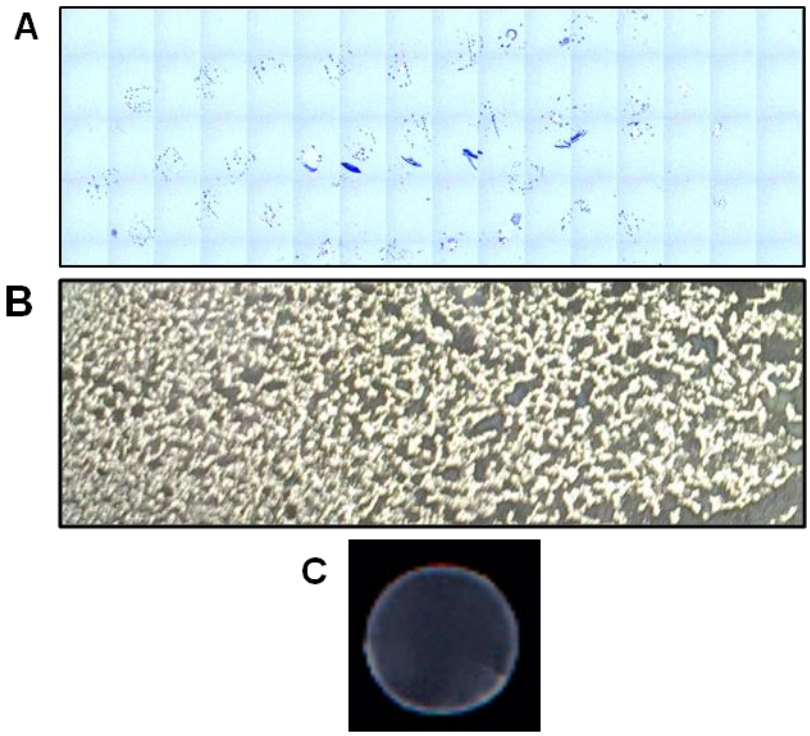

Figure 4.1: Types of CHCA matrix crystallization. A) Deposition of matrix using the Scienion SciFlex Arrayer. B) Matrix deposition using the Bruker ImagePrep system. C) Pre-spotted AnchorChip technology by Bruker.

On the other hand, highly reproducible arrays could be obtained through the use of prespotted anchorchip (PAC) plates (Figure 4.1C). The PAC plates used in this study has matrix (CHCA) prespotted on specific locations with a diameter of 800 µm and spacing of ~4.5 mm between spots, limiting the total number of array elements that could be printed to 4 per PAC spot, or 384 per plate (Figure 4.2). Given the dimensions of each array element (ca. 250 µm), a uniformly matrix coated PAC plate (7.7 x 11.7 cm) could theoretically fit as many as 122000 microarray spots on it, where a uniformly coated microscope slide could result in ~25000 microarray spots on a single slide. Both options

would allow for a high quantity of reactions to be monitored in quick succession and greatly increase the throughput. The use of microarray technology greatly reduces the cost of assays, primarily though reduction of assay volume, and can increase throughput owing to the potential for parallelization of some assay steps. Based on our reaction conditions and printing paramters, our arrays contained approximately $4.5x10^5$ molecules per μm^2 or about 10^8 molecules per array element in our assay.

Each new PAC plate was also tested for location specificity by printing and viewing digital images of a 2x2 array in the corner positions, with any variation corrected from plate-to-plate to fit the full 2x2 array in each spot. The precoated matrix plates provided a surface with uniform matrix crystallization for deposition of arrays (Figure 4.2).

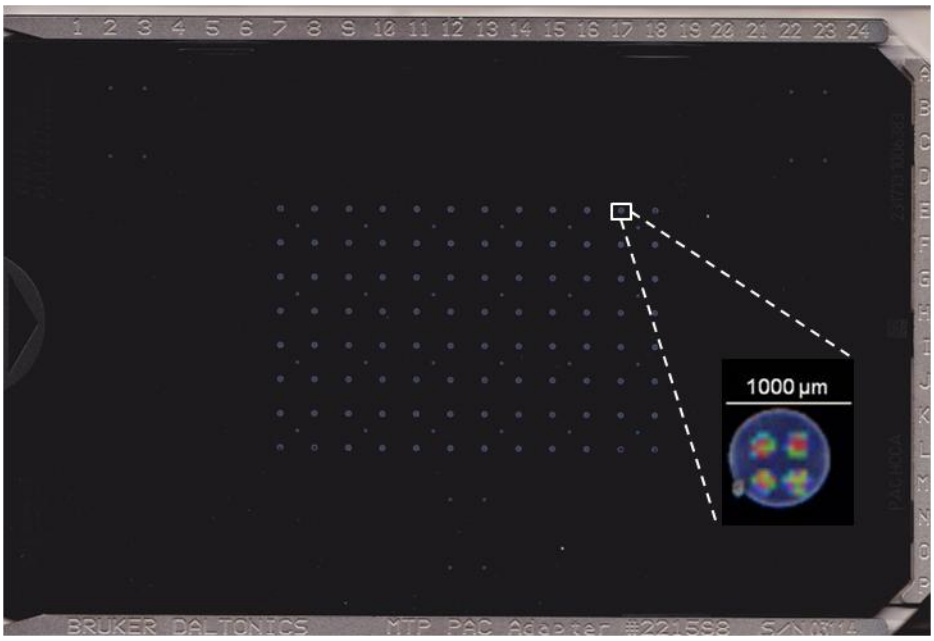

Figure 4.2: PAC-96 plate with a small array within one of the 800 µm spots.

Imaging MALDI-TOF Detection of Product and Substrate.

MALDI-MS was chosen as the given detection method due the presence of moderately high ionic strength, resulting from the co-factors of the reaction, and based on previous successes using a similar method. [5, 14] In addition to those benefits previously mentioned, the current MALDI-TOF system provides the further benefit of imaging capability, which could increase assay throughput due to rapid qualitative identification of hits, and the ability to obtain high mass resolution data, reducing the need for MS/MS experiments. Following deposition of analytes using a microarray platform (Figure 4.3A) and with the aforementioned detection method, the substrate molecule kanamycin was found adducted to Na^+ with a theoretical monoisotopic mass of 507.227 Da (Figure 4.3B). The phosphorylated product was also found to be in agreement with its adducted form with a theoretical monoisotopic mass of 587.194 Da (Figure 4.3C); both values were collected within 0.003% of the theoretical value.

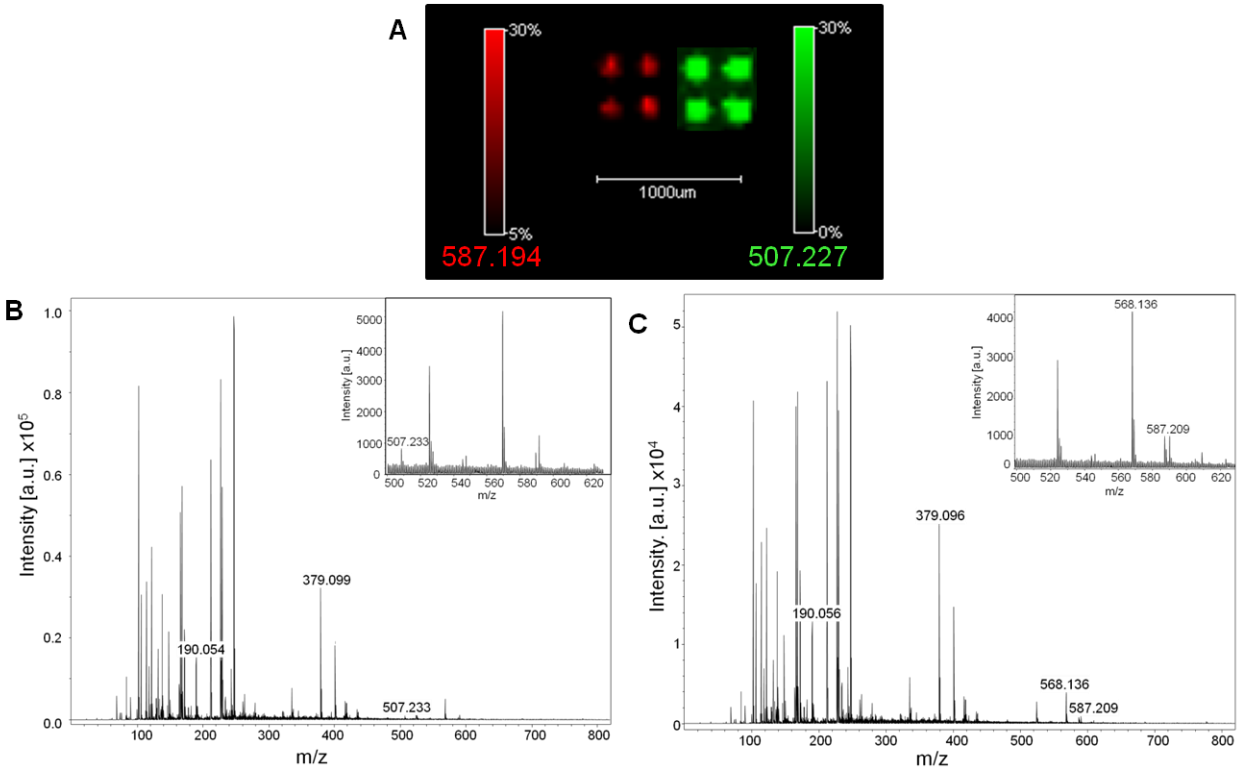

Figure 4.3: A) Deposited analyte spots as a microarray for both product (red) and substrate (green). MS spectra of B) kanamycin and C) phosphorylated kanamycin in the presence of co-factors obtained on a Bruker Ultraflexextreme MALDI MS.

Instrument Response.

The response of the MALDI-IMS instrument to varying concentrations of both kanamycin and phosphorylated kanamycin was found through construction of two calibration curves. Both curves were repeated in triplicate in addition to the 2x2 replicate array of each analyte concentration. Qualitative information was denoted through the increasing color intensity, as shown in Figure 4.4A. Following calibration, the peak area for the 507.227 Da peak was extracted to obtain quantitative data resulting in R^2 values of 0.97 and 0.99 for kanamycin (Figure 4.4B) and phosphorylated kanamycin (Figure 4.4C) respectively, illustrating the utility of the platform for obtaining quantitative data.

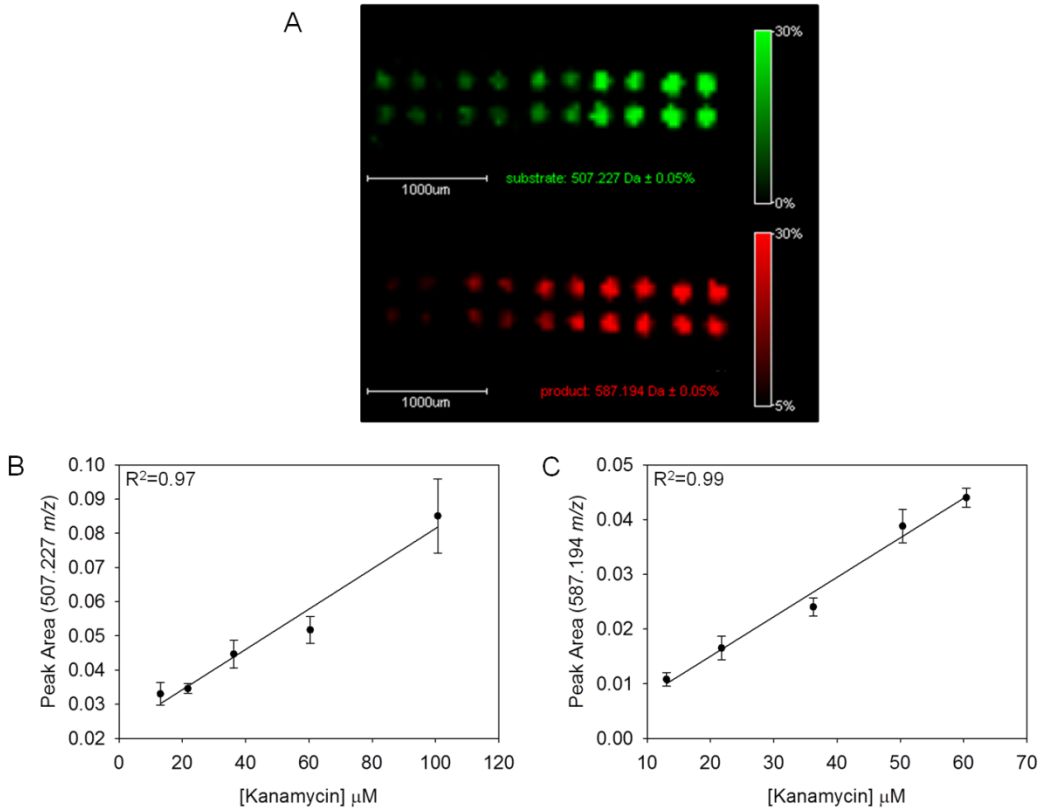

Figure 4.4: Kanamycin calibration curve A) Qualitative images obtained by selecting an m/z of 507.227 Da (green) or 587.194 Da (red). B) Quantitative calibration curve obtained by integrating the 507.227 m/z peak. C) Quantitative calibration curve obtained by integrating the 587.194 m/z peak.

APH3′IIIa Assay Validation by MALDI-MS.

Previously, we showed that while MALDI-MS was typically not used for obtaining quantitative data, that the use of internal standards, and more specifically, the use of a product-to-substrate ratio (P/(P+S)) provided an excellent internal standard for obtaining quantitative data (Z′, IC_{50}, etc.). [5, 14] A Z′-factor was once again obtained in this study,

however we used only MS, rather than MS/MS data due to the high mass resolution capabilities discussed previously. Ten replicates of each HC and LC were used in calculation of the Z′-factor resulting in a value of 0.80, which corresponds to an excellent assay, characterized by the large gap between HC and LC, as well as minimal deviation between replicates (Figure 4.5).

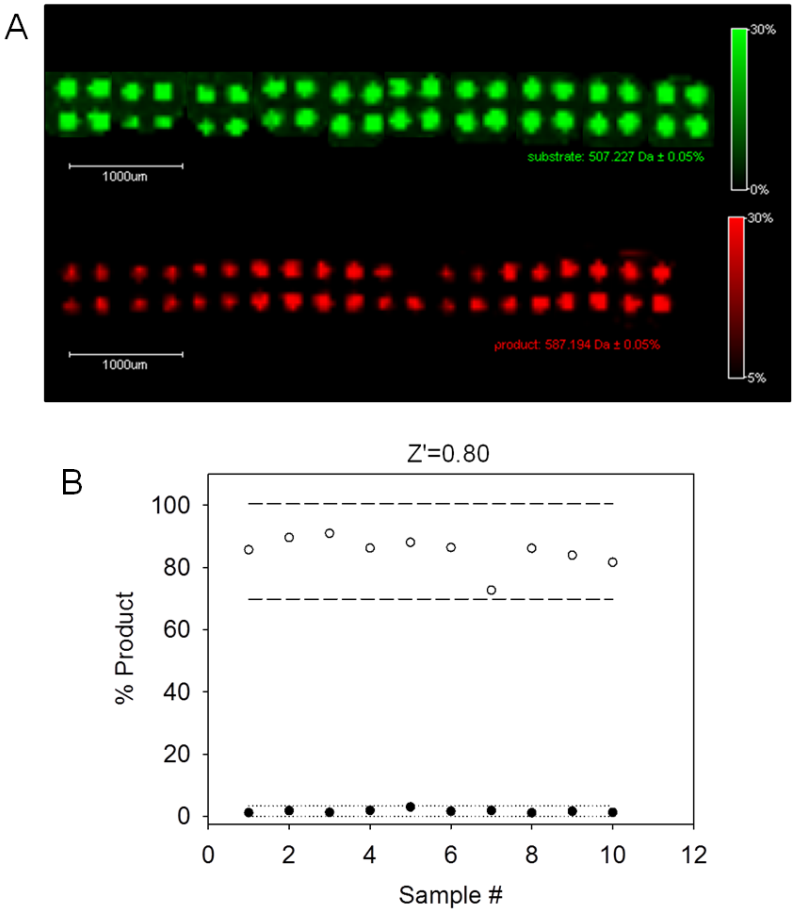

Figure 4.5: A) Image of Z´ data signifies qualitative data of the reaction of 3′IIIa with kanamycin in the presence of 0.2% v/v MeOH. B) Quantitative Z´plot. Dashed lines signify 3 standard deviations of high and low control averages.

Secondary validation procedures were performed by producing a quantitative dose-dependent response curve with a known inhibitor, tobramycin (Figure 4.6).

Through the use of the Cheng-Prusoff equation,[16] the inhibition constant of tobramycin was found to be 1.6 ± 0.5 µM, which is in excellent agreement with the theoretical value of 2 µM.[13] As previously discussed, obtaining quantitative data on MALDI-MS instruments is a well known difficulty. Reduction of the error bars seen in Figure 4.6 may allow for a smoother curve fit and hence a more accurate IC_{50} and K_I value.

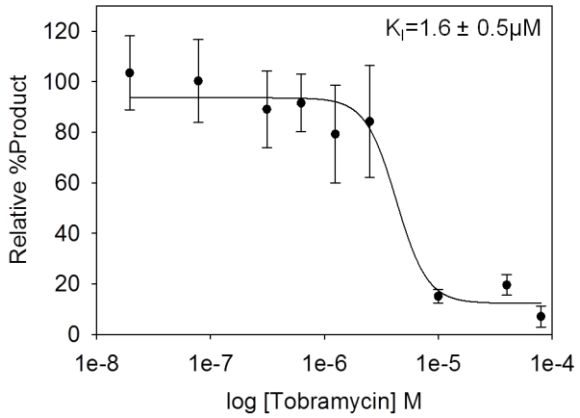

Figure 4.6: Dose-response curve of known inhibitor tobramycin.

4.5 Conclusions

Imaging MALDI-MS of microarrays has shown promise for the use as a kinase screening platform. While difficulties in matrix deposition were encountered, they were addressed through the use of PAC plates for uniform matrix deposition and high quality imaging data. Assay validation further showed the utility of the platform for screening studies with generation of an excellent Z′-factor. The imaging microarray platform was also tested for accurate identification of inhibition with a known inhibitor, tobramycin. Following several software or instrument advances, including alternative matrix

deposition methods such as sublimation and further automation of data acquisition and processing, the platform could be used for screening kinases in a multiplexed high density array.

4.6 Acknowledgements

The authors thank Dr. G. D. Wright and Tushar Shakya for providing the pPCRG6 plasmid for overexpression of the APH3'IIIa enzyme. The authors also thank Elna Luckham and Mehdi Keramane of the Biointerfaces Institute for their assistance with microarray printing and MALDI-IMS, and Brandon Aubie of the Biointerfaces Institute for producing the Spectrometry Analysis software. The authors thank the Natural Sciences and Engineering Research Council of Canada, the Canada Foundation for Innovation, the Ministry of Research and Innovation, Ontario, and MDS-Sciex for financial support of this work. JDB holds the Canada Research Chair in Bioanalytical Chemistry and Biointerfaces.

4.7 References

[1] P. Cohen, *Nature Reviews Drug Discovery* **2002**, *1*, 309-315.

[2] M. D. Shults, I. A. Kozlov, N. Nelson, B. G. Kermani, P. C. Melnyk, V. Shevchenko, A. Srinivasan, J. Musmacker, J. P. Hachmann, D. L. Barker, M. Lebl, C. Zhao, *Chembiochem* **2007**, *8*, 933-942.

[3] D. H. Min, J. Su, M. Mrksich, *Angewandte Chemie International Edition* **2004**, *43*, 5973-5977.

[4] D. H. Fong, A. M. Berghuis, *Embo Journal* **2002**, *21*, 2323-2331.

[5] A. M. E. Smith, J. D. Brennan, *Chembiochem* **2014**, *15*, 587-594.

[6] X. Ge, J. M. Lebert, M. R. N. Monton, L. L. Lautens, J. D. Brennan, *Chemistry of Materials* **2011**, *23*, 3685-3691.

[7] M. Schutkowski, U. Reimer, S. Panse, L. Y. Dong, J. M. Lizcano, D. R. Alessi, J. Schneider-Mergener, *Angewandte Chemie International Edition* **2004**, *43*, 2671-2674.

[8] K. Y. Horiuchi, Y. Wang, S. L. Diamond, H. Ma, *Journal of Biomolecular Screening* **2006**, *11*, 48-56.

[9] D. T. McLachlin, B. T. Chait, *Current Opinion in Chemical Biology* **2001**, *5*, 591-602.

[10] N. Ibarrola, D. E. Kalume, M. Gronborog, A. Iwahori, A. Pandey, *Analytical Chemistry* **2003**, *75*, 6043-6049.

[11] M. R. Groseclose, P. P. Massion, P. Chaurand, R. M. Caprioli, *Proteomics* **2008**, *8*, 3716-3724.

[12] D. S. Cornett, M. L. Reyzer, P. Chaurand, R. M. Caprioli, *Nature Methods* **2007**, *4*, 828-833.

[13] G. A. McKay, P. R. Thompson, G. D. Wright, *Biochemistry* **1994**, *33*, 6936-6944.

[14] A. M. Smith, E. Awuah, A. Capretta, J. D. Brennan, *Analytica Chimica Acta* **2013**, *786*, 103-110.

[15] J. H. Zhang, T. D. Y. Chung, K. R. Oldenburg, *Journal of Biomolecular Screening* **1999**, *4*, 67-73.

[16] Y. Cheng, W. H. Prusoff, *Biochemical Pharmacology* **1973**, *22*, 3099-3108.

4.8 Supplementary Information

Software or instrument advancements required for large scale screening

- Automated designation of probe (analyte) location from 384-well plate to target (PAC plate) in Scienion software
- Automated designation of analyte spots from PAC plate for MALDI analysis
    - Circle selection tool would reduce the time for manually drawing around each PAC spot
    - A preloaded PAC plate in the software would allow the user to select spots to analyze with a simple click of a button
    - Readable files with array positions from Scienion arrayer to the MALDI-IMS instrument would provide the ideal solution.
- Access to a sublimation unit
    - Could provide an alternative reproducible matrix deposition method
    - Uniform coating of slide would make designating location for Scienion microarray spotting and MALDI positioning quicker and allow a greater density of array elements on each surface
    - Creation of uniform matrix coated ITO slides by Bruker, similar to the PAC plates would provide the same aforementioned benefit at a much greater ease.
- Data analysis software
    - More unified and simplified manner for data analysis that allows the user to export the spectra as a txt files from FlexImaging would prove useful in expediating data analysis

Chapter 5 : An Automated Materials Screening Approach for the Development of Sol-Gel Derived Monolithic Silica Enzyme Reactor Columns

Author's Preface:

The following chapter was published as a full paper in the journal RSC Advances under the citation:

Anne Marie E. Smith, Jordan Fortuna, Erica M. Forsberg and John D. Brennan, **An automated materials screening approach for the development of sol-gel derived monolithic silica enzyme reactor columns**, RSC Advances, **2014**, 4, 15952-15960.

Jordan Fortuna collected the data for the AChE entrapped silica reactor columns involving both IMER and dose-response under the supervision of myself and Erica M. Forsberg. Erica M. Forsberg also collected preliminary data not included in this chapter. I designed and performed all other experiments, data collection, analysis and interpretation. I wrote the first draft of the manuscript and Dr. Brennan provided editorial input to generate the final draft for submission.

This chapter describes a process by which silica enzyme reactor columns can be developed and fabricated. The process is amenable to the entrapment of a variety of enzymes and has been tested in the presence of the robust enzyme, AChE for the purpose of proof of principle. Implementation of this process to a reactor column fabricated for the entrapment of kinases could improve the high throughput nature of the previously described platforms through enzyme re-use, reducing assay cost. Mounting the column

on a nano-LC system with integration to a fractionation or spotting device could again further increase throughput providing an alternative platform for inhibitor screening.

5.1 Abstract

Fabrication of monolithic protein-doped capillary columns was reported almost 10 years ago. These columns were derived from a diglycerylsilane precursor, however this material is not commercially available, is difficult to produce in large quantities and has very short phase separation and gelation times, which leads to issues with column reproducibility. Herein, we investigate the use of sodium silicate (SS), a commercially available biofriendly sol-gel precursor, for the fabrication of bimodal meso/macroporous protein-doped monolithic silica columns that are suitable for immobilized enzyme reactor (IMER) assays. Using an automated liquid handler and platereader, a hierarchical materials screening approach was applied to ~1400 formulations, from which we have identified materials with long gelation times that can form robust bimodal meso/macroporous materials suitable for fabrication of monolithic silica columns. A subset of these materials was observed to have good chromatographic behavior (appropriate backpressure and good stability). A secondary screen around lead materials was performed to identify optimal materials for fabrication of IMER columns. These materials were tested for leaching and activity of immobilized acetylcholine esterase to identify an optimal material for IMER column fabrication. The optimal material was formed from 2% (w/v) silica which was combined with 1.25% PEG 600 at pH 6.4 in 100 mM TRIS buffer. Such columns showed reproducible IMER performance and were able to quantitatively measure the inhibition of immobilized AChE by galanthamine with an inhibition constant of 175 ± 5 nM, which is in excellent agreement with the literature value.

Keywords: sodium silicate, sol-gel process, bioaffinity, automated screening

5.2 Introduction

Sol-gel processing has been employed as a means of creating biologically-doped materials for a variety of applications, including biosensing, small molecule screening and bioaffinity chromatography. Early studies utilized tetramethylorthosilicate (TMOS) or tetraethylorthosilicate (TEOS), which proved to be detrimental to the stability of biological species owing to evolution of alcohol (methanol and ethanol, respectively) during hydrolysis of the precursor.[1,2] Later studies utilized more "biofreindly" precursors and processing conditions, such as materials that had alcohol byproducts removed by evaporation prior to introduction of biological species,[3] novel synthetic silica precursors that did not liberate alcohol[4,5] such as polyglyceryl silicate (PGS)[6] and diglycerylsilane (DGS),[5,7-15] or commercially available precursors such as sodium silicate.[4]

For the development of monolithic protein-doped columns it is necessary to produce a material that undergoes spinodal decomposition (phase separation) prior to gelation in order to produce macropores that allow liquid flow with reasonable backpressure. The silica skeletons around the macropores must also have a high proportion of mesopores, which are critical for entrapping the protein within the column. Prior work from Nakanishi's group demonstrated that TEOS or TMOS based materials could be used to form monolithic columns with bimodal meso/macroporous pore morphology. However, the processing conditions (high alcohol concentration, low pH, heating to condense the silica) were not compatible with protein entrapment.[16] Our group reported on the fabrication of monolithic columns using a biocompatible processing method with the DGS precursor.[12] However, there are two key issues with the use of this precursor for

column fabrication: 1) DGS is not commercially available and can be produced only in limited quantities; and 2) the phase separation and gelation time of DGS under the conditions used for column fabrication are very short (<5 min), making column fabrication challenging and leading to poor column-to-column reproducibility.[8]

The key goals of this study were to apply an automated formulation and screening approach to evaluate the potential of the commercially available biofreindly precursor sodium silicate as a precursor for column fabrication, and to identify reaction conditions that provided long phase separation and gelation times (> 2 hr). We chose sodium silicate as we have previously reported on the ability to form macroporous films using this precursor.[17] Our approach, which is similar to that previously reported to identify materials for microarray fabrication,[18,19] utilized a hierarchical screening approach where rapid, low information content methods were used initially, followed by progressively slower but higher information methods on hits that passed the prior stage of screening. However, while microarray fabrication focused on the ability to print the materials, have them remain adhered and crack-free after printing on a surface, and ultimately be compatible with a fluorescence assay, the parameters that affect column performance related primarily to the ability to generate macroporous materials that have low backpressure and retain a significant amount of active protein under pressure driven flow.

For column screening, we first used automated liquid handlers for high-throughput formulation, and platereaders to evaluate phase separation and macropore formation (which leads to an opaque material). From ~1440 initial formulations, those that passed the initial screen were further tested for uniformity (i.e., monolith formation vs.

flocculation), gelation time, mechanical stability, and finally performance in column format (backpressure, leaching). A small secondary screen was then done around a lead material, based on activity for an entrapped enzyme, to find an optimal material. From our screening data we also identified the key formulation parameters (including pH, buffer type and concentration, amount and molecular weight of poly(ethylene glycol) porogen, inclusion of glycerol) that led to the development of an optimal macroporous SS derived material with long working times. The entrapment of acetylcholine esterase (AChE) into SS derived monolithic capillary columns, and the use of such columns as immobilized enzyme reactors (IMER) is shown.

5.3 Results and Discussions

High Throughput Screening Studies*:*

Figure 5.1 shows the overall screening workflow, the criteria used to assess "hit" compositions, and the number of compositions that passed through each stage of the screening process. A large selection of materials, derived from a total of 1440 formulations, were originally created using varying silica concentrations, buffer types and concentrations (which control gelation time) pH values (which control gelation and phase separation times), and polymer concentrations and molecular weights (which control the timing and extent of phase separation). These 1440 formulations were first studied for opacity by measuring the absorbance at 400 nm, which increases for macroporous materials owing to increased scattering from the silica particles.

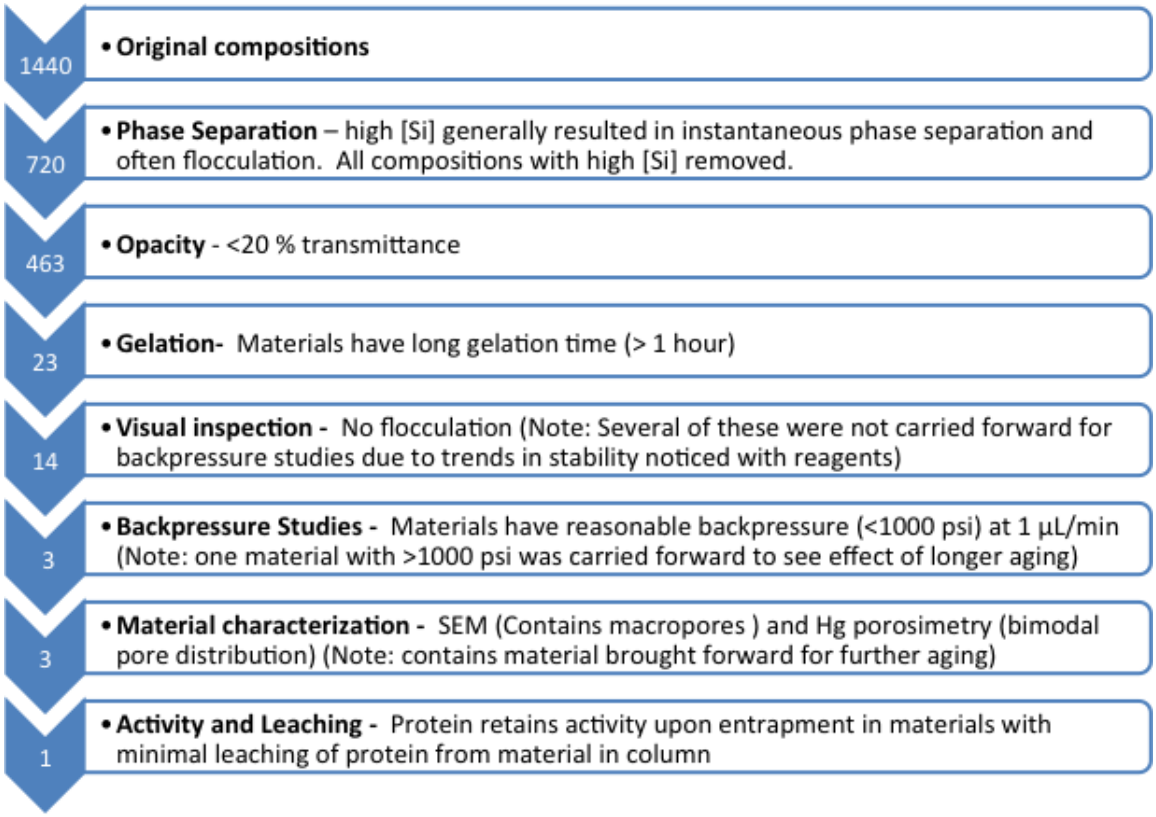

Figure 5.1: Approach to optimization of materials. A selection of materials were chosen and optimized for porosity and mechanical stability through opacity, backpressure, SEM, porosimetry and activity based techniques.

Figure 5.2 (HEPES) and supplementary Figures S5.1 (TRIS) and S5.2 (BIS-TRIS) show how the opacity changes as a function of buffer concentration, pH, and PEG concentration and molecular weight, and demonstrates that lower PEG molecular weights give an ability to finely tune the opacity, while higher molecular weight PEG have only a narrow range over which opacity can be tuned. Macroporosity increases with higher concentrations and molecular weights of PEG, as higher amounts of polymer will drive phase separation due to the repulsive interaction between the solvent mixture (buffer) and the PEG/silica oligomers.[20] However, high concentrations and molecular weights of PEG

were found to result in flocculation, likely due to the instability and lack of solubility of the PEG chains and were thus not generally used for further studies.

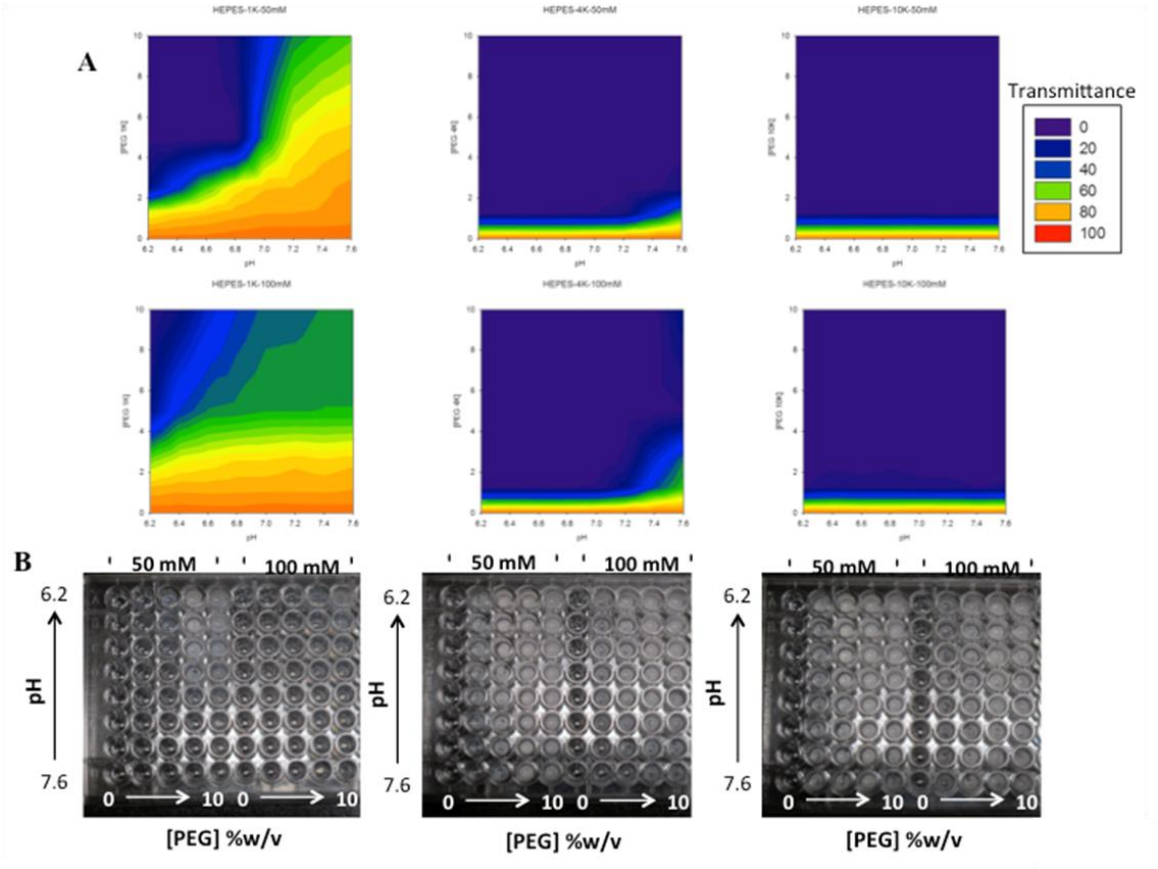

Figure 5.2: A) Opacity plots of a selection of materials tested. Scale bar indicates % transmittance. B) Optical images of materials showing a range in opacity.

Decreases in pH produced more macroporous materials, as lower pH samples have longer gelation times,[16,21] and hence samples have time to phase separate before the material gels and locks in the specific pore morphology allowing only minimal changes in porosity with time. Hence, low pH buffers were key in creating materials amenable to column fabrication, as seen previously with DGS materials.[8] Materials made of high concentrations of silica were generally observed to undergo very rapid gelation or

flocculation (particle aggregation prior to gelation) under almost all conditions, and were thus removed from further study.

A final parameter tested in the initial screen was phase separation and gelation time. Gelation normally occurs after phase-separation, and so, the point at which phase-separation occurs is taken as the earliest point at which gelation could occur. Phase separation time was tested for all 463 materials with <20% transmittance while gelation time was tested only for those materials with phase-separation times over 1 h. Gelation cannot be determined in an automated fashion using our current instrumentation. As such, we used a manual method wherein the gelation time was monitored by tilting the microwell plate and assessing the time when the sample was unable to flow. Once this occurred we also assessed whether the material formed a self-supporting solid by scraping a pipette tip along the surface of the material – if the tip moved across the surface only, the material was gelled, if it moved through the material it was not gelled, and if particles stuck to the tip it showed that flocculation had occurred, likely as a result of rapid aggregation of sol particles before they could form a self-supporting gel;[22] these materials were also removed from further study. Based on these preliminary screens of the 1440 initial formulations, half (720) of the compositions with high silica concentrations were removed as these flocculated or gelled too quickly, and a total of 463 low silica concentration formulations were sufficiently macroporous to move forward. Of these, only 23 showed gelation times of over 2 h, and only 14 of these formed self-supporting monoliths. The compositions of these 14 materials are listed in Table 5.1. The general trend existing within this selection is that a low PEG percentage and molecular weight

results in formation of self-supporting monoliths. Interestingly, while trends for pH, PEG and buffer concentrations were consistent with previous reports, phase separation has not previously been observed when using low molecular weight PEG (MW < 10,000) with the DGS or TEOS systems.[8,16,20] This unexpected finding may be a function of the fact that the SS materials are fully hydrolyzed and partially condensed prior to addition of PEG, and do not contain either glycerol or ethanol byproducts, which could help promote spinodal decomposition even with low molecular weight PEG.

Buffer	[Buffer] mM	pH Buffer	PEG MW Da	[PEG] %
HEPES	100	6.2	1000	5
HEPES	50	6.8	1000	10
HEPES	100	7.6	4000	5
TRIS	50	7.2	1000	1.25
TRIS	50	7.4	1000	1.25
TRIS	100	7.0	1000	1.25
TRIS	100	7.2	1000	1.25
TRIS	100	7.4	1000	2.5
TRIS	100	7.0	10000	1.25
BIS-TRIS	50	6.2	1000	1.25
BIS-TRIS	50	6.4	1000	1.25
BIS-TRIS	50	6.6	1000	1.25
BIS-TRIS	100	6.2	1000	1.25
BIS-TRIS	100	6.4	1000	1.25

Table 5.1: Compositions of materials proceeding past the final test of the initial screen.

To further probe material compositions, Figure S5.3 shows the absorbance vs. time for a small sub-library of 13 materials which formed self-supporting monoliths, both with and without glycerol (12.5% v/v) added, since glycerol is a known protein stabilizer and is a byproduct of the DGS based fabrication of columns. At this stage we also evaluated PEG 600 as a porogen based on our finding that PEG 1K was most often observed to form robust macroporous columns with extended gelation times, and we wanted to see if

even lower MW PEG would further extend gelation time and still produce a macroporous robust material. We found that the use of PEG 600 further extended the phase separation time, but tended to form materials that were often less opaque and thus not sufficiently macroporous. In addition, we found that the glycerol-doped materials tended to have a significantly delayed phase separation and slightly lower transmittance than those without glycerol, indicative of somewhat more macroporous materials relative to those without glycerol. However, glycerol-doped materials tended to be softer and less mechanically robust, as judged by scraping a pipette tip across the surface of the material, and thus were not further evaluated for column development. The effect of glycerol concentration on material properties was not fully assessed, and will be the subject of a follow up study.

Column Chromatography.

The 14 materials discovered in the initial screen, along with one material from the sub-library above (Material M1) were used to prepare monolithic columns within 150 µm i.d. polyimide coated capillaries. These initial studies used untreated capillaries that were simply washed with water and ethanol to clean the inner surface prior to use. At this stage some columns showed excessive backpressure (insufficient porosity), some showed a rapid rise followed by a dramatic drop in backpressure, indicative of collapse of the material in the column (insufficient cross-linking), some detached from the capillary wall and thus produced flow channelling (no backpressure) and excretion of silica materials from capillaries, while a subset of materials were sufficiently robust to withstand moderate pressure (~1000 psi) without material collapse (supplementary Table S5.1). We

note that pull away can in some cases be addressed by either activating the column walls with base or by grafting of 3-aminopropyltriethoxysilane (APTES), or by reduction of inner diameter of the capillary (see below). However, we chose the wider bore column with APTES activation for this stage of screening to provide a more stringent test of column performance. A total of 3 column materials produced stable backpressure values of <1000 psi, and were thus considered to be sufficiently macroporous and mechanically stable to be used as column materials. This included one material (material iv) that was originally showing high backpressure at short aging times and was retested after 15 days to produce adequate backpressure values.

Qualitative Pore Assessment by SEM.

A selection of three materials showing either adequate or excessive backpressure values were further assessed for macroporosity by SEM imaging, which gives a qualitative assessment of the morpohology of the material. In general, the SEM images were found to correspond well with backpressure measurements previously obtained. Sample i and iv of Figure 5.3 are highly cross-linked materials and these had been observed to have a higher backpressure that caused the instrument to overpower as flow rate was increased. The moderately cross-linked structure seen in sample ii (Figure 5.3) was also one of the materials that showed a backpressure of < 1000 psi, and thus was expected to be useful for column fabrication as the higher percentage of macropores should allow for a lower backpressure, while the mesopores will allow for a biomolecule to be readily entrapped, and retained within the sol-gel-derived material. Material iii was not tested as it failed the

backpressure test owing to the column being excreted from the capillary at high pressure (see Supplementary Table S5.1).

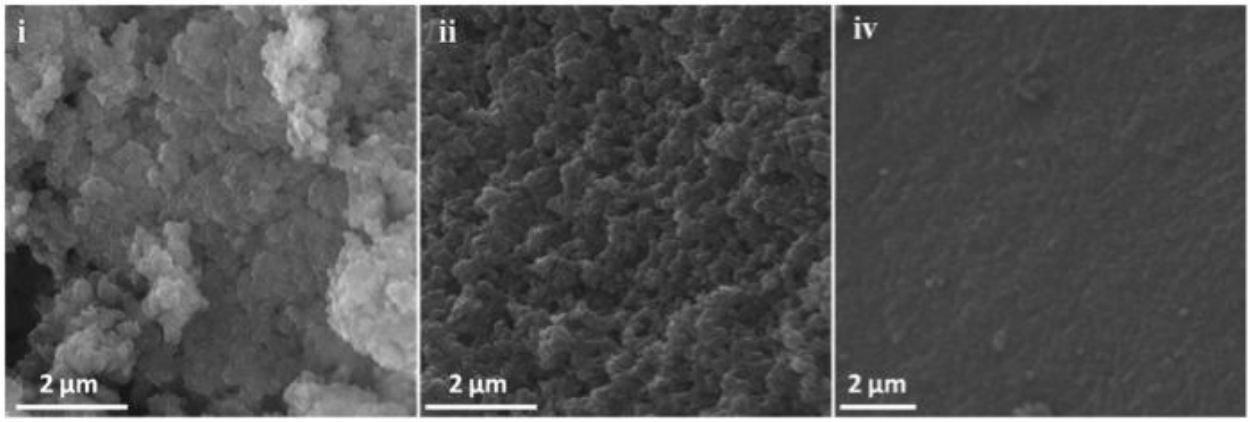

Figure 5.3: i/ii) SEM images of materials found with adequate backpressure at 1 µL/min. Materials showing macropores in SEM image were included in further optimization studies. iv) Material allowed to age longer due to lack of macropores.

Quantitative pore assessment by Hg Porosimetry.

The morphology of materials that showed acceptable backpressure values was quantitatively assessed using mercury intrusion porosimetry (Figure S5.4A), which provides information on the size and pore volume of macropores. Columns with good performance generally showed a bimodal pore structure (two peaks in pore size distribution plots), with one peak in the mesopore range and the second in the macropore range (Figure S5.4). Initial work suggested that the bimodal structure seen in Figure S5.4B (Material ii) was more desirable for column fabrication, however later work described below showed that materials with a morphology similar to that shown in Figure S5.4C (Material iv) were actually more amenable to column fabrication with proteins,

since polycondensation continues as the materials age, resulting in the formation of more macropores.

Leaching and Activity Studies.

Materials amenable to column fabrication and chromatography that showed prolonged gelation times, enabling uniform column casting, and a combination of meso and macropores were examined for enzyme leaching and activity. At this stage, a small sub-library of materials was prepared using PEG 600 as a porogen to perform "lead optimization" on Material M1 (aka material iv) so as to further fine tune the materials for chromatography applications by further modifying pH and buffer concentrations over a narrow range. The optimized monolith compositions were used to synthesize columns in APTES activated columns with or without AChE at a final concentration of 42.5 U/mL and were investigated using the Ellman assay and galanthamine, a weak inhibitor of AChE. Activity was detected using a UV-Vis flow cell interfaced to an Eksigent LC pump using column types 1-6 (Table S5.2). Columns 1-4 were active and responsive to galanthamine addition/removal during the analysis following an 8 day curing period (Figure 5.4A), while columns 5 and 6 were found to be too mesoporous and required further aging (15 days) to fully form the required bimodal pore structure. However, columns showed varying stability ranging from complete stability (column 1) to low stability (column 2-4) as determined by the large drop in activity over the progress of the experiment (Fig. 4A). It is expected that the reduction in activity is most likely due to protein leaching from the silica monoliths as a result of the size and/or quantity of

macropores and so these materials were deemed unsuitable. All of columns 1-4 showed low activity after 15 days, and were not tested further.

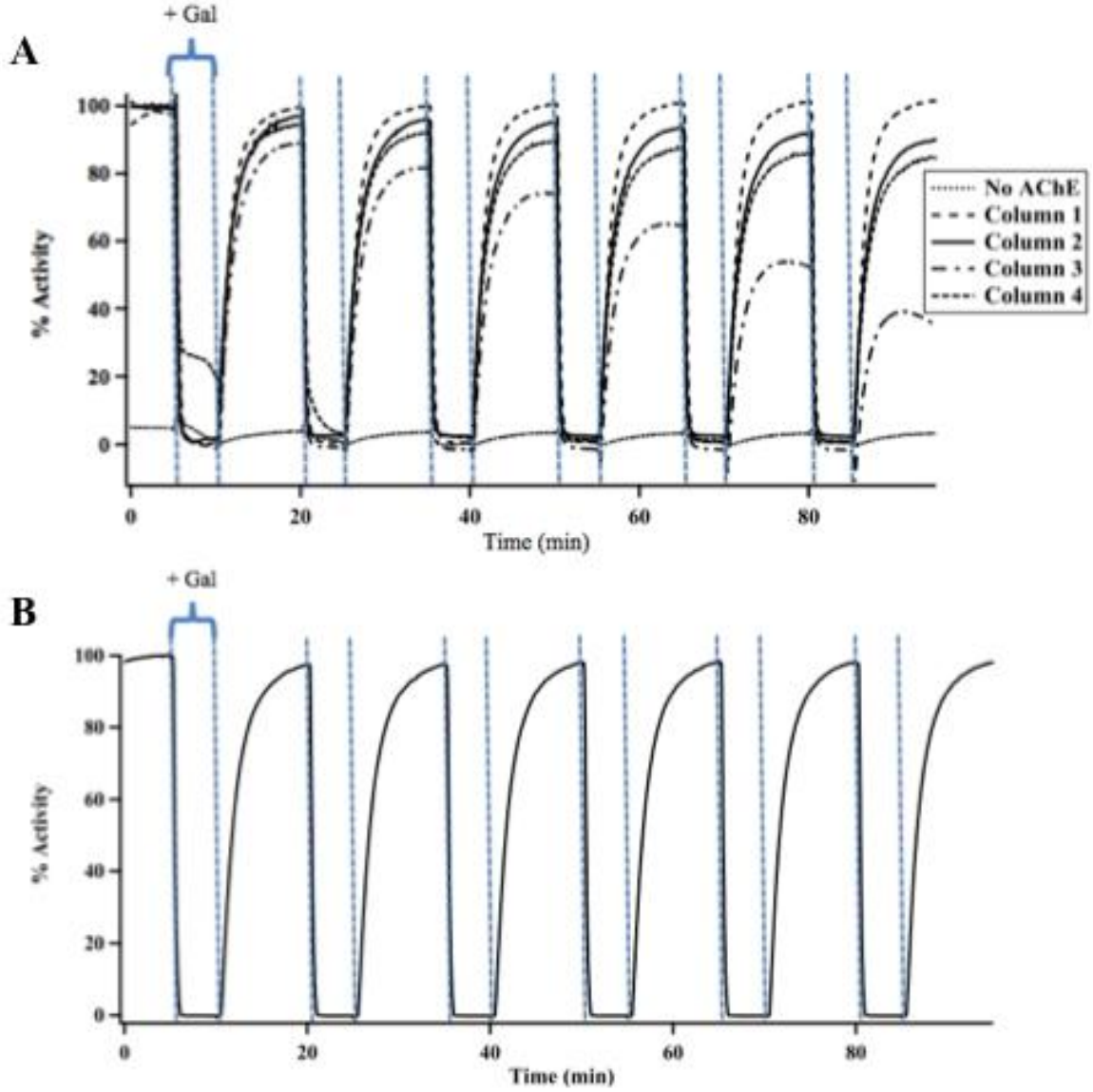

Figure 5.4: AChE activity over time in SS-derived columns measured in IMER mode. A. Activity of column 1 returns to a constant level in comparison leaching seen in column 2 (10% reduction), column 3 (60 % reduction) and column 4 (15% reduction) over the course of the trial. B. Following 15-day storage, column 6 showed reproducible activity with no leaching over throughout the duration of the trial. The dashed lines indicate the addition of galanthamine. Activity was determined through absorbance measurements at $\lambda = 412$nm.

Analysis of columns 5 and 6 eight-to-ten days post-synthesis was not possible due to extremely high backpressures in the columns and thus no flow of mobile phase through the column (data not shown). However, 15 days after synthesis these columns were not only capable of mobile phase flow-through and high enzyme activity (illustrated here with column 6), but also remained stable over the duration of an IMER experiment (Fig. 4B). This data suggests an increase in macroporosity over time (as previously seen in Figure S5.3A/B), and indicates that 15 days is the minimum aging time to form stable columns. Column 6 was tested for on-column inhibition of entrapped AChE by injecting increasing concentrations of the inhibitor galanthamine, ranging from 0.025 μM to 1.60 μM (Fig. 5A) with injections performed for 5 minutes followed by a 10 minute buffer rinse between injections. Increasing galanthamine concentrations lead to an increase in inhibition with activity returning to baseline upon removal of the inhibitor (~100 % activity). The experimentally determined K_I value was 175 ± 5 nM (error based on curve fitting, Figure 5.5B), which is in excellent agreement with the previously determined K_I of galanthamine in a DGS derived material of 180 nM. [19]

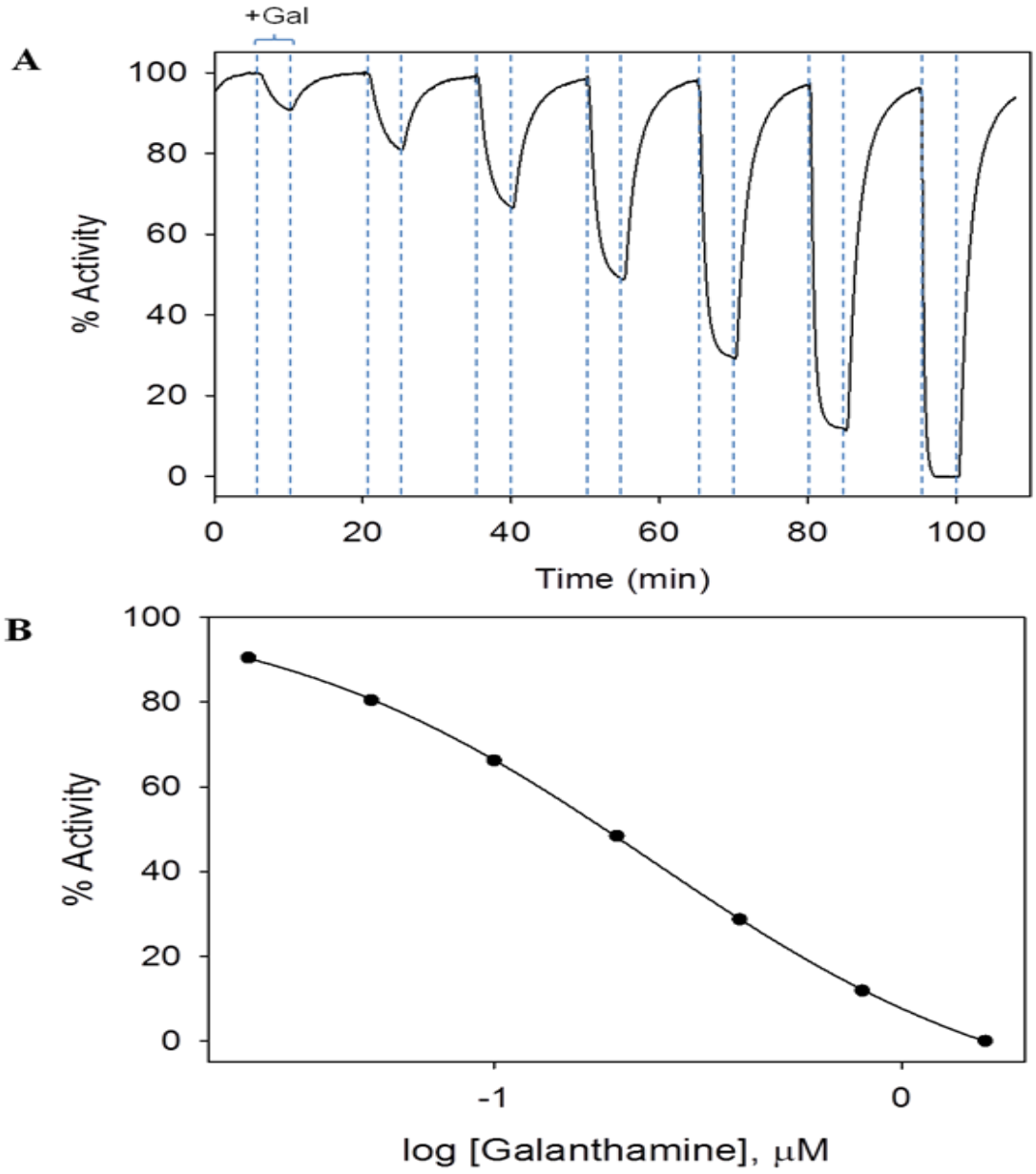

Figure 5.5: AChE-doped SS-derived columns are active in a dose-dependent manner. A) Inhibition of AChE by galanthamine in column 6: at varying concentrations of galanthamine (0.025, 0.050, 0.100, 0.200, 0.400, 0.800, 1.600 μM). Column activity decreases with increasing galanthamine concentration and is restored after removal of inhibitor. B) Dose-response curve of AChE in the presence of increasing concentrations of galanthamine. Activity was determined through absorbance measurements at λ = 412nm.

When compared to DGS columns, the SS-based columns show longer phase separation and gelation times, leading to much longer working time to prepare columns, which has been shown to lead to more reproducible columns.[9] In addition, the SS columns demonstrate phase separation using low molecular weight PEG (MW = 600 or 1000), which has not been previously observed for DGS columns. A potential drawback of SS columns is the need for a much longer aging time (15 days) to provide stable materials; relative to as little as 5 days for DGS derived columns.[8] Even so, the data clearly show that SS materials can be used to form IMER columns, and provide high activity and stability for entrapped AChE, allowing for on-column evaluation of inhibitor potency.

5.4 Experimental Section

Materials.

Poly(ethylene) glycol (PEG, 600-10,000 Da), tris(hydroxymethyl)aminomethane (TRIS), 4-(2-hydroxyethyl)-1-piperazineethanesulfonic acid (HEPES), Bis(2-hydroxyethyl)amino-tris(hydroxymethyl)-methane (BIS-TRIS), acetylcholinesterase (AChE) from *Electrophorus electricus* (EC 3.1.1.7), acetylthiocholine iodide, galanthamine, 5,5'-dithiobis(2-nitrobenzoic acid) (DTNB), Dowex 50x8-100 cation exchange resin and Ludox HS-40 were obtained from Sigma Aldrich (Oakville, ON). Sodium silicate (SS solution, ultrapure grade, ~14 % Na_2O, ~29 % silica) was obtained from Fisher Scientific (Pittsburgh, PA). Glycerol was purchased from Fluka Biochemika (Buchs, Switzerland). Ammonium acetate was purchased from Caledon Laboratory Chemicals (Georgetown, Ontario, Canada). Fused silica tubing (100 and 150 μm i.d.)

was purchased from Polymicro Technologies (Phoenix, AZ, U.S.). Polystyrene 96-well plates were purchased from Costar (Corning, NY). All water was distilled and deionized using a Milli-Q synthesis A10 water purification system. All other reagents were of analytical grade and were used as received.

General Procedures.

Preparation of Sodium Silicate Sol.

A primary screen of 1440 materials was performed using a range of silica compositions prepared from: two silica concentrations (2% and 7.3% w/v SiO_2), three buffer types (TRIS, BIS-TRIS, HEPES) at two concentrations (50 or 100 mM) and 8 pH values (6.2-7.8, 0.2 pH steps), and tested with three polymers (PEG 1K, PEG 4K, PEG 10K) at five concentrations (0, 1.25, 2.5, 5 or 10% w/v). Secondary screens evaluated additional buffer concentrations (25 mM), an additional molecular weight of PEG (600 Da) and evaluated a selection of materials with addition of glycerol (12.5 %, v/v, ~2:1 molar ratio glycerol:Si). Samples derived solely from sodium silicate were prepared as described elsewhere. [4,7] Briefly, the sol was prepared by diluting 2.6 g of sodium silicate in 10.0 ml of *dd*H_2O. This solution was then passed through Dowex strong cation-exchange resin (5.5 g) for 2.5 minutes, followed by additional filtration with a 0.2 µm membrane syringe filter to yield a sol solution with a pH of ~4 [23] with a working time of approximately one day. It should be noted that the preparation of the Dowex resin is a critical step in the resulting sol chemistry. The most consistent sols were prepared by adding Dowex resin (300 mL) to a plastic beaker, enough hydrochloric acid (0.1 M) to cover the resin was

then added and the mixture was stirred for 1 hour using a magnetic stirrer. The resulting solution was filtered with a Büchner funnel, followed by rinsing with *dd*H_2O until the filtrate was clear. The resin was left under vacuum until dry and transferred to sealed vials for use in sol preparation. High concentration SiO_2 samples were derived from a combination of sodium silicate and Ludox AM30. Materials were prepared mixing dilute sodium silicate (3.6 % SiO_2, 61.8 µL) with Ludox in HCl (32.2% SiO_2/0.8 M HCl 38.2 µL) forming the concentrated silica sol.

Preparation of Silica Monoliths for Screening of Opacity.
Monoliths for screening studies were prepared by mixing 50 µL of PEG (varying MW and % w/v) with 50 µL of buffer (varying type, concentration and pH) and 100 µL of the SS precursor sol (4.0 % or 14.5 % SiO_2 prior to addition of buffer/PEG) into a well of a 96-well clear bottom microplate, followed by immediate mixing using a pipette based Biomek FX liquid handler to move liquid in and out of the pipette tip 5 times; the use of disposable pipette tips is important in work with silica sols to prevent gelation within syringe-based liquid dispensers. Glycerol containing monoliths were prepared by dispensing 50 µL of PEG (varying MW and % w/v) with 25 µL of buffer (varying type, concentration and pH), 25 µL of glycerol (anhydrous) and 100 µL of the high or low concentration SS precursor sol. Following mixing, plates were left for 8 h and then placed into a plate reader (Tecan M1000) to monitor absorbance at 400 nm, which increases upon spinodal decomposition, indicating a macroporous material. Any samples that showed a transmittance of < 20% and formed self-supporting monoliths were retested by

monitoring absorbance as a function of time over an 8 h period to assess the time when phase separation occurred. Gelation time was also determined for these samples in a manual test involving scraping a pipette tip across the surface of the sol-gel derived material to determine which samples that formed self-supporting monoliths and which had flocculated and thus had particle clusters dispersed in the remaining liquid.

Preparation of Monolithic Chromatography Columns for Backpressure Studies. Monolithic columns were prepared for opaque silica compositions with gelation times ranging from 2 to 8 hours that did not show flocculation. Materials were mixed as previously stated (final volume 200 µL) and infused into 60 cm of 150 µm i.d. polyimide coated fused silica capillary. Columns were laid flat at room temperature in air until gelation occurred. Following sufficient time for aging (three times the gelation time), the ends of the capillaries were immersed into Eppendorf tubes containing the same final concentration of buffer as the respective material and the Eppendorf tubes were covered with Parafilm^{TM} to prevent evaporation of buffer and drying of the materials. The materials were further aged for 3-7 days at 4 ºC, and in some cases for up to 15 days before testing. Columns were then cut into 5 cm length pieces, the initial 10-15 cm at each end was discarded, and columns were formed from the central region, giving a minimum of six columns segments from each full length capillary. These columns were attached to an Eksigent nanoLC pump (Dublin, California, U.S.A.) using standard UpChurch Scientific fittings and pH 7.5 NH_4OAc was introduced to the column from

both channels A and B at a total flow rate of 1 µL/min to measure backpressure and column robustness.

Porosity Studies.
Materials showing sufficient opacity, no flocculation and an ability to withstand moderate backpressure were prepared as bulk monoliths for SEM imaging and mercury porosimetry studies using 75 times the original volume of each reagent (15 mL final volume). These materials were mixed with a vortexer immediately upon addition of the SS precursor sol to the aqueous solution. Gelation was assessed as before. Following gelation, bulk monoliths were aged for 10 days followed by washing with water, three times a day for 3 days to remove excess salts, PEG and/or glycerol. For SEM imaging, the samples were dried at 80 ºC (3 hours) followed by heating to 120 ºC (16.5 hours), placed on carbon tape and sputter coated with platinum (5 nm) followed by imaging on a TESCAN VP-SEM to qualitatively assess the porosity of the materials. Samples were further heated, and calcined at 200 ºC (3.5 hours), 350 ºC (4 hours), 500 ºC (1 hour) and finally 600 ºC (2 hours) followed by removal from the furnace and storage in a desiccator for Hg porosimetry studies. The macropore morphology of the materials was quantitatively assessed using Hg intrusion porosimetry measurements on a Quantachrome Poremaster® GT mercury intrusion porosimeter using methods described elsewhere.[12]

Synthesis of AChE Doped Columns.
Materials that showed good column performance were doped with acetylcholinesterase for testing of on-column enzyme activity. These studies used a capillary with a lower

inner diameter (100 μm i.d.) and the capillary walls were activated to promote silica bonding and reduce radial shrinkage. Activation involved flushing the capillary tubing with 3 bed volumes of 1.0 M NaOH, 1.0 M HCl, ddH_2O and finally EtOH. The capillary tubing was then baked at 120 °C for 4-5 hours followed by cooling and storage at room temperature. For column-casting purposes, 100 μL of the 2% SiO_2 SS sol was added to 50 μL of TRIS buffer (with or without AChE) and 50 μL of 600 Da PEG at the optimized reagent concentrations determined from secondary screening studies. The final AChE concentration in the mixture was calculated to be 42.5 U/mL. The solutions were vortexed and injected into the activated 100 μm i.d. fused silica capillaries using a syringe pump. After casting, columns were left to gel (ca. 2 h) and aged for three times the gelation time at room temperature, followed by storage at 4 °C for a minimum of 3 days to allow monolith curing/formation. Prior to column testing, a syringe pump was used to remove impurities (buffer salts and excess PEG) by flowing 20 mM NH_4OAc, pH 7.0 through 5 cm column sections (bed volume of 0.4 μL containing 0.017 U of AChE) at a variety of flow rates (0.5μL/min, 2μL/min, 5μL/min, and 10μL/min) for a total of 10 min at each flow rate. The ammonium acetate buffer was chosen to allow comparisons to previous studies of AChE IMERs that were formed using DGS.[24]

Activity and Inhibition of AChE in Sodium Silicate Derived Columns.

A 2 channel Eksigent nanoLC pump was used for mobile phase delivery to a GL Sciences Inc. Model 701 UV-Vis detector equipped with a 6 nL flow-cell (40 μm i.d., 4 mm path length) (Veldhoven, Netherlands). Eksigent nanoLC software v 2.08 was used to control

mobile phase delivery and attain absorbance chromatograms using the UV-Vis detector. Channel A of the nanoLC contained DTNB and ATCh (100 μM each in 20 mM NH_4OAc, pH 7.0). Channel B contained a similar solution to that found in channel A with the addition of galanthamine (2.5 μM), an inhibitor of AChE. Mobile phase delivery was set to a rate of 10 μL/min and programs were created to test both IMER and dose-dependent inhibition involving cycling between flow from channels A and B, or running a step gradient from 100% A to 100% B in 7 equal steps (15 min each). All absorbance measurements were made at 412 nm to monitor the colorimetric by-product 2-nitro-5-thiobenzoate (NTB) produced from the Ellman assay [25] .

5.5 Conclusions

The use of a hierarchical screening approach allowed the screening of a large number of materials quickly using a rapid assay (transparency), and the attrition of materials was such that slower, higher information content methods could be applied to a small number of materials to identify optimal leads for column fabrication. Development of small sub-libraries around primary leads allowed the identification of an optimal column material composed of 2% SiO_2, 100 mM TRIS, pH 6.4, 1.25 % PEG 600, which was shown to be suitable for IMER studies. This material had a long gelation time, providing sufficient time to reproducibly fabricate columns, and was able to retain the activity of an entrapped enzyme for at least 15 days. Unlike columns formed from TEOS or DGS, the SS derived materials could undergo phase separation to form macroporous materials using low molecular weight PEG (600 or 1000 Da), which leads to slower phase separation and

gelation, but also to continued evolution of the final material over a period of weeks. Interestingly, the optimal materials initially showed a high backpressure after 1 week of aging, but further evolved over a second week to become sufficiently macroporous to support flow. Future studies will investigate the long-term stability and reproducibility as a function of column aging and methods to scale up the production of columns. When compared to trial and error methods to develop monoliths, the screening approach is far more efficient as it avoids the need to prepare and test individual columns manually, and allows far more materials to be assessed in a short time, which provides a significant amount of data to allow modeling and thus better understanding the factors that affect column performance.

5.6 Acknowledgements

The authors thank the Natural Sciences and Engineering Council of Canada for operating grant support and the Canada Foundation for Innovation and Ministry of Research and Innovation, Ontario for infrastructure funding in the Centre for Microbial Chemical Biology and the Biointerfaces Institute. J.D.B. holds the Canada Research Chair in Bioanalytical Chemistry and Biointerfaces.

5.7 References.

(1) Ellerby, L. M.; Nishida, C. R.; Nishida, F.; Yamanaka, S. A.; Dunn, B.; Valentine, J. S.; Zink, J. I. *Science* **1992**, *255*, 1113-1115.

(2) Yamanaka, S. A.; Nishida, F.; Ellerby, L. M.; Nishida, C. R.; Dunn, B.; Valentine, J. S.; Zink, J. I. *Chemistry of Materials* **1992**, *4*, 495-497.

(3) Ferrer, M. L.; del Monte, F.; Levy, D. *Chemistry of Materials* **2002**, *14*, 3619-3621.

(4) Bhatia, R. B.; Brinker, C. J.; Gupta, A. K.; Singh, A. K. *Chemistry of Materials* **2000**, *12*, 2434-2441.

(5) Brook, M. A.; Chen, Y.; Guo, K.; Zhang, Z.; Brennan, J. D. *Journal of Materials Chemistry* **2004**, *14*, 1469-1479.

(6) Gill, I.; Ballesteros, A. *Journal of the American Chemical Society* **1998**, *120*, 8587-8598.

(7) Besanger, T. R.; Chen, Y.; Deisingh, A. K.; Hodgson, R.; Jin, W.; Mayer, S.; Brook, M. A.; Brennan, J. D. *Analytical Chemistry* **2003**, *75*, 2382-2391.

(8) Besanger, T. R.; Hodgson, R. J.; Green, J. R. A.; Brennan, J. D. *Analytica Chimica Acta* **2006**, *564*, 106-115.

(9) Besanger, T. R.; Hodgson, R. J.; Guillon, D.; Brennan, J. D. *Analytica Chimica Acta* **2006**, *561*, 107-118.

(10) Hodgson, R. J.; Besanger, T. R.; Brook, M. A.; Brennan, J. D. *Analytical Chemistry* **2005**, *77*, 7512-7519.

(11) Hodgson, R. J.; Brook, M. A.; Brennan, J. D. *Analytical Chemistry* **2005**, *77*, 4404-4412.

(12) Hodgson, R. J.; Chen, Y.; Zhang, Z.; Tleugabulova, D.; Long, H.; Zhao, X. M.; Organ, M.; Brook, M. A.; Brennan, J. D. *Analytical Chemistry* **2004**, *76*, 2780-2790.

(13) Lin, T. Y.; Wu, C. H.; Brennan, J. D. *Biosensors & Bioelectronics* **2007**, *22*, 1861-1867.

(14) Sui, X. H.; Lin, T. Y.; Tleugabulova, D.; Chen, Y.; Brook, M. A.; Brennan, J. D. *Chemistry of Materials* **2006**, *18*, 887-896.

(15) Braun, S.; Rappoport, S.; Zusman, R.; Avnir, D.; Ottolenghi, M. *Materials Letters* **1990**, *10*, 1-5.

(16) Nakanishi, K. *Journal of Porous Materials* **1997**, *4*, 67-112.

(17) Carrasquilla, C.; Li, Y. F.; Brennan, J. D. *Analytical Chemistry* **2011**, *83*, 957-965.

(18) Ge, X.; Lebert, J. M.; Monton, M. R. N.; Lautens, L. L.; Brennan, J. D. *Chemistry of Materials* **2011**, *23*, 3685-3691.

(19) Monton, M. R. N.; Lebert, J. M.; Little, J. R. L.; Nair, J. J.; McNulty, J.; Brennan, J. D. *Analytical Chemistry* **2010**, *82*, 9365-9373.

(20) Nakanishi, K.; Soga, N. *Bulletin of the Chemical Society of Japan* **1997**, *70*, 587-592.

(21) Iler, R. K. *The Chemistry of Silica*; John Wiley and Sons: New York, 1979.

(22) Rodriguez, R.; Rojas, G.; Estevez, M.; Vargas, S. *Journal of Sol-Gel Science and Technology* **2002**, *23*, 99-105.

(23) Rupcich, N.; Nutiu, R.; Li, Y. F.; Brennan, J. D. *Analytical Chemistry* **2005**, *77*, 4300-4307.

(24) Forsberg, E. M.; Green, J. R. A.; Brennan, J. D. *Analytical Chemistry* **2011**, *83*, 5230-5236.

(25) Ellman, G. L.; Courtney, K. D.; Andres, V., Jr.; Feather-Stone, R. M. *Biochemical Pharmacology* **1961**, *7*, 88-95.

5.8 Supporting Information

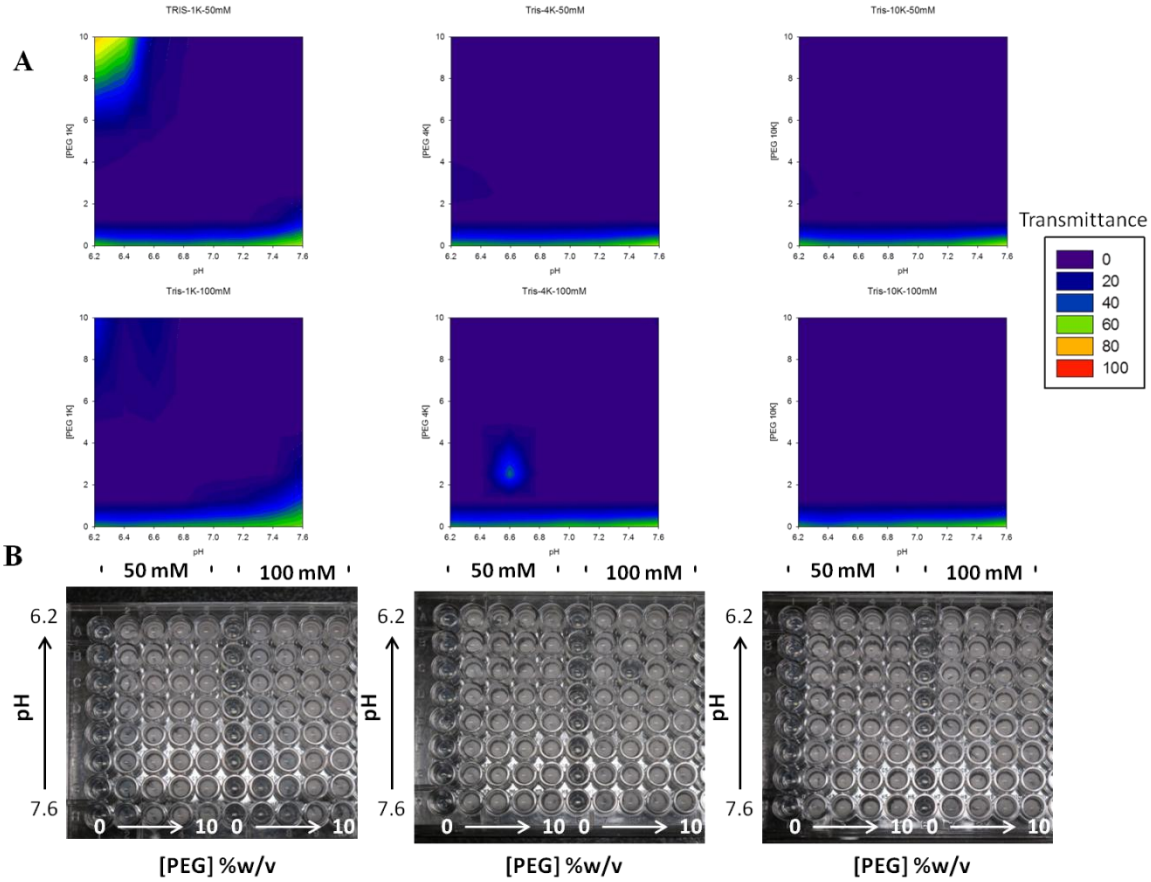

Figure S5.1: A) Opacity plots of a selection of materials tested involving the use of TRIS buffer. Scale bar indicates % transmittance. B) Optical images of materials showing a range in opacity.

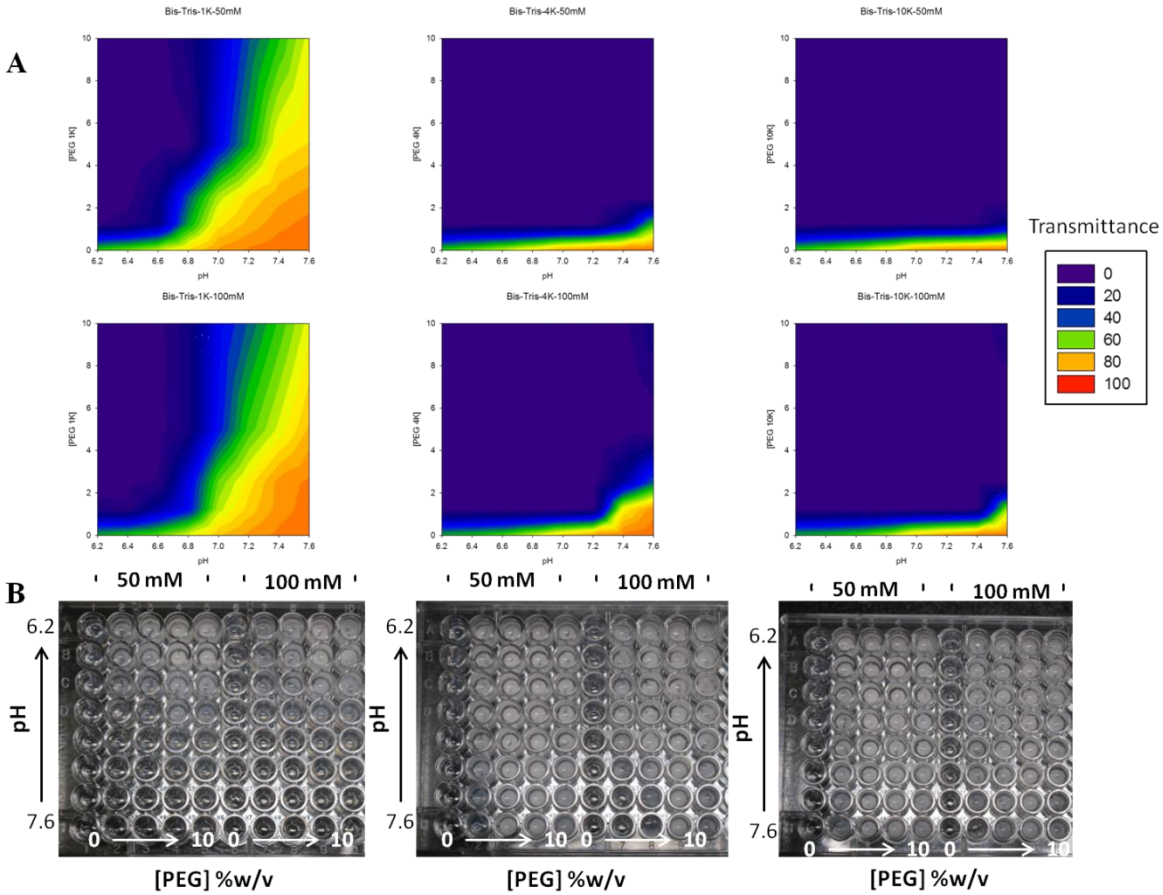

Figure S5.2: A) Opacity plots of a selection of materials tested involving the use of BIS-TRIS buffer. Scale bar indicates % transmittance. B) Optical images of materials showing a range in opacity.

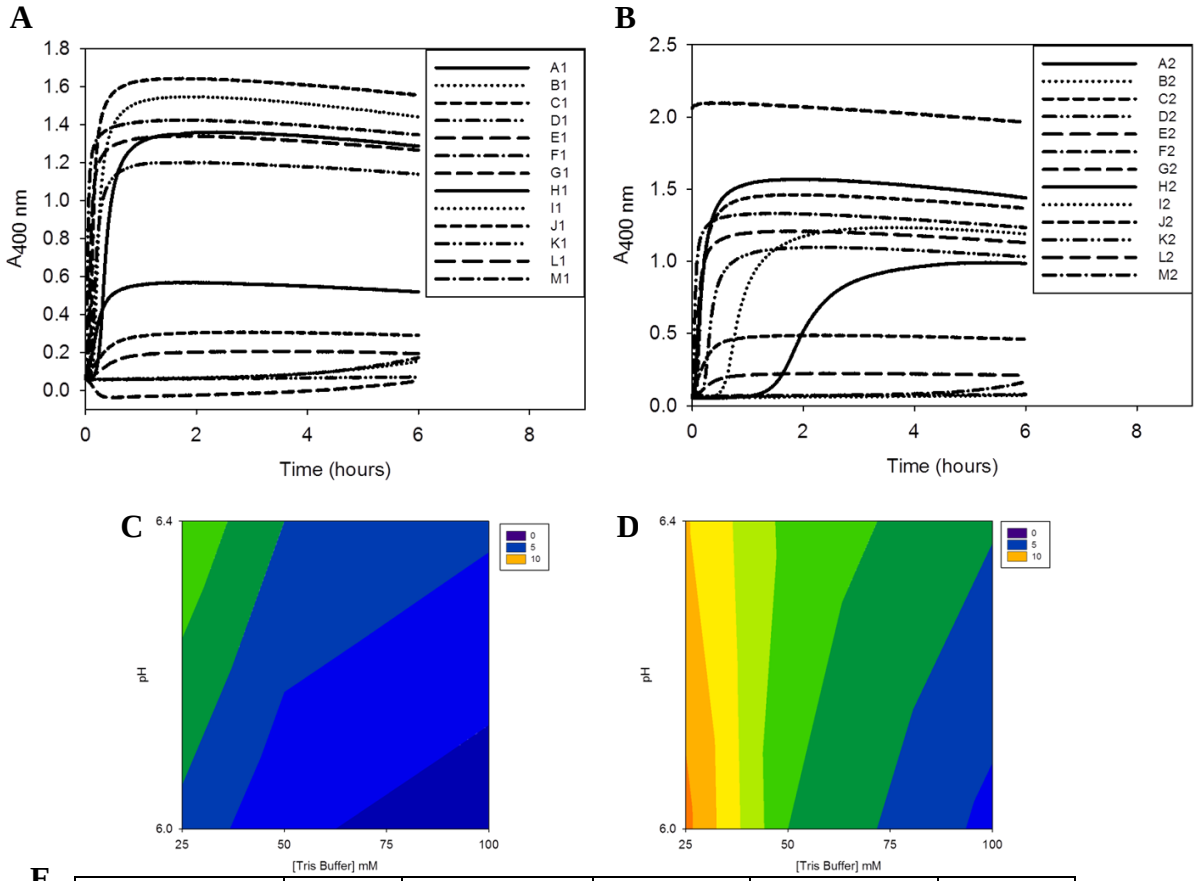

E

Sample Name	Buffer	[Buffer] mM	pH buffer	PEG MW Da	[PEG] %
A (1,2)	Hepes	100	6.2	1000	1.25
B (1,2)	Hepes	100	6.2	1000	10
C (1,2)	Hepes	25	7.0	1000	1.25
D (1,2)	Hepes	25	7.0	1000	10
E (1,2)	Hepes	50	7.0	1000	1.25
F (1,2)	Hepes	50	7.0	1000	10
G (1,2)	Hepes	50	8.0	10,000	1.25
H (1,2)	Tris	25	6.0	600	1.25
I (1,2)	Tris	50	6.0	600	1.25
J (1,2)	Tris	100	6.0	600	1.25
K (1,2)	Tris	25	6.4	600	1.25
L (1,2)	Tris	50	6.4	600	1.25
M (1,2)	Tris	100	6.4	600	1.25

Samples denoted with a "1" contain no glycerol, samples denoted with a "2" contain 12.5% glycerol.

Figure S5.3: Kinetic study of a selection of materials showing varying ranges of phase separation onset and resulting in various opacities for A) materials in the absence of glycerol and B) materials in the presence of glycerol. Opacity plots of a selection of

materials tested for PEG 600 1.25 % in C) absence of glycerol and D) presence of 12.5% glycerol. Scale bar indicates % transmittance. E) Table of material formulations used in glycerol study.

Sample	Buffer	[Buffer] mM	Buffer pH	PEG MW (Da)	[PEG] %	Pc (psi) 1 µL/min	Pc (psi) 5 µL/min	Pc (psi) 10 µL/min
Blank	--	--	--	--	--	154	232	302
i	HEPES	100	6.2	1000	10	950	--	--
ii	HEPES	50	6.2	1000	10	275	360	460
iii	HEPES	50	7.0	1000	10	194*	--	--
iv	TRIS	100	6.4	600	1.25	>3500	--	--

Table S5.1: Table of backpressure readings performed on the Eksigent NanoLC for materials used for SEM imaging. * indicates material excreted from capillary.

A

Sample	Bulk Particle Density (g/cc)	Macropore Volume (%)	Mesopore Volume (%)
i	0.5	8	92
ii	0.7	30	70
iii	0.3	98	1
iv	1.12	1	99

B

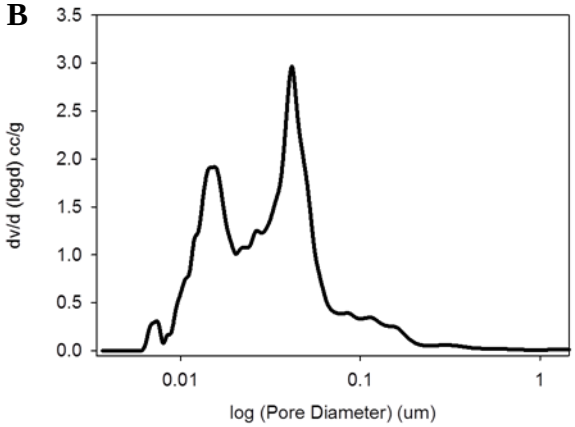

Material ii

C

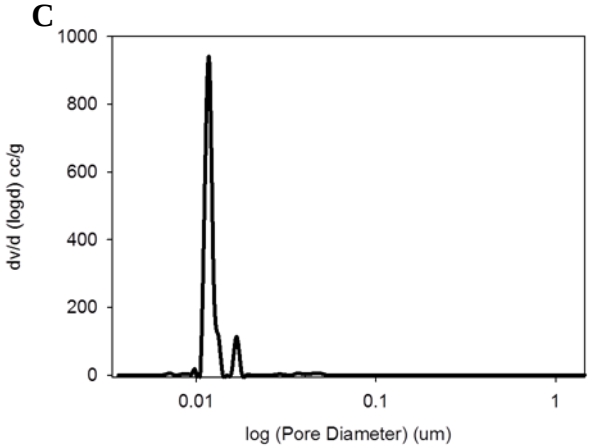

Material iv

Figure S5.4: A) Mercury porosimetry data obtained for materials shown in backpressure and SEM studies. Pore size distribution curves for B) Material ii, and C) Material iv.

Monolith #	**[TRIS] (mM)**	**[PEG 600] (% w/v)**	**pH**
1	25	1.25	6.0
2	25	1.25	6.4
3	50	1.25	6.0
4	50	1.25	6.4
5	100	1.25	6.0
6	100	1.25	6.4

Table S5.2: Table of compositions tested for leaching and activity of AChE.

Chapter 6 : Conclusions and Future Outlook

6.1 Summary of thesis projects

The primary goal of the research presented herein was to develop a robust, high-throughput technology for direct assaying of kinase activity and inhibition in a multiplexed fashion. This goal was achieved through development of a kinase assay that utilized MALDI-MS/MS detection to directly detect phosphorylation of substrates. It was demonstrated that the assay could provide quantitative data on the degree of phosphorylation, and could be multiplexed to simultaneously assay two enzymes. Furthermore, proof-of-concept studies showed that it was possible to extend this platform to allow imaging of kinase reaction microarrays using imaging mass spectrometry of reactions that were printed onto pre-coated MALDI plates. The final chapter examined an alternative method for producing a solid-phase assay that could increase assay throughput through the development of biofriendly sodium silicate bioaffinity chromatography columns.

In chapter 2 it was shown that the phosphorylation reaction of the aminoglycoside antibiotic, kanamycin, which is catalyzed by APH 3′IIIa, could be followed in a quantitative manner using a MALDI-ion trap MS/MS platform, and employed for screening mixtures of modulators against APH 3′IIIa. Not only was a method developed which showed the generation of an excellent assay, but the assay also showed utility in obtaining quantitative data. Importantly, it was shown that this platform could be applied to detection of small molecules, which has traditionally been a challenge for MALDI-MS,

which highlighted the importance of the ability to perform tandem mass spectrometry of the desorbed ions using an ion trap.

To further extend the throughput and utility of the assay, Chapter 3 demonstrated that the assay could be multiplexed to detect two kinase assays at once. This allowed simultaneous assaying of both a bacterial kinase (APH 3′IIIa) and a human protein kinase, protein kinase A, to more rapidly identify selective inhibitors of APH3′IIIa. Once again the assay was shown to be highly reproducible and amenable to quantitative assays, though it was necessary to replace DMSO with methanol to achieve adequate assay performance. Screening the two kinases concurrently not only increased assay throughput, but also allowed for the investigation into mechanism of action to be carried out, further demonstrating the utility of this assay.

Chapter 4 illustrated a proof of concept method for semi-automated high throughput assaying of kinases using imaging MALDI-MS of reaction microarrays. After optimization of printing, matrix deposition and MS analysis methods, the use IMS to detect the extent of phosphorylation of printed droplets of the reaction mixture was successfully demonstrated. In addition, it was shown that the method could provide quantitative data on the extent of the reaction and inhibition of kinases. Interestingly, the high resolution attainable from reflectron TOF-MS made it possible to utilize selected ion monitoring with a single mass analyzer rather than selected reaction monitoring by tandem MS, thereby increasing sensitivity. Furthermore, the use of this high-throughput platform allows for screening a multitude of kinases in cost-effective, individual reactions eliminating potential substrate cross-reactions.

Chapter 5 examined an alternative method to produce a solid-phase assay format that could ultimately be integrated with mass spectrometric detection. The major focus was to develop a column that would be suitable for entrapment of enzymes, including kinases, and could be interfaced to ESI or MALDI MS. The key focus of Chapter 5 was to develop a high-througput process for the identification of optimal materials for creating capillary-scale bioaffinity chromatography columns. Through high throughput, low information techniques (opacity, phase separation, visual inspection) it was possible to rapidly identify suitable materials for more in-depth analysis, reducing optimization time. Lead optimization was carried out to refine the materials for ultimate use as immobilized enzyme reactors. Lead optimization allowed for the use of high content, but more time consuming methods (SEM, porosimetry, leaching and activity) to be carried out on a smaller subset of materials. The activity of a robust enzyme, AChE, was then carried out on an optimal material, and showed not only minimal protein leaching, but also the ability to obtain quantitative information, such as the K_I of a known inhibitor in the sol-gel derived material. The development of such a column should ultimately allow for the entrapment of more fragile, expensive proteins such as kinases into chromatography columns for HTS.

Taken together, the data presented in this thesis demonstrates that MALDI-MS methods can be used to follow enzymatic reactions involving small molecular weight compounds (~500 Da), and allow these reactions to be performed under conditions of high ionic strength the better mimic physiological conditions. This overcomes the need for desalting prior to MS analysis, which is required for some other methods. In addition,

when using optimized matrix deposition methods, it is possible to obtain quantitative information on kinase reactions using either ion trap or TOF analyzers. This has traditionally been a major drawback of MALDI based assay methods, and has slowed the use of the method for HTS.

While the potential for MALDI-MS as a platform for HT kinase assays has been demonstrated, there are several aspects of the assay method that should be further improved. This includes increased automation, improved deposition of reaction mixtures onto alternative surfaces, higher density microarrays to increase throughput, increased multiplexing and more automated data analysis. Kinases are known to be very costly; a further decrease in assay volume would provide a great benefit to the developed assay. To achieve this, liquid handlers capable of handling very low volumes, or possibly microarray printers, could be used not only for the deposition of kinase reaction microarrays, but also to perform the kinase reactions. Using a series of overspotting steps, reaction microarrays could be created whereby enzyme and co-factors are deposited together, followed by overspotting of inhibitor compounds and finally substrate solutions. This process would require precise spotting by the arrayer and could pose enzyme turnover problems due to the rate of evaporation and decrease in reaction time. An alternative method would be to perform the reactions offline, for instance using a liquid handler for mixing and carrying out all reactions, followed by deposition of reaction microarrays as before.

The implementation of new matrix deposition methods would also show a large improvement to the aforementioned assay. The use of either a pre-coated microscope

slide purchased from a manufacturer or created through the use of sublimation could reduce assay cost by simplifying programming time on both the microarray liquid handler and the IMS system while also allowing for a greater number of array elements to be printed on a single surface, further reducing IMS analysis time.

Enhanced data analysis programs would reduce user time with automated analysis performed on designated spots from the liquid handler. A method to export reaction microarray positions from the robot to the IMS system would provide the first level of enhancement, followed by software that can export the data from these positions for automated smoothing, calibration and integration of the collected spectra. These improvements would allow a vast selection of kinases (5-10) to be assayed against thousands of potential modulators and show the utility of the assay for high-throughput screening.

6.2 Future Outlook: MALDI-MS Based Solid Phase Assays for HTS

The assay methods described in this thesis typically utilized solution based assays that were subsequently deposited onto the surface of MALDI plates for analysis, though it was demonstrated that immobilized enzymes could be used for solid-phase reactions, which provides a platform that could be integrated to MS. HTS methods are often employed as a means to reduce sample volumes and analysis times, thus reducing the overall cost of performing an assay. Furthermore, immobilization methods also allow for reduction of assay costs due to the ability to reuse the immobilized biomolecules, and, in the case of microarrays, provide multiplexed assays. Two methods of immobilization which could

extend the assays developed in this thesis would be the entrapment of kinases in the sodium silicate columns or the use of covalent linkage of kinases to magnetic nanoparticles (MNPs) to allow for either affinity or turnover based assays.

Kinase immobilization in sol-gel derived column materials with MALDI-MS/MS detection.

Immobilization of the biological component of an assay in sol-gel derived materials offers a variety of advantages, as described in Chapter 5. Using the previously developed SS chromatography columns, slight adjustments in the material parameters (pore morphology and distribution) could be done to optimize the entrapment of relatively small, fragile kinases such as APH3'IIIa (molecular weight of ~31 kDa[1]) into the monolithic support. Pore sizes will likely need to be minimized as a result of the small enzyme size compared to the previously entrapped AChE, a robust, large 230-260 kDa protein [2] to reduce protein leaching. Furthermore, the activity of the fragile kinase would need to be tested upon immobilization to determine specific factors needed to maintain activity (i.e. co-factors or increased salt concentrations). If immobilization of the kinase shows success, methods to integrate the column to MALDI-MS would be needed such as attachment of the column to a MALDI spotting system, [3] or collection of the flow through into individual wells of a 384-well plate and deposition onto the aforementioned microarray platform potentially allowing for IMER kinase reaction microarrays to be studied to give an inexpensive HTS method for functional and affinity based screening of modulators of kinases.

Immobilization of kinases to Magnetic Nanoparticles (MNPs)

MNPs have emerged as an assay platform for isolation and enrichment of the analyte(s) of interest.[4-5] Matrix MNP immobilization has previously been shown to be a simple, reliable way of performing MALDI experiments in a "matrixless" manner. [4] The use of a covalently immobilized matrix reduced the interferences observed when performing experiments with MALDI-MS and may provide additional benefits to the current assay design by not only reducing background interference but also potentially increasing assay throughput by allowing direct identification of modulators by their binding to kinase-derivatized MNPs. A comparison of immobilized to free matrix could be carried out to determine any benefit to the kinase system.

The use of a covalently tethered matrix-target may not provide any additional benefits to some of the current work completed on this project due to the use of tandem MS. Furthermore, the orientation of covalent immobilization of the kinase to MNP surface would need to be verified to ensure the active site of the protein is not blocked and that there is sufficient product turnover, which could be done by using His_6 tagged proteins. Should this method prove possible for the given kinases, it will allow for facile identification of enzyme modulators ideally in mass encoded mixtures with ligand identification performed directly from the surface of the MNP. The ability of direct ionization from the bead surface without the need for an elution step as previously performed in our group[5] would allow for an increase in throughput. In addition, ionization directly from the bead surface is more amenable to the work flow seen in traditional HTS facilities.

6.3 References

[1] G. A. McKay, P. R. Thompson, G. D. Wright, *Biochemistry* **1994**, *33*, 6936-6944.

[2] W. Leuzinger, M. Goldberg, E. Cauvin, *Journal of Molecular Biology* **1969**, *40*, 217-225.

[3] P. Kovarik, R. J. Hodgson, T. Covey, M. A. Brook, J. D. Brennan, *Analytical Chemistry* **2005**, *77*, 3340-3350.

[4] P. C. Lin, M. C. Tseng, A. K. Su, Y. J. Chen, C. C. Lin, *Analytical Chemistry* **2007**, *79*, 3401-3408.

[5] M. J. McFadden, M. S. Junop, J. D. Brennan, *Analytical Chemistry* **2010**, *82*, 9850-9857.